

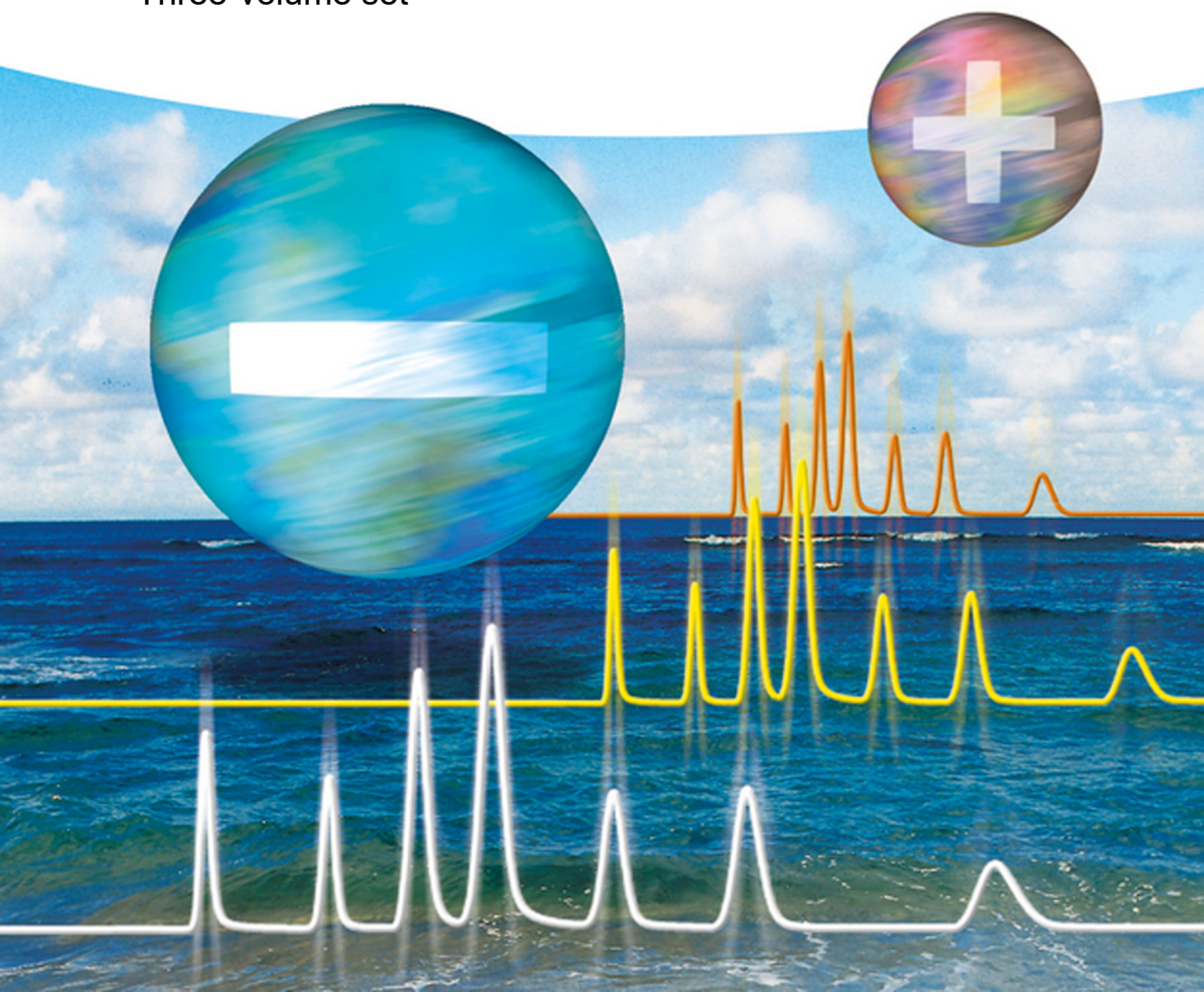
Joachim Weiss

# Handbook of Ion Chromatography

Foreword by Oleg Shpigun

Fourth Edition

Three-volume set



## Author

**Dr. Joachim Weiss**  
Thermo Fisher Scientific GmbH  
Im Steingrund 4-6  
63303 Dreieich  
Germany

**Cover credits:** CreativCollection  
(photograph of the sea)

All books published by **Wiley-VCH** are carefully produced. Nevertheless, authors, editors, and publisher do not warrant the information contained in these books, including this book, to be free of errors. Readers are advised to keep in mind that statements, data, illustrations, procedural details or other items may inadvertently be inaccurate.

**Library of Congress Card No.:** applied for

## **British Library Cataloguing-in-Publication Data**

A catalogue record for this book is available from the British Library.

## **Bibliographic information published by the Deutsche Nationalbibliothek**

The Deutsche Nationalbibliothek lists this publication in the Deutsche Nationalbibliografie; detailed bibliographic data are available on the Internet at <http://dnb.d-nb.de>.

© 2016 Wiley-VCH Verlag GmbH & Co. KGaA,  
Boschstr. 12, 69469 Weinheim, Germany

All rights reserved (including those of translation into other languages). No part of this book may be reproduced in any form – by photoprinting, microfilm, or any other means – nor transmitted or translated into a machine language without written permission from the publishers. Registered names, trademarks, etc. used in this book, even when not specifically marked as such, are not to be considered unprotected by law.

**Print ISBN:** 978-3-527-32928-1

**ePDF ISBN:** 978-3-527-65164-1

**ePub ISBN:** 978-3-527-65163-4

**Mobi ISBN:** 978-3-527-65162-7

**oBook ISBN:** 978-3-527-65161-0

**Cover Design** Grafik-Design Schulz, Fußgönheim,  
Germany

**Typesetting** Thomson Digital, Noida, India

Printed on acid-free paper

## 8.5.2

**IC–MS Coupling**

The second important hyphenation is the coupling of an ion chromatograph to a mass spectrometer; this combination provides the analyst with information on analyte structure and molecular weight. While mass-selective detection in gas chromatography became routine years ago, the coupling of a liquid chromatograph to a mass spectrometer used to be problematic, because the relatively large amounts of liquid mobile phase are not compatible with the high vacuum in the ion source of a mass spectrometer. To solve these incompatibility problems, various types of LC–MS interfaces have been developed. The discussion below focuses on the electrospray interface. Particle-beam and thermospray interfaces, which were also briefly introduced in the third edition of this handbook, are not used anymore. To the interested reader I refer to the monographs by Yergey *et al.* [230] and Niessen [231] for more indepth reading about other interface

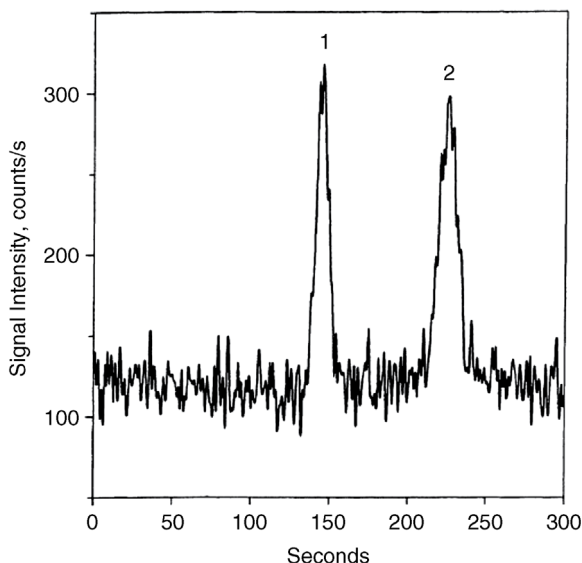


**Figure 8.97** Separation of Sb(III) and Sb(V) with element-specific detection. Separator column: IonPac AS14; column dimensions: 250 mm  $\times$  4 mm i.d.; eluent: 1.25 mmol/L EDTA, pH 4.7; flow rate: 1.5 mL/min; injection volume: 100  $\mu$ L; detection: ICP-MS; peaks: 50 ng/L each of Sb(V) (1) and Sb(III) (2) (reproduced with permission from Ref. [222]. Copyright 2001, Elsevier Science BV).

types. The most important characteristic of an LC-MS interface is the transfer of analyte molecules from the separator column into the high vacuum of a mass spectrometer. This means that an analyte molecule dissolved in the mobile phase has to make the transition to an analyte molecule isolated in the gas phase. To achieve high sensitivity, as many analyte molecules as possible have to be transferred, while the mobile-phase constituents have to be largely removed. The maximum amount of liquid that can be introduced into the high vacuum of a mass spectrometer without increasing pressure in the ion source depends solely on the capacity of the vacuum pumps. Given the feed rate of modern turbomolecular pumps, the practical upper limit to flow rate is 10–20  $\mu$ L/min, depending on the composition of the solvent and on the use of coaxial sheath flow. However, conventional 4 mm separator columns in ion chromatography are operated at 1 mL/min, so only 1–2% of that amount of liquid can be directly introduced into the vacuum system. These numbers impressively demonstrate the dimension of this incompatibility problem. It can be solved by removing a large amount of solvent before the analytes enter the high vacuum. Split techniques and microbore columns with a small inner diameter of 2 mm and low flow rates of 0.25 mL/min also help to significantly decrease the amount of liquid. Combinations of all these measures can also be applied.

An additional problem is the electrolytes that are used for separating ionic species on ion-exchangers. Such separations cannot be performed without

electrolytes. Therefore, volatile eluents such as ammonium sulfate have to be used, which can be pumped out of the ion source. The second solution to this problem is continuously regenerated suppressor systems (see Sections 3.6 and 4.3), with which eluents can be converted to water prior to entering the MS interface. It is true that the use of a suppressor system limits the choice of eluent [232]. Meanwhile, however, so many ion exchangers for anion and cation chromatography are available that allow anions and cations to be eluted efficiently and with high resolution using KOH or mineral acids eluents. Because these ion exchangers are usually also solvent compatible, even polarizable ions can be eluted by adding organic solvents to the mobile phase. As early as 1990, Simpson *et al.* [233] successfully employed a micromembrane suppressor for desalting eluents. They placed it between an anion exchanger and the thermospray interface and determined a residual sodium concentration of 13–30  $\mu\text{mol/L}$  when pumping an eluent concentration of 10–100 mmol/L. Conboy *et al.* [234] also utilized suppressors for their investigations on quaternary ammonium compounds and organic sulfonates and sulfates, placing them between separator column and interface.

#### 8.5.2.1 Electrospray Interface

Electrospray ionization (ESI) [235] is an atmospheric-pressure ionization technique (API) that allows the transfer of ions from solution to the gas phase, from which the ions can be subjected to mass spectrometric analysis. Electrospray is of great importance because a large number of chemical and biochemical processes involve ions in solution. It affords ion transfer of a wide variety of ions dissolved in a wide variety of solvents. The ions include

- single and multiple charged inorganic cations such as alkali and alkaline-earth metal ions,
- single and double charged transition metal ions and their complexes with mono- and polydentate ligands,
- inorganic and organic anions,
- single and multiple protonated organic bases such as amines, alkaloids, peptides, and proteins, and
- single and multiple deprotonated organic acids or organophosphates such as nucleic acids.

The solvents include practically all protic solvents such as water, methanol, and ethanol or aprotic solvents such as acetone, acetonitrile, and dimethylsulfoxide.

Electrospray ionization mass spectrometry was introduced by Yamashita and Fenn in 1984 [236] and independently in a very similar way at approximately the same time by Aleksandrov *et al.* [237]. Development of ESI–MS since 1984 has established it as a method of outstanding importance, in particular for biochemical applications.

The transfer of ions from solution to the gas phase is a strong endothermic process, because in solution the ion interacts with solvent molecules that form a solvation sphere around the ion. The energy required to transfer an ion from

aqueous solution to the gas phase is larger than the energy required to break a carbon C—C bond. If that energy is supplied at once over a short period of time, the act of freeing an ion from the solvent can lead to fragmentation. The softness of the ion transfer method can be defined as the degree to which fragmentation of the ions is avoided. From that standpoint, ESI-MS is the softest technique available.

There are three major steps in the production of gas-phase ions from electrolytic ions in solution by electrospray:

- Production of charged droplets at the electrospray capillary tip
- Shrinkage of the charged droplets by solvent evaporation and repeated droplet disintegrations, ultimately leading to very small, highly charged droplets capable of producing gas-phase ions
- The actual mechanism by which gas-phase ions are produced from the very small and highly charged droplets

As shown in the schematic representation in Figure 8.98, a voltage of 2–3 kV is applied to the metal spray capillary (needle) that typically has an inner diameter of 0.1 mm and is located 1–3 cm from the counterelectrode. In ESI-MS, this counterelectrode may be a plate with an orifice leading to the mass spectrometric sampling system. Because the capillary tip is very thin, the electric field in the air at the tip is very high ( $E_c \approx 10^6$  V/m). Considering a typical solution present in the capillary with methanol as the solvent and a low concentration ( $10^{-5}$ – $10^{-3}$  mol/L) of an organic base as the salt, the field  $E_c$ , when turned on, will penetrate the solution at the capillary tip, and the positive and negative electrolyte ions in the solution will move under the influence of the electric field until a charge distribution results that counteracts the imposed field and leads to essentially field-free conditions inside the solution. When the capillary is the positive electrode, positive ions will drift toward the meniscus of the liquid, and negative ions will drift away from the surface. The mutual repulsion of the positive ions at

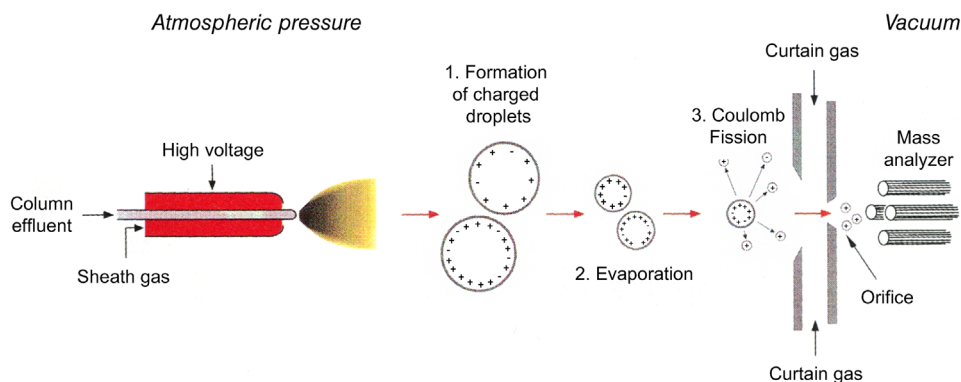


**Figure 8.98** Schematic diagram of the ionization process in electrospray ionization ("IonSpray," Perkin-Elmer Sciex).

the surface overcomes the surface tension of the liquid and the surface begins to expand, allowing the positive charges and liquid to move downfield. The so-called Taylor cone [238] is formed, and if the applied field is sufficiently high, a fine jet emerges from the cone tip, which breaks up into small charged droplets. The charged droplets produced by the spray then shrink, owing to the solvent evaporation while the charge remains constant. The energy required for solvent evaporation is provided by the thermal energy of the ambient air. The charge of the droplet is expected to remain constant because the emission of ions from the solution to the gas phase is highly endoergic. The decrease of the droplet radius  $R$  at constant droplet charge  $q$  leads to an increase of the electrostatic repulsion of the charges at the surface until the droplets reach the Rayleigh stability limit [239]:

$$q_{\text{Ry}} = 8 \pi (\epsilon_0 \gamma R^3)^{1/2} \quad (8.61)$$

The Rayleigh equation describes the condition at which the electrostatic repulsion becomes equal to the force due to the surface tension  $\gamma$ , which holds the droplet together. The charged droplet becomes unstable when its radius  $R$  and charge  $q$  satisfy Eq. (8.61). In a very complex process [240] that is not yet completely understood, droplets undergo fission when they are close to the Rayleigh limit. The fragmentation is generally referred to as coulombic fission. Two mechanisms have been proposed to account for the formation of gas-phase ions from very small and highly charged droplets. The first one, proposed by Doyle *et al.* [241], is based on the formation of extremely small droplets containing only one ion. Solvent evaporation from such a droplet will lead to a gas-phase ion. Iribarne and Thomson [242] predict that, after the radii of the droplets decrease to a given size, direct ion emission from the droplets become possible and that this process, which is called ion evaporation, becomes dominant over coulomb fission for droplets with radii  $R \leq 10$  nm. The emitted ions are then directed into the mass analyzer by electrostatic lenses. More detailed information on the mechanism of ESI-MS has been published by Kebarle and Ho [243].

The electric field required to generate an aerosol largely depends on the surface tension of the solvent. If the composition of the column effluent remains constant, nebulization is not a problem. However, in the case of gradient elution, where eluent composition and, consequently, surface tension change with time, nebulization can be a problem. A rather elegant solution to this problem is the pneumatically assisted electrospray ionization ("IonSpray") developed by Perkin-Elmer Sciex, in which a sheath gas assists in the formation of droplets. Electrospray is a low-flow rate technique. When the flow rate is increased for a given analyte concentration, the analyte ion signal does not increase. Thus, in terms of analyte concentration, sensitivity remains constant, but in terms of mass flow, sensitivity drops when the flow rate of the analyte solution is increased. This is an unusual situation in mass spectrometry because a mass spectrometer operating in the electron ionization (EI) or chemical ionization mode (CI) is a mass-flow sensitive detector. If the liquid flow rate is increased too much, the ion

signals become lower and less stable. Therefore, microbore columns are usually employed for IC/ESI–MS with flow rates of approximately 250  $\mu\text{L}/\text{min}$ . These flow rates are compatible with thermally assisted electrospray [244], which heats the spray capillary to 150–240  $^{\circ}\text{C}$ . Manufacturers have also claimed good performance of ultrasonically assisted electrospray [245] in combination with a sheath gas for drying and focusing suitable for flow rates up to 1  $\text{mL}/\text{min}$ , which can be used for conventional separator columns with 4 mm diameters. High-flow electrospray is always combined with the supply of heat to assist the evaporation of the solvent.

The position of the spray capillary relative to the ion sampling orifice within the sampling plate is of significant importance. By avoiding directly spraying at the sampling plate orifice, the instance of charged droplets being sampled (as opposed to gas-phase ions) is lowered, hence increasing instrument response. In most modern MS instruments, the sprayer position may be adjusted in one, two, or three axes that will allow optimization relative to the sampling orifice. In the first published report of successful electrospray mass spectrometry [236], the spray capillary was positioned in the center of the source (on-axis position), as schematically depicted in Figure 8.99. By moving to an off-axis position, the ion signal observed by the mass spectrometer is more stable and at least as high

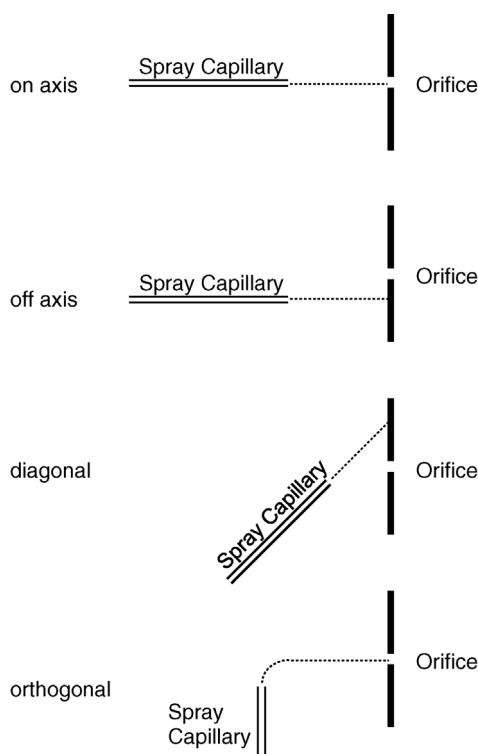


**Figure 8.99** Arrangements for the sprayer capillary in an electrospray ion source.



as in the on-axis position. It is desirable to take ions, but no droplets into the mass analyzer. Charged droplets transported into the mass spectrometer may impinge on the ion optics or on the mass analyzer, creating spikes in the mass spectra. Off-axis positioning can be taken a step further by placing the sprayer in a diagonal position inside the source. The spray is not aimed at the sampling orifice, but at a position beyond, in order to reduce the chance of shooting droplets into the mass spectrometer. Diagonal positioning is most effective for pneumatically assisted electrospray. Optimization of the sprayer position and the capillary voltage are interrelated and should be optimized empirically together. The most important practical advance in sprayer positioning has come with the introduction of orthogonal source designs, where the sprayer is positioned orthogonally to the sampling orifice. This design has several advantages, including sampling of fewer charged droplets relative to ions and the ability to tolerate higher flow rates.

In an interface for chemical ionization at atmospheric pressure (APCI), aerosol formation occurs in a heated tube with nitrogen as a reagent gas; the solvent is completely evaporated in the tube. The gas-vapor mixture is then directed into the atmospheric-pressure ion source, in which chemical ionization is initiated by electrons that are generated at the corona discharge needle. The solvent vapor acts as a reagent gas. The charge is transferred to the analyte molecules by ion-molecule reactions (cluster formation and declustering of ions). Subsequently, the ions generated are sampled into the high vacuum of a mass spectrometer for mass analysis. Figure 8.100 schematically depicts the APCI ionization process.

Both ionization modes can be operated in the positive and negative ion mode to obtain either protonated or deprotonated molecular ions as well as sodium, potassium, ammonium, formate, or acetate adducts. Because atmospheric-pressure ionization is a “soft” ionization technique (i.e., molecular ions are

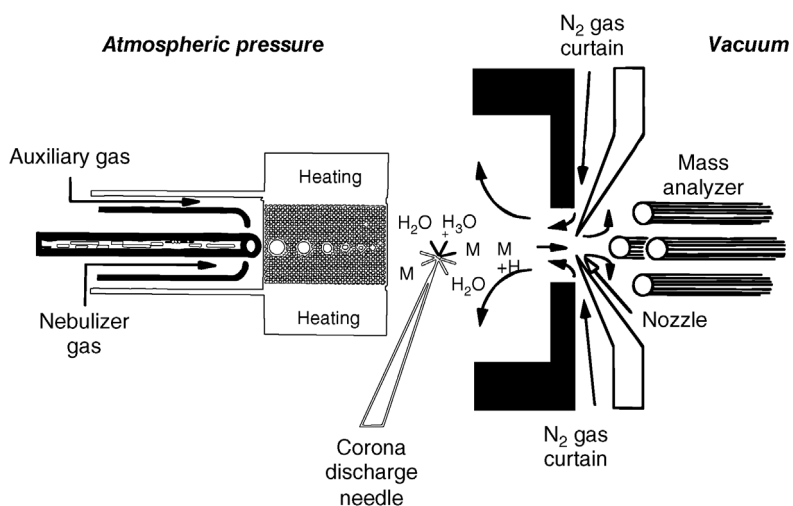


**Figure 8.100** Schematic diagram of the ionization process in APCI (“Heated Nebulizer,” Perkin-Elmer Sciex) (adapted with permission © 1992 John Wiley & Sons, Ltd.; [244]).

predominantly formed and fragmentation is very rare), the mass spectra of single components do not exhibit many signals. Under suitable MS conditions (voltage increase at the electrostatic lenses) or in tandem mass spectrometry, fragmentations can be induced for a more detailed structural elucidation. Such fragmentations, however, differ from those observed in electron impact ionization (EI). Because spectral libraries for API-MS do not exist at present, the ability to identify unknowns is rather limited.

**Collision-Induced Dissociation** Classical API spectra tend to show very little fragmentation due to the “soft” nature of the ionization processes, that is, during the formation of ions, the analyte ions do not receive enough energy to break the intramolecular bonds. However, some fragmentation may easily be induced in one of the higher pressure regions, so that some structural information may be gathered. Acceleration of ions between the orifice and the skimmer, or between the skimmer and the RF-only multipole, results in collision of ions with the background gas. This process is known by various different names depending upon the instrument manufacturer and includes “in-source collision-induced dissociation” (CID), “nozzle-skimmer fragmentation,” “cone-voltage fragmentation,” and so on. By increasing the potential difference between the skimmer and the quadrupole, or between the nozzle and the skimmer, the energy imparted to the analyte molecule through increasing frequency and collision energy can be high enough to cause intramolecular bonds to be broken and for fragmentation to occur [246,247]. In the case of larger molecules such as peptides and proteins, the excess energy can often be absorbed in several vibrational modes and high potential differences are required to fragment these kinds of molecules. The major advantage of this technique for the production of spectra containing a greater amount of structural information is its simplicity. One voltage needs to be adjusted and there is neither need for switching or adjustment of collision gases nor any retuning of ion optics. In negative ion mode, for instance, the degree of collision-induced dissociation (CID) can be estimated using the drug naproxen that normally only shows the  $[M-H]^-$  ion at  $m/z$  229. With small nozzle-skimmer potential differences, the naproxen molecule readily loses  $CO_2$ , giving rise to a peak at  $m/z$  189.

Collision-induced dissociation can also be used to improve baseline noise and increase signal-to-noise ratios in LC-MS. When ions pass through the sampling orifice into the vacuum region, the background density of neutral gas ions falls rapidly. If ions moving in a low-density gas are accelerated by the nozzle-skimmer region, mild CID may be affected, which will be enough to cleave the hydrogen bonds inside the ion-water or ion-neutral gas clusters. In addition, heating of the ion clusters, which occurs during collisions, will also aid desolvation of the cluster ions. Moderate acceleration of clusters is effective and widely used to decluster ions.

**Considerations in IC/ESI-MS Instrumentation** A typical IC-MS system consists of an ion chromatographic system, a mass spectrometer, and a delivery system for

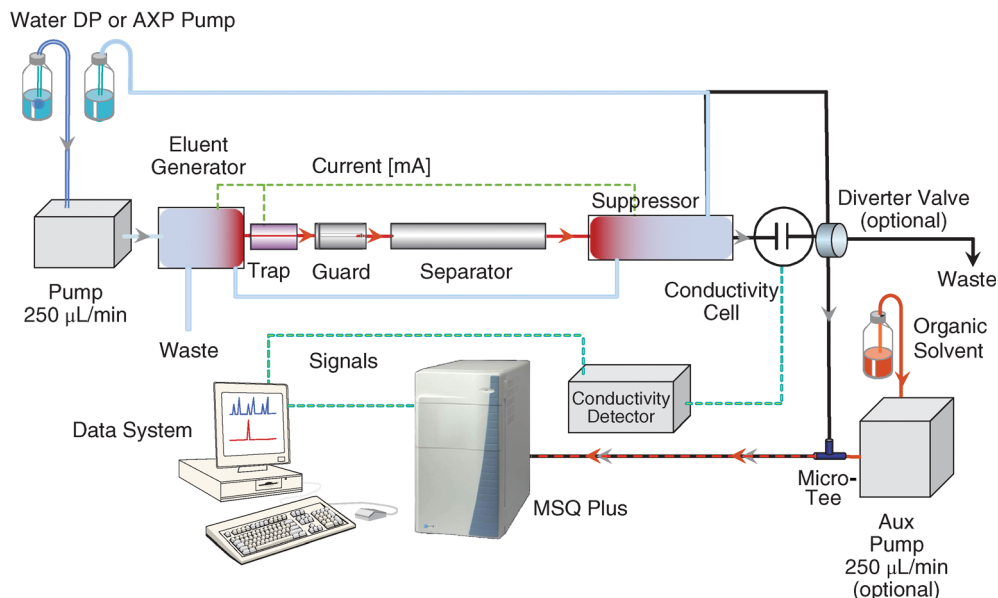


**Figure 8.101** Schematic diagram of a reagent-free IC-MS system.

the addition of a desolvation solution (usually an AXP-MS pump and a static mixing tee). Figure 8.101 shows the configuration of a preferred IC-MS system setup. A standard microbore IC system is recommended for routine MS detection, because it has a flow rate range from 0.1 to 0.5 mL/min that is within the preferred flow characteristics of most electrospray ionization sources. In principle, higher flow rates (used for 4 mm columns) are feasible, but the excessive flow ends up diverted to waste, with no benefit of sensitivity enhancement. Therefore, 2 mm columns and consumables are recommended for MS applications. Reagent-free ion chromatography (RFIC) systems are the preferred systems for the delivery of a highly reproducible mobile phase that is electrolytically generated from an eluent generator. An electrolytically operated suppressor is used to continuously convert the high-ionic strength eluent to deionized water prior to entering the conductivity and MS detectors by exchanging the eluent counterions for hydronium or hydroxide ions. Because the eluent is not recoverable in MS, the suppressor has to be operated in external water mode, with deionized water as the regenerant delivered by an auxiliary pump. To enhance desolvation, the effluent from the conductivity cell is combined with an organic desolvation solvent, delivered by another pump through a static mixing tee and a grounded union, prior to entering the electrospray ionization source of the MS detector. The grounding union between the conductivity cell and the high-voltage potential prevents possible current backstreaming in case the connection tubing becomes filled with a conductive solution. An additional back pressure of 30–40 psi is recommended for the proper functioning of the suppressor and

conductivity cell to prevent eluent in the cell from outgassing due to abrupt volume changes. However, excessive back pressure may cause adverse effects such as peak tailing or peak broadening and a decrease in resolution due to the expanded flow path. It also may cause irreversible damage to the suppressor hardware. The current ERS 500 suppressors should be operated at back pressures <100 psi (0.689 MPa) for IC–MS application; back pressures >450 psi (3.100 MPa) are not recommended.

Because ion-exchange separations are essentially carried out in 100% aqueous media, they require a higher nebulizer gas volume and higher temperatures for desolvation. Therefore, an organic solvent is usually added for IC–MS applications to the column effluent prior to entering the ion source of the MS detector. Different solvents may be used for this purpose, including acetonitrile, methanol, or 2-propanol. The best signal improvements are always observed with 100% organic solvent. While acetonitrile demonstrates the best improvements for inorganic anions and organic acids, 2-propanol is very well suited for cation applications. As shown with the MS spectra of lithium in Figure 8.102, 2-propanol as the desolvation solvent provides the cleanest adduct MS spectrum with the best intensity for the main adduct. Its use improves the desolvation/

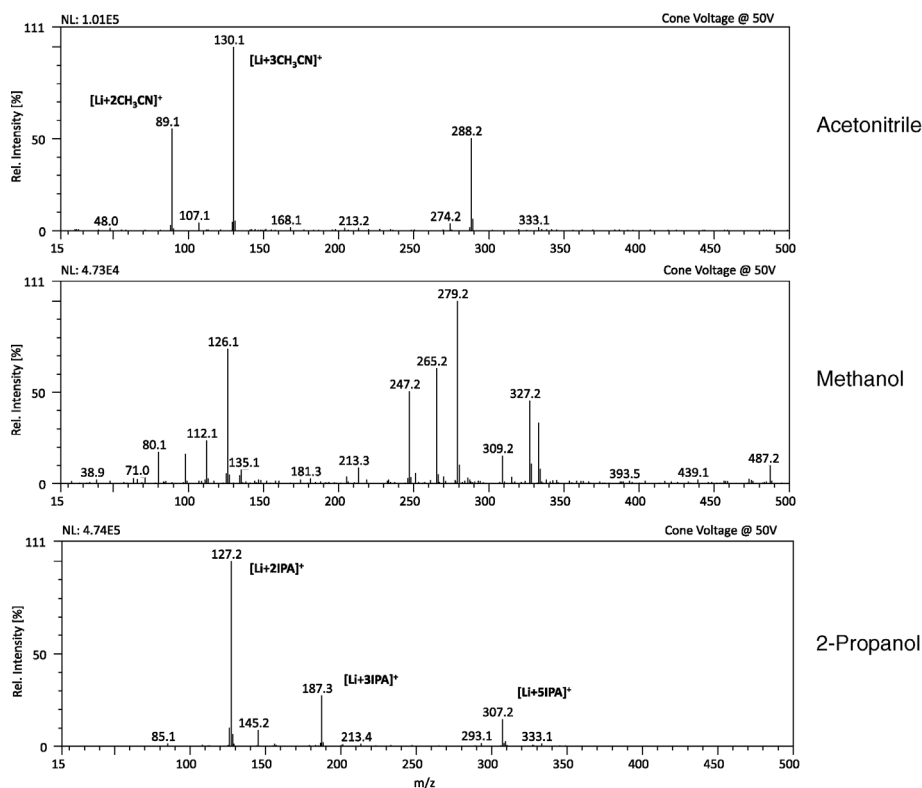


Figure 8.102 MS spectra of Li with different organic desolvation solvents.

ionization process and the detection sensitivity, forming adducts that facilitate the detection of analyte ions with an extremely low nominal mass. Lithium ions, for instance, are single charged species with  $m/z$  7, which is below the lowest calibrated mass of any MS detector. With the addition of 2-propanol (IPA),  $[\text{Li} + n\text{IPA}]^+$  clusters are observed, that is,  $[\text{Li} + 2\text{IPA}]^+$ ,  $[\text{Li} + 3\text{IPA}]^+$ , and  $[\text{Li} + 5\text{IPA}]^+$ , with  $m/z$  127, 187, and 307, respectively, which are within the calibrated mass range.

Another consideration that is important for IC–MS configurations is the dimension of the inner diameter and length of the connection tubing between the ion chromatograph and the MS detector, which has to be minimized to reduce the extracolumn volume. However, the total additional back pressure should not exceed 300 psi (2.067 MPa). Recently, Wang and Schnute described a systematic method of optimizing mass spectrometric detection for ion chromatographic analysis of common inorganic anions and selected organic acids using response surface methodology (RSM) [248]. As suggested there, general conditions can be used as a starting point for further system optimization: when operating the ion chromatography system at a flow rate of 0.25 mL/min, the probe temperature should be set at 400–450 °C and the nebulizer gas at 85 psi. Acetonitrile is typically used as the desolvation solvent with a flow rate of 0.2–0.3 mL/min.

#### 8.5.2.2 IC–MS Applications

**Environmental Applications** Although ESI–MS was originally developed for the analysis of high-molecular weight organic compounds, it can also be applied to the analysis of strongly polar and low-molecular weight ionic compounds. Charles *et al.* [249] applied this technique for the first time to the trace analysis of bromate in water at submicrogram/Liter levels. The ion chromatographic separation was carried out on an IonPac AG9-SC guard column. The optimal flow rate for ESI–MS/MS detection of 50  $\mu\text{L}/\text{min}$  was obtained by a 1:20 split utilizing a T-piece of very low dead volume. However, the traditional carbonate/bicarbonate eluent for this column is not very suitable with ESI–MS/MS detection, because bicarbonate forms a nonvolatile residue during the evaporation process. This residue would precipitate around the entrance cone and eventually block it. Also, sensitivity is compromised when using a carbonate/bicarbonate eluent compared to pure deionized water. One of the two ways to reduce the electrolyte content in the column effluent prior to entering the electrospray interface is the use of a suppressor system. Alternatively, an electrolyte has to be selected that is compatible with ESI and capable of eluting bromate. For example, ammonium sulfate can be used; it elutes bromate at a concentration of  $c = 27.5 \text{ mg/L}$ . If the ammonium sulfate solution is prepared with 90% (v/v) methanol instead of pure deionized water, nebulization and subsequent evaporation is supported that, in turn, increases sensitivity by a factor of 10. Because the stationary phase used for the separation is solvent compatible, such an eluent can be used without any problem. In the course of sample preparation, anions

that have a negative influence on separation or detection have to be removed. These anions include bicarbonate, sulfate, and chloride. The negative effect of bicarbonate on ESI-MS/MS detection was mentioned above. However, it can easily be removed by using an SPE cartridge filled with a cation exchanger in the hydrogen form (Thermo Scientific Dionex OnGuard-H). As a result of this cation-exchange process, carbon dioxide is formed due to the sample acidification. The carbon dioxide can then be removed by sparging the sample with helium. Sulfate at concentrations  $c > 20$  mg/L also interferes with the analysis. If sulfate is present in the sample at higher concentrations, SPE cartridges such as OnGuard-Ba (cation exchanger in the barium form) are used for precipitating sulfate. Higher concentrations of chloride are precipitated with the cation exchanger in the silver form (OnGuard-Ag).

In the mass spectrum, bromate is detected at  $m/z = 127$  and  $129$ , which reflects the natural occurrence of the two evenly distributed bromine isotopes  $^{79}\text{Br}$  and  $^{81}\text{Br}$ . After fragmentation of both ions in the second quadrupole (Q2), the product ions can be analyzed in the third quadrupole (Q3). In the course of fragmentation, bromate can lose one, two, or three oxygen atoms to yield  $\text{BrO}_2^-$ ,  $\text{BrO}^-$ , and  $\text{Br}^-$ , respectively, as the products. Due to the isotope distribution, six transitions generally result that can be registered in the multiple reaction-monitoring mode (MRM):  $127/111$ ,  $127/95$ ,  $127/79$ ,  $129/113$ ,  $129/97$ , and  $129/81$ . Because a high background signal is observed after the elution of bromate, which is attributed to the formation of  $\text{HSO}_4^-$  ( $m/z = 97$ ), only the first four transitions are selected to obtain a perfectly resolved chromatographic signal such as that of a  $1\text{ }\mu\text{g/L}$  bromate standard in Figure 8.103. With this technique, Charles *et al.* calculated a minimum detection limit for bromate of  $0.1\text{ }\mu\text{g/L}$ ; the standard deviation for  $n = 7$  is 1.9% at this concentration level.

In another paper published around that time, Charles and Pépin [250] extended the ESI-MS/MS technique developed for trace analysis of bromate to the analysis of other oxyhalides such as chlorite, chlorate, and iodate, which can occur when ozonating drinking water (see Section 10.1). Because chlorine also occurs in two isotopic forms, oxychlorides are detected in the negative ion mode at two different  $m/z$  values:  $m/z = 67$  and  $69$  for  $\text{ClO}_2^-$ , and  $m/z = 83$  and  $85$  for  $\text{ClO}_3^-$ . Iodate is detected at  $m/z = 175$ . The fragmentation of these ions also results from the successive loss of oxygen atoms. The eluent mixture consisting of ammonium sulfate and methanol developed for the analysis of bromate cannot be used for the analysis of oxyhalides, because it is contaminated with chlorate. For this reason, the authors used ammonium nitrate as an eluting agent. Because the affinity of nitrate toward the stationary phase is lower than that of sulfate, its concentration has to be increased accordingly. Optimal separations between iodate and chlorite, the elution order of which is reversed due to the high methanol content in the mobile phase [251], are obtained with  $65\text{ mg/L}$  ammonium nitrate in the mobile phase. As an example, Figure 8.104 shows the chromatogram of a drinking water sample, in which  $1.95\text{ }\mu\text{g/L}$  chlorate could be detected. Detection was carried out following the transitions  $^{35}\text{ClO}_3^- / ^{35}\text{ClO}_2^-$  ( $83/67$ ) and  $^{37}\text{ClO}_3^- / ^{37}\text{ClO}_2^-$  ( $85/69$ ). With this technique, the minimum

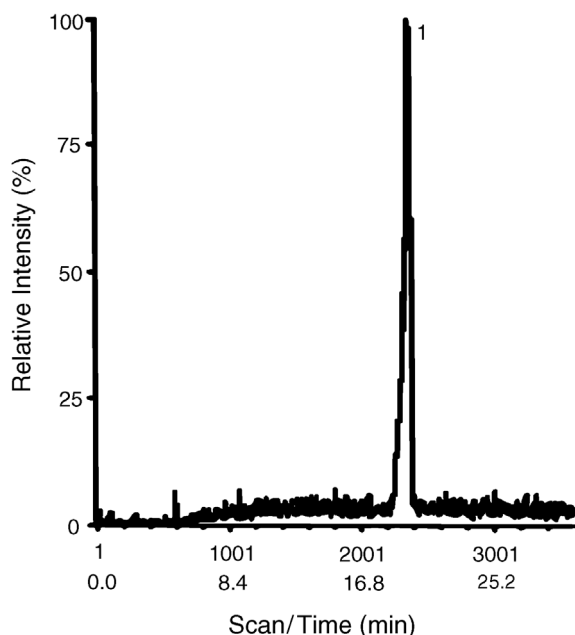


**Figure 8.103** Chromatogram of a 1 µg/L bromate standard with ESI-MS/MS detection. Separator column: IonPac AG9-SC; eluent: 27.5 mg/L ammonium sulfate/MeOH (10:90 v/v); flow rate: 1 mL/min; detection: ESI-MS/MS in the negative MRM mode

(127/111, 127/95, 127/79, and 129/113); sample volume: 5 µL; sample: 1 µg/L bromate standard (1) in deionized water (reproduced with permission from Ref. [247]. Copyright 2008, American Chemical Society).

detection limits for iodate, chlorite, and chlorate are 0.5, 1.0, and 0.05 µg/L, respectively.

While bromate is a by-product from disinfecting drinking water via ozonation, haloacetic acids (HAAs) are disinfection by-products produced during chlorination of water and natural organic matter. EPA Methods 552.1, 552.2, and 552.3 used to determine HAAs require derivatization and multiple extraction steps followed by gas chromatography with electron capture detection (ECD) and mass spectrometry. In contrast, IC-MS and IC-MS/MS offer a sensitive and selective alternative that does not require sample pretreatment [252]. Water samples can be injected directly into an ion chromatograph coupled to a single quadrupole MS detector or to a triple quadrupole mass spectrometer. The separation of all nine haloacetic acids, dalapon (2,2-dichloropropanoic acid), and bromate can be carried out on IonPac AS24 (see Section 3.4.1.5), which was specifically developed for use with MS and MS/MS, and is specified in the US EPA Method 557 [253]. The unique selectivity of this column under hydroxide gradient conditions allows the separation of these analytes from common inorganic matrix ions such as chloride, nitrate, bicarbonate, and sulfate, which are diverted to waste during the chromatographic run by switching the matrix diversion valve as shown with the

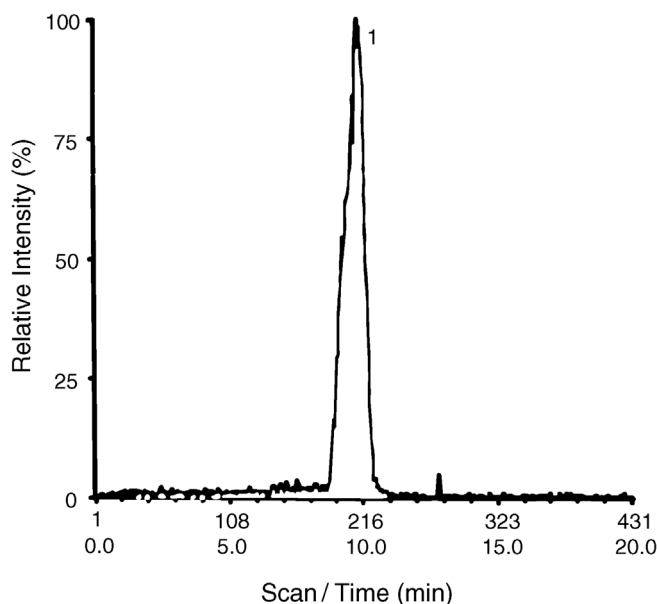


**Figure 8.104** Trace analysis of chlorate in drinking water with ESI-MS/MS detection. Separator column: IonPac AG9-SC; eluent: 65 mg/L ammonium nitrate/MeOH (10:90 v/v); flow rate: 1 mL/min; detection: ESI-MS/MS in the negative MRM mode (83/67, 85/69); sample volume: 5 mL; sample: drinking water with 1.95 µg/L chlorate (1) as well as 11.9 mg/L chloride, 6.7 mg/L nitrate, 19.3 mg/L sulfate, 129.4 mg/L bicarbonate, 13.7 mg/L sodium, 3.7 mg/L potassium, 9.4 mg/L magnesium, and 25.8 mg/L calcium (reproduced with permission from Ref. [250]. Copyright 1998, American Chemical Society).

configuration in Figure 8.101. Thus, contamination of the ion source of the mass spectrometer can be avoided. Figure 8.105 shows the separation of all nine haloacetic acids with MS/MS detection in the form of an MRM channel overlay. The gray boxes indicate the matrix diversion windows where the analytical flow is diverted to waste during elution of the matrix ions. The hydroxide gradient is illustrated above the chromatogram. In this method, four isotope-labeled internal standards have been used for all analytes due to availability issues. The chosen internal standards elute in each of the three sections of the gradient method, because the composition of the background changes over the course of the run. Period 1 of the gradient uses 7 mmol/L KOH as the eluent; during this time, monochloroacetic acid (MCAA) and monobromoacetic acid (MBAA) elute. Chloride elutes at the end of this region, that is, a matrix diversion window separates this first section of the gradient from the second one. Brominated acetic acids, in particular MBAA, are known to be susceptible to decomposition at higher temperature and pH. Thus, MBAA-1-13C is used for accurate determination of MBAA. MCAA-1-13C is used as an internal standard in the first section for the quantification of MCAA. In period 2, dihaloacetic acids and dalapon elute by ramping up the concentration of KOH to 18 mmol/L. The internal standard for



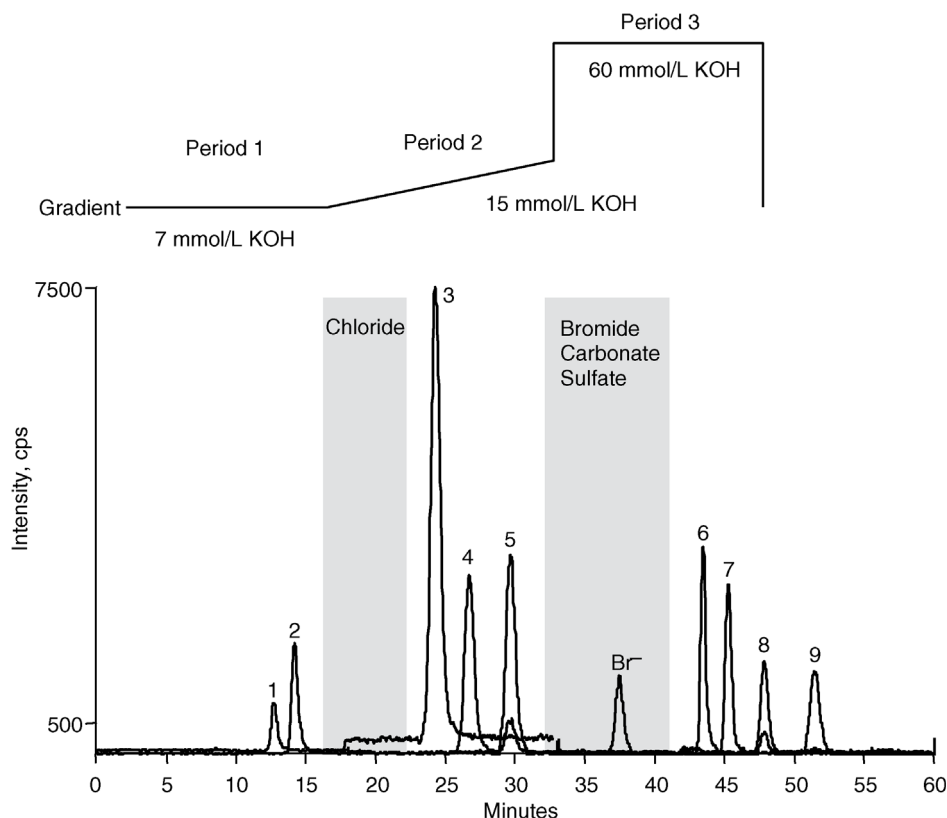


**Figure 8.105** Separation of nine haloacetic acids (HAAs) with ESI-MS/MS detection. Separator column: IonPac AS24; column dimensions: 250 mm  $\times$  2 mm i.d.; column temperature: 15  $^{\circ}$ C; eluent: KOH (EG); gradient: 7 mmol/L from 0–18 min, linearly to 18 mmol/L in 18.5 min and then to 60 mmol/L in 0.3 min; flow rate: 0.3 mL/min; detection: ESI-MS/MS in the negative MRM mode; desolvation solvent:

MeCN at 0.3 mL/min; injection volume: 100  $\mu$ L; peaks: 1  $\mu$ g/L each of monochloroacetic acid (1), monobromoacetic acid (2), dichloroacetic acid (3), monobromomonochloroacetic acid (4), dibromoacetic acid (5), trichloroacetic acid (6), monochlorodibromoacetic acid (7), monobromodichloroacetic acid (8), and tribromoacetic acid (9).

this period is DCAA-2-13C. The second section ends with the diversion of sulfate, nitrate, and bicarbonate to waste. In period 3, the concentration of KOH is ramped up to 60 mmol/L to elute the trihaloacetic acids, using TCAA-2-13C as the internal standard (not commercially available) for this section. For method simplicity, 15  $^{\circ}$ C was chosen as the column temperature as the recovery of seven of the haloacetic acids is better than 90% (relative to a column temperature of 10  $^{\circ}$ C) at this temperature level. Only MBAA and monochlorodibromoacetic acid (CDBAA) show losses at a column temperature of 15  $^{\circ}$ C.

Using IC-MS with a single quadrupole MS detector and method programming of the cone voltage, sensitivity can be optimized for each of the haloacetic

acids. This is important for minimizing the formation of undesirable fragments or adducts that can reduce sensitivity. Haloacetic acids can be detected as their pseudomolecular ions  $[M-H]^-$  or as the decarboxylated species  $[M-H-COO]^-$ . With continuous aspiration of higher HAA concentrations (e.g., 1–100  $\mu\text{mol/L}$ ), dimer ions  $[2M-H]^-$  are also observed. The relative distribution of the different species is mostly controlled by the ESI probe temperature and by the source CID voltage used. In general, decarboxylation is favored for the more heavily substituted haloacetic acids, as shown in the mass spectra in Figure 8.106. Compared to the pseudomolecular ion, the signal for the decarboxylated ion is clearly lower for dibromomonochloroacetic acid (Figure 8.106a) than for tribromoacetic acid (Figure 8.106b). Because the loss of  $\text{CO}_2$  results in a mass difference of 44 Da, which is the same as the mass difference between  $^{35}\text{Cl}$  and  $^{79}\text{Br}$  (and  $^{37}\text{Cl}$  and  $^{81}\text{Br}$ ), several haloacetic acids are detected at more than one of the  $m/z$  values.

Despite the high capacity of the IonPac AS24 anion exchanger, overloading with sample matrix may cause peak broadening and significant shifts in retention times. However, the ion-exchange capacity of 140  $\mu\text{equiv}$  for the 2 mm column format is high enough to tolerate a simulated matrix consisting of 250 mg/L sulfate and chloride, 20 mg/L nitrate, and 100 mg/L ammonium chloride. Table 8.6 shows stable peak areas and retention times, even in a high-ionic strength matrix.

Table 8.7 provides linearity in deionized water and high-ionic strength matrix for this method at optimized MRM conditions for maximum sensitivity.

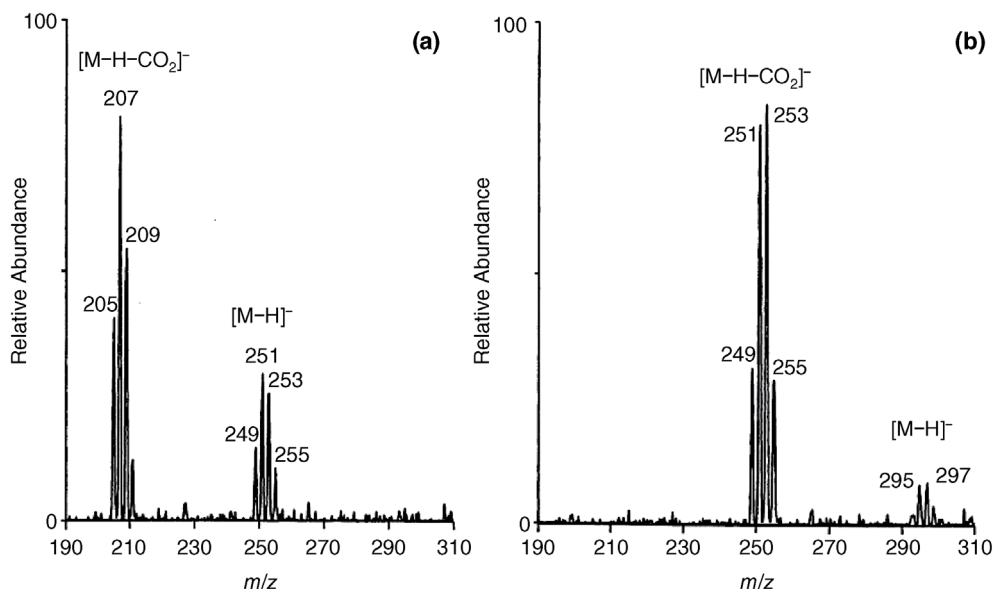


**Figure 8.106** Mass spectra of dibromomonochloroacetic acid (a) and tribromoacetic acid (b). Detection: negative ESI-MS; ESI probe temperature: 300 °C; ESI probe voltage: –2.5 kV; source CID voltage: 20 V; analytes: 1  $\mu\text{mol/L}$  each.

**Table 8.6** Retention time stabilities and recoveries for nine haloacetic acids in deionized water and simulated matrix<sup>a)</sup>.

Analyte	Concentration ( $\mu\text{g/L}$ )	Peak area $\times 10^4$ DI water $n = 7$	Peak area $\times 10^4$ matrix $n = 7$	% Recovery	Retention time (min) DI water $n = 7$	Retention time (min) matrix $n = 7$	Shift (min)
MCAA	3	11.1	11.6	104	10.56	10.48	-0.08
MBAA	2	16.0	17.2	107	11.86	11.80	-0.06
DCAA	3	126	132	105	19.26	19.28	0.02
BCAA	2	19.3	20.0	103	20.72	20.72	0.00
DBAA	1	11.6	12.0	102	23.08	23.10	0.02
TCAA	1	9.15	9.22	100	37.16	36.70	-0.46
BDCAA	2	8.96	9.13	101	40.18	40.10	-0.08
CDBAA	5	14.8	15.3	103	43.34	43.34	0.00
TBAA	10	14.8	15.5	104	47.00	47.02	0.02

a) Simulated matrix: 250 mg/L sulfate, 250 mg/L chloride, 20 mg/L nitrate, and 100 mg/L ammonium chloride.

**Table 8.7** Transitions, linearity, detection limits, and accuracy for nine haloacetic acids.

Analyte	Transition	ISTD 3 or 5 µg/L	$r^2$ 0.25–20 µg/L DIW/matrix	$r^2$ 0.25–5 µg/L matrix with NH <sub>4</sub> Cl	MDL (µg/L/% RSD) ( <i>n</i> = 7, 1 µg/L in matrix)	Accuracy (%) (at 500 ng/L) DIW/Hi matrix with NH <sub>4</sub> Cl
MCAA	92.9/34.9	MCAA-1-13C	0.0007/0.9989	0.9962	0.440/14.7	87.5/81.6
MBAA	137/78.8	MBAA-1-13C	0.9999/0.9990	0.9981	0.126/4.2	102/74
DCAA	127/82.9	DCAA-2-13C	0.9999/0.9991	0.9924	0.095/3.3	96.7/73.3
BCAA	170.8/78.8	DCAA-2-13C	0.9999/0.9992	0.9964	0.100/0.8	93.5/88.8
DBAA	214.7/170.7	DCAA-2-13C	0.9999/0.9993	0.9957	0.325/10.8	107.0/79.9
TCAA	161/116.9	TCAA-2-13C	0.9999/0.9993	0.9970	0.091/0.3	113.0/87.3
BDCAA	207/81 79/79	TCAA-2-13C	0.9991/0.9991	0.9963	0.637/18.9	105/89.0
CDBAA	207/78.8	TCAA-2-13C	0.9992/0.9994	0.9972	0.521/16.4	128/108.0
TBAA	250.75/78.8	TCAA-2-13C	0.9994/0.9998	0.9954	0.360/9.9	102/95.6

Standards in matrix were used to calculate worst-case minimum detection limits against the deionized water calibration. The high-ionic strength matrix comprised 350 mg/L chloride, 250 mg/L sulfate, 150 mg/L bicarbonate, and 30 mg/L nitrate. This chloride content includes 250 mg/L sodium chloride and 100 mg/L ammonium chloride that is typically added for sample preservation. The transition for monobromodichloroacetic acid (BDCAA) is 287/81, but the intensity for this transition is low resulting in high % RSD and MDL. Better quantification is observed by monitoring the 79/79 signal for this analyte. This method has been applied to water samples from Southwest Water Users Public Water Authority (Benton, AZ, USA). Present regulatory levels of 1 and 2 µg/L for the five most important haloacetic acids can easily be achieved (see Section 10.1) and show good correlation to data generated using EPA Method 552.2 for real-world samples.

Perchlorate has been used as an oxidant in rockets, munitions, and fireworks since the 1950s, and has been found to cause thyroid dysfunctions in humans. The conventional ion chromatographic method for the trace analysis of perchlorate based on suppressed conductivity detection (EPA Method 314.0) [254] requires the use of a large injection volume and a 4 mm high-capacity IonPac AS16 anion exchanger that allows the quantification of perchlorate down to 2 µg/L. Lower detection limits employing suppressed conductivity detection are possible only by using matrix elimination (EPA Method 314.1) or IC×IC techniques (EPA Method 314.2) (see also Section 10.1). Electrospray ionization mass spectrometry provides lower detection limits for perchlorate than suppressed conductivity detection, particularly in high-ionic strength matrices. The IC–MS method (EPA Method 332.0 [255]) uses the same separator column, substituting a microbore format, and the same instrument configuration with a diverter valve as shown in Figure 8.101. It may be used with a single quadrupole MS detector or with a tandem mass spectrometer as outlined in EPA Method 331.0 [256]. Perchlorate is separated from constituent cations and anions in the sample using a potassium hydroxide mobile phase [257]. Due to the use of a nonvolatile mobile phase, the column effluent is passed through a suppressor to exchange the potassium ions from the mobile phase and the analyte counteranions by hydronium ions prior to entering the mass spectrometer. The two predominant perchlorate anions that occur naturally at a ratio of 3086:1 are  $^{35}\text{Cl}^{16}\text{O}_4^-$  ( $m/z$  99) and  $^{37}\text{Cl}^{16}\text{O}_4^-$  ( $m/z$  101), respectively. Due to fewer mass spectral interferences, the concentration of perchlorate using  $m/z$  101 is typically reported. The  $m/z$  99/101 area count ratio and relative retention time are used for confirmation of perchlorate in samples. The sodium perchlorate internal standard is enriched with  $^{18}\text{O}$  ( $m/z$  107) for improved accuracy and ruggedness. Because the internal standard and the analyte are chemically indistinguishable, the two species exhibit the same behavior in the analytical method and are affected in the same way by chemical and instrumental variations. Two SIM channels are used in the mass spectrometer for selective detection. Selected ion monitoring (SIM) is a mass spectrometry scanning mode in which only a limited  $m/z$  range is transmitted and/or detected by the instrument, as opposed to the full spectrum range. This mode of operation typically

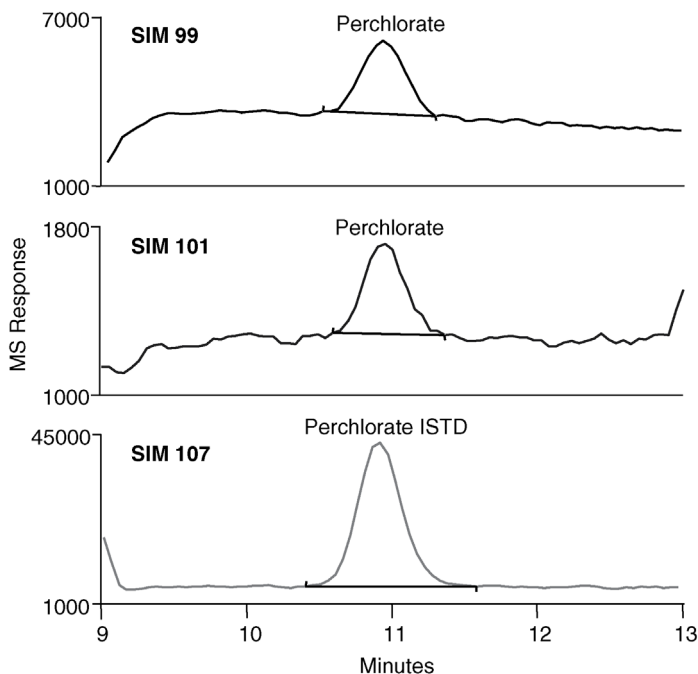


**Figure 8.107** Mass chromatograms of a high-ionic strength matrix spiked with 125 ng/L perchlorate. Separator column: IonPac AS16; column dimensions: 250 mm  $\times$  2 mm i.d.; eluent: 45 mmol/L KOH (EG); flow rate: 0.3 mL/min; detection: ESI-MS in the negative ion mode; cone voltage: 70 V; probe voltage: –3 kV; probe temperature: 450 °C; SIM channels:  $m/z$  99, 101, 107; desolvation solvent: MeCN at 0.3 mL/min; injection volume: 100  $\mu$ L; sample: perchlorate standards in 1000 mg/L each of chloride, sulfate, and bicarbonate; peaks: 125 ng/L perchlorate (1) and 1000 ng/L internal standard (1).

results in significantly increased sensitivity. Figure 8.107 shows mass chromatograms of a high-ionic strength matrix (1000 mg/L each of chloride, sulfate, and carbonate) spiked with 125 ng/L perchlorate.

As a large polarizable anion, perchlorate elutes much later than common inorganic anions such as chloride, sulfate, and bicarbonate. Separation of perchlorate from the matrix combined with the specificity of mass spectrometry has resulted in a method that minimizes interferences from drinking water matrices. However, high concentrations of other polarizable anions such as condensed phosphates, thio compounds, or aromatic sulfonates are potential chromatographic interferences, but usually elute well before perchlorate under the chromatographic conditions being used. Of all the common inorganic anions found in drinking water, sulfate can be most problematic. Although sulfate elutes well before perchlorate, large concentrations of sulfate may result in very large peaks with a tailing into the retention time of perchlorate.  $\text{H}^{32}\text{SO}_4^-$  ( $m/z$  97) and  $\text{H}^{34}\text{SO}_4^-$  ( $m/z$  99) are formed in the electrospray interface and thus can interfere

with the determination of perchlorate at  $m/z$  99. As a result, high sulfate concentrations can lead to an inability to detect the  $m/z$  99 ion or to an area count ratio  $m/z$  99/101 that does not meet the QC requirement. If either of these effects is observed, sample dilution or pretreatment to reduce/remove the sulfate is required to meet the  $m/z$  99/101 area count ratio requirement for perchlorate confirmation.

Trace-level perchlorate analysis can also be done with IC-MS/MS. Three multiple reaction monitoring (MRM) transitions are usually monitored to quantify perchlorate in drinking water samples:  $^{35}\text{Cl}^{16}\text{O}_4^- / ^{35}\text{Cl}^{16}\text{O}_3^-$  ( $m/z$  98.8/82.8),  $^{37}\text{Cl}^{16}\text{O}_4^- / ^{37}\text{Cl}^{16}\text{O}_3^-$  ( $m/z$  100.9/84.8), and  $^{35}\text{Cl}^{18}\text{O}_4^- / ^{35}\text{Cl}^{18}\text{O}_3^-$  ( $m/z$  107.0/89.0). The last transition is for the  $^{18}\text{O}$ -enriched internal standard that is used in this method. The isotopic ratio of  $^{37}\text{Cl}/^{35}\text{Cl}$  is used to further confirm the presence of perchlorate and to detect any coeluting isobaric interferences. The MDL of perchlorate in reagent water is 4 ng/L using MRM 98.8/82.8, based on a 100  $\mu\text{L}$  injection volume. Linear calibration is typically performed from the MDL up to approximately 10  $\mu\text{g}/\text{L}$ . Figure 8.108 shows the measurement of perchlorate near the detection limit at 5 ng/L. MRM is a standard technique for quantitative LC-MS/MS analysis and performs equally well in IC-MS/MS. This approach

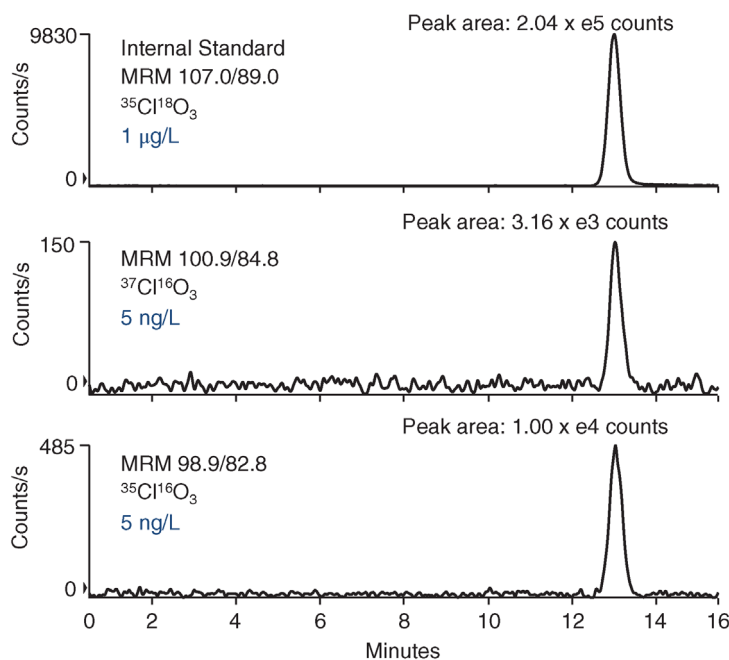


**Figure 8.108** Determination of 5 ng/L perchlorate in reagent water by IC-MS/MS with an  $^{18}\text{O}$ -enriched internal standard. Separator column: IonPac AS16; column dimensions: 250 mm  $\times$  2 mm i.d.; eluent: 45 mmol/L KOH

(EG); flow rate: 0.3 mL/min; detection: ESI-MS/MS; desolvation solvent: MeCN at 0.3 mL/min; injection volume: 100  $\mu\text{L}$ ; sample: 5 ng/L perchlorate standard in reagent water with 1  $\mu\text{g}/\text{L}$   $^{18}\text{O}$ -enriched internal standard.

has been used in many environmental applications to generate unmatched limits of detection, precision, and accuracy. Diversion of the total dissolved solids (TDS) matrix anions away from the mass spectrometer while eluting perchlorate from the IC results in robust method performance. The IC–MS/MS method has been successfully tested under high matrix conditions of 1800 mg/L each of chloride, sulfate, and bicarbonate for extended periods. The MRM lowest concentration minimum reporting limit (LCMRL) as determined by the protocol outlined in Method 332.0 is 0.0157  $\mu\text{g/L}$ .

Fast analysis of low-level perchlorate can also be done by LC–MS/MS [258]. The IonPac AS21 anion exchanger (see Section 3.4.2.5) was specifically developed for this purpose and is the specified column in US EPA Method 331.0 [256]. The resin material of the IonPac AS21 is extremely hydrophilic and, therefore, has a very high selectivity for both methylamine and hydroxide eluents. Minimum reliable quantification levels of perchlorate using this separator column are typically less than 50 ng/L. Figure 8.109 shows the determination of trace perchlorate in a drinking water sample using a 200 mmol/L methylamine mobile phase. The mass chromatograms of perchlorate at a level of 0.5  $\mu\text{g/L}$  in reagent water and high-ionic strength matrix are illustrated in Figure 8.110.

Another application of IC–MS is the direct determination of fluoroacetate (compound 1080), which is a very effective rodenticide and predacide. Fluoroacetic acid is also an intermediate metabolite of many compounds such as anti-cancer drugs 5-fluorouracil and 2-fluoroethyl nitrosourea. Because fluoroacetate

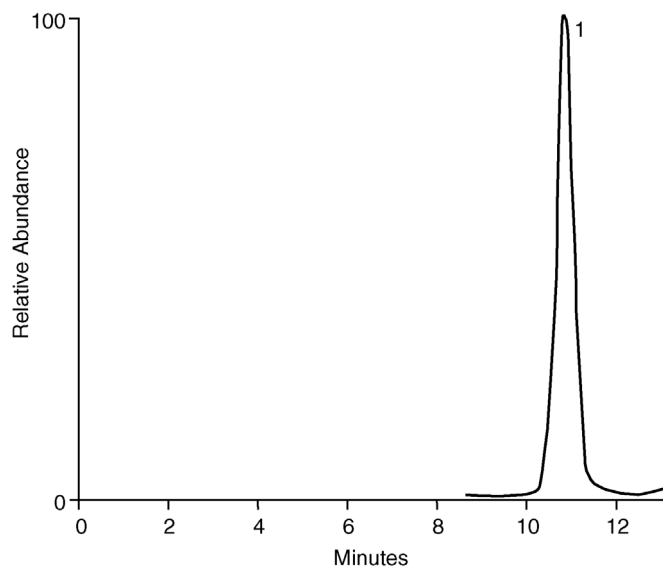


**Figure 8.109** Determination of perchlorate in drinking water by LC–MS/MS. Separator column: IonPac AS21; column dimensions: 250 mm  $\times$  2 mm i.d.; column temperature:

30  $^{\circ}\text{C}$ ; eluent: 200 mmol/L methylamine; flow rate: 0.35 mL/min; detection: ESI–MS/MS (LCQ Deca Ion Trap), transition  $m/z$  99/83; injection volume: 100  $\mu\text{L}$ ; peak: 2  $\mu\text{g/L}$  perchlorate (1).



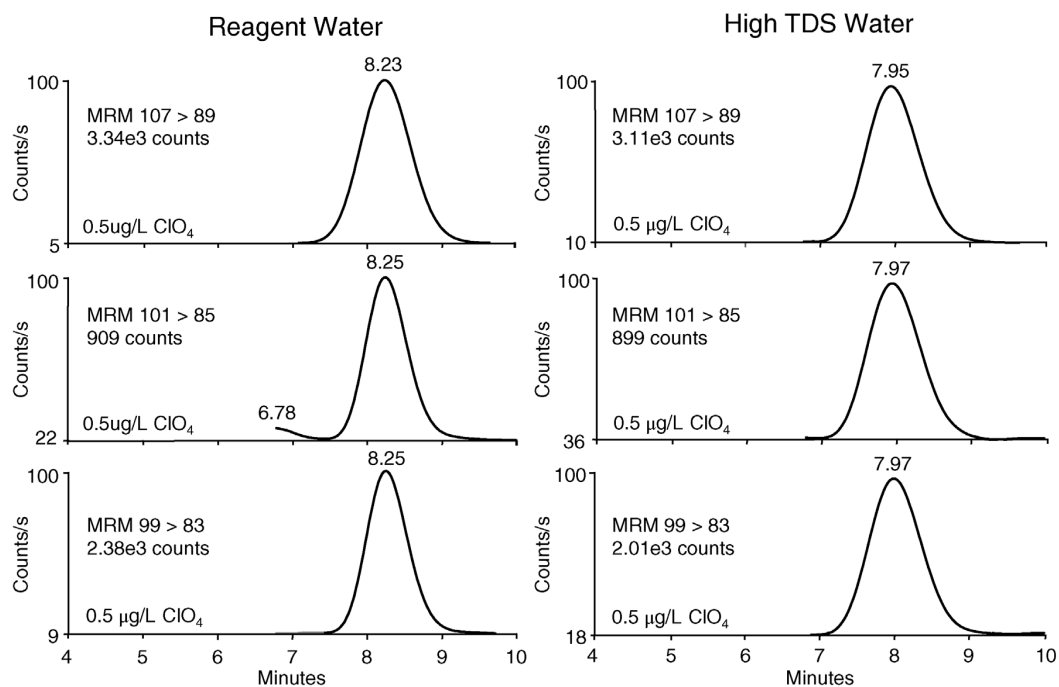
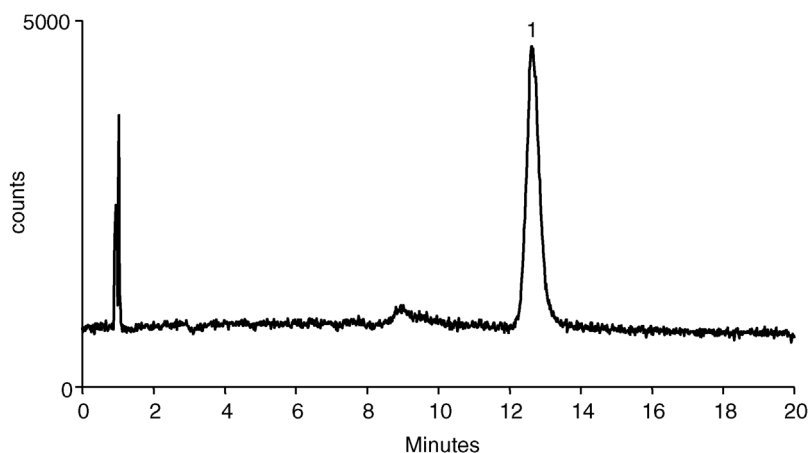


Figure 8.110 Mass chromatograms of perchlorate in reagent water and high-ionic strength matrix by LC-MS/MS using EPA Method 331.0.

is highly toxic to mammals and insects (it disrupts the Krebs cycle) [259], its use has been banned or restricted in many countries. The US EPA has placed sodium fluoroacetate in Toxicity Category I, indicating the highest degree for acute oral toxicity. Conventional methods for the analysis of fluoroacetate include GC [260] and HPLC [261]. Some of these techniques rely upon derivatization and lack adequate sensitivity for low-level detection [262]. In contrast, anion-exchange chromatography hyphenated with SIM mass spectrometry allows a reliable determination of this compound at trace level in water samples. The required RFIC–MS configuration is the same as illustrated in Figure 8.101. A flow of 0.1 mL/min of acetonitrile is added via a low-volume mixing tee prior to the MS to aid with the thermally assisted pneumatic nebulization of the ESI source. The separation of fluoroacetate is carried out on IonPac AS24 in the microbore format (Figure 8.111). Due to its high capacity, it provides sufficient retention of the target compound from anionic matrix interferences. It also allows large injection volumes and improves detection limits, especially in high-ionic strength samples. After the elution of fluoroacetate at 12.5 min under the given chromatographic conditions, the separator column is flushed with a strong eluent to remove any strongly retained anions. This improves method ruggedness when analyzing high ionic strength water samples. Under IC conditions, fluoroacetate shows a strong deprotonated molecular ion at  $m/z$  77 in negative ESI mode. Detection limits are 0.3  $\mu\text{g/L}$  for fluoroacetate in deionized water and 1.8  $\mu\text{g/L}$  in fortified water. This is better than reported results on GC analyses that require ethylation and solid-phase microextraction, yet only achieve a 1  $\mu\text{g/L}$  detection limit in deionized



**Figure 8.111** SIM chromatogram of a fluoroacetate ( $m/z$  77) standard in deionized water. Separator column: IonPac AS24; column dimensions: 250 mm  $\times$  2 mm i.d.; column temperature: 15  $^{\circ}\text{C}$ ; eluent: 5 mmol/L KOH (EG) for 10 min; flow rate: 0.25 mL/min; detection: ESI–MS; probe temperature: 450  $^{\circ}\text{C}$ ; needle voltage: 2 kV; cone voltage: 45 V; desolvation solvent: MeCN at 0.1 mL/min; injection volume: 100  $\mu\text{L}$ ; sample: 2  $\mu\text{g/L}$  fluoroacetate standard (1) in deionized water.

water and a 10 µg/L limit in more complex samples such as blood and plasma matrices.

Low-molecular weight organic acids in the marine environment play important roles in adjusting pH, forming a variety of complexes, and increasing the solubility of trace metals in seawater. In light of the significant growth in aquaculture for farmed fish and shellfish, several feed additives – including acidifiers consisting of organic acids and their salts – may provide promising alternatives to the use of in-feed antibiotics in aquaculture. Previously, organic acid analyses in aqueous matrices were carried out using gas chromatography methods with derivatization, which allow fisheries to monitor the water environment and control its impact on the health of the fish. However, direct analysis of organic acids at trace level by IC–MS provides a faster, more direct approach that does not require sample pretreatment. An IC×IC–MS method has been developed that allows low levels of short-chain organic acids (C1–C5) to be analyzed in a high-ionic strength matrix. The first channel of the system separates the low-level analytes from the seawater matrix, while the second channel resolves each of the target analytes. By connecting the second channel separator column to a mass spectrometer, the identity of the target analytes can be confirmed and low-level detection limits be achieved for a sensitive and selective assay. Figure 8.112 illustrates the schematic of such IC×IC–MS system that requires two diverter valves, one enabling the IC×IC setup to operate and the other one to direct

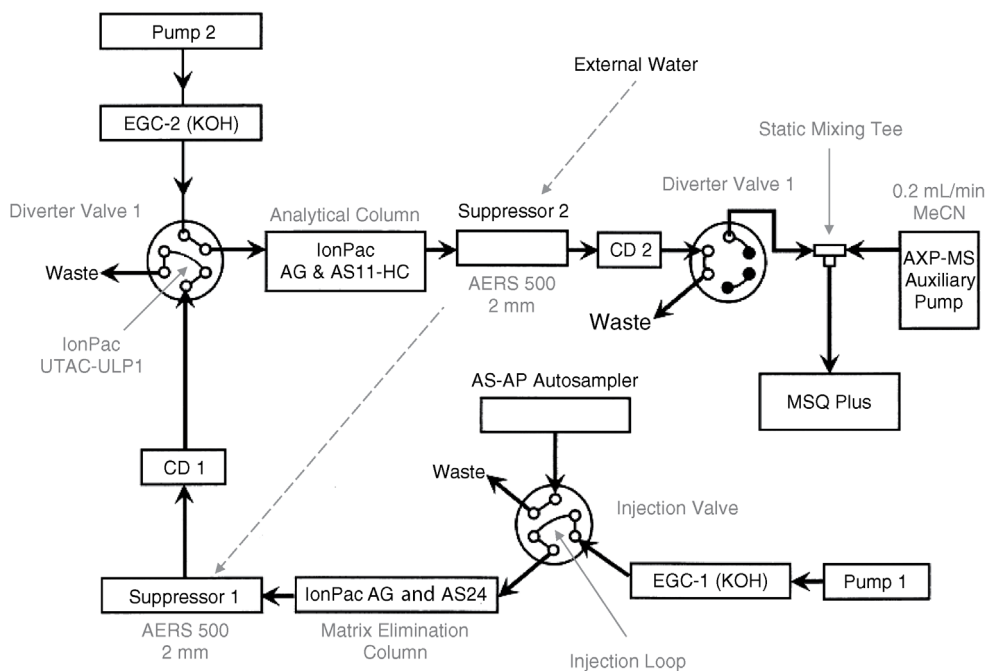
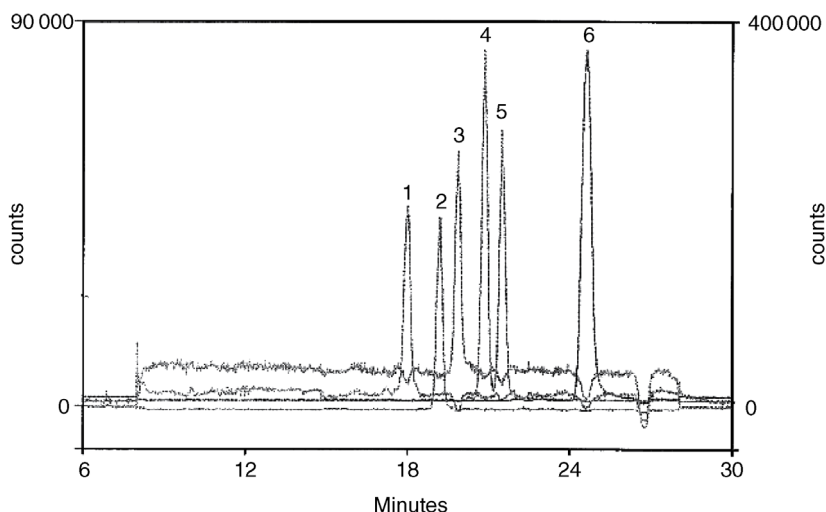


Figure 8.112 Schematic diagram of a reagent-free IC×IC–MS system.

unwanted components away from the mass spectrometer. Both diverter valves are positioned behind the respective conductivity detectors. A flow of 0.4 mL/min of acetonitrile is added via a low-volume mixing tee prior to the MS to aid with the thermally assisted pneumatic nebulization of the ESI source.

The seawater matrix necessitates the use of an IC  $\times$  IC setup. In the first channel, the IonPac AS24 anion exchanger weakly retains the organic acids, but retains the inorganic anions much more strongly. Thus, the early eluting organic acids can be trapped onto an IonPac UTAC-ULP1 concentrator column. The Diverter Valve 1 in Figure 8.112 controls the flow to this concentrator column, allowing the trapping from the IonPac AS24 column initially and then connecting the concentrator column to the IonPac AS11-HC column flow path at a later stage for the separation of just the organic acids. With the help of the second Diverter Valve 2, the analytes eluting from IonPac AS11-HC are directed to the mass spectrometer for detection, while all other matrix ions are directed to waste to avoid contamination of the electrospray interface. The two IC channels can be plumbed in the way that while one column is used for analyte separation, the other column is being cleaned and equilibrated for the next sample. After the analytes are eluted off the IonPac AS24 column and the Diverter Valve 1 changes position to connect this column directly to waste, other inorganic anions are quickly washed off with a high eluent concentration. Eluent concentration is then decreased to starting conditions, allowing the column to equilibrate while completing the organic acid analysis on the IonPac AS11-HC column. Likewise, while IonPac AS11-HC is equilibrating for the next sample, IonPac AS24 will be loading the concentrator column. By overlapping functionality in this way, the total run time for multiple samples is significantly reduced. Because all of the small-molecular weight organic acids ionize easily in the ESI source, optimization of the ionization parameters is straightforward with respect to cone voltage, needle voltage, and probe temperature. Selectivity for the organic acids, including acetate, propionate, formate, butyrate, pyruvate, and valerate, is established through the use of SIM scans on the pseudomolecular ion  $[M-H]^-$ , as illustrated in Figure 8.113. When combined with the respective retention times, verification of the analytes is ensured. Method detection limits for propionate, butyrate, pyruvate, and valerate can be estimated through standard deviation of nine replicate injections of a 20  $\mu\text{g/L}$  standard to be 8  $\mu\text{g/L}$ . MDLs for acetate and formate are based on the minimum level needed to achieve a  $S/N \geq 3$  (see Table 8.8).

**Chemical and Agrochemical Applications** Mohsin [263] developed an IC–MS method using thermospray and electrospray interfaces for the analysis of organophosphorus and organosulfur compounds in an insecticide such as monomethyl phosphate, monomethyl sulfate, and dimethyl phosphate. All three compounds were separated on an IonPac AS11 anion exchanger using a NaOH/methanol mixture as an eluent. Mohsin used an Alltech 1000HP suppressor to convert the eluent to water prior to entering the MS interface. The Alltech 1000HP suppressor contains two packed-bed suppressor columns. One of the



**Figure 8.113** SIM traces for six low-molecular weight organic acids in synthetic seawater from MS Peaks: (1) acetate, (2) propionate, (3) formate, (4) butyrate, (5) pyruvate, and (6) valerate.

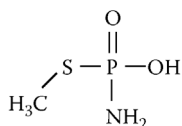
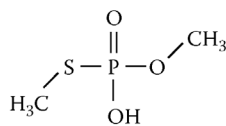
suppressor columns is used for suppression, while the other one is electrochemically regenerated at the same time. The suppressor effluent is split 99:1 and mixed with acetonitrile/water (90:10 v/v) containing 0.5% ammonium hydroxide. Detection is carried out in the negative ion mode. Ammonium hydroxide increases the pH of the mobile phase entering the electrospray interface and thus supports negative ion formation. The two compounds monomethyl phosphate and monomethyl sulfate, identified in the insecticide by electrospray MS, exhibit the same mass-to-charge ratio of  $m/z$  111 but differ in their mass spectra due to differences in the fragmentation and isotope distribution of the  $[M-H]^-$  ions.

In a subsequent publication, Mohsin [264] applied ion chromatography coupled to electrospray mass spectrometry for the separation and structure elucidation of anionic compounds in a complex organophosphate matrix. CID was used to fragment molecular ions for obtaining mass spectral information. With a maximum voltage difference between entrance cone and skimmer of 200 V, the

**Table 8.8** Linearity, minimum detection limits, and recovery for organic acid analysis in synthetic seawater by IC-MS.

Analyte	Linearity $r^2$	MDL ( $\mu\text{g/L}$ )	% Recovery 100 $\mu\text{g/L}$	% Recovery 1 mg/L
Acetate	0.999 93	100	—	88
Formate	0.999 95	200	—	103
Propionate	0.999 91	15.5	102	99
Butyrate	0.999 98	7.8	90	96
Pyruvate	0.999 91	5.6	105	107
Valerate	0.999 87	3.8	93	108

degree of fragmentation of the  $[M-H]^-$  ions can be controlled. Mohsin clearly identified monomethyl sulfate and monomethyl phosphate that have the same  $m/z$  111, yet their mass spectra are different. The mass spectrum of monomethyl sulfate shows the typical isotopic cluster resulting from the presence of sulfur in this compound, while the isotopic cluster of monomethyl phosphate is consistent with lack of sulfur in this compound. Mohsin could identify two other compounds in the sample, *S*-methyl phosphoramidothioate and *O,S*-dimethyl phosphorothioate.

*S*-methyl phosphoramidothioate*O,S*-dimethyl phosphorothioate

A widely used herbicide for both terrestrial and aquatic weeds is endothall (see Section 10.1). Human exposure in excess of the maximum contamination level (MCL) may cause gastrointestinal problems. Endothall is regulated by the US EPA with an MCL of 0.1 mg/L for drinking water. The current analytical method for quantitation of endothall in water samples is described in EPA Method 548.1 [265] as gas chromatography with either flame ionization or mass spectrometric detection. This method involves ion-exchange solid-phase extraction, sample enrichment, and dimethylester derivatization, followed by a 20 min GC separation with FID or MS detection. In contrast, IC-MS allows the direct analysis of trace-level endothall without labor-intensive sample preparation. Because endothall is a dicarboxylic acid, ion chromatography is the preferred separation technique. Major interferences are inorganic matrix ions such as chloride and sulfate, and other ionizable organic compounds at high concentrations. Several high-capacity anion exchangers such as IonPac AS16, AS19, and AS20 were evaluated for their selectivity. IonPac AS16 exhibits the best performance for providing a wide elution window for endothall between chloride and sulfate. It also provides substantially less chromatographic run time in comparison to IonPac AS19. A TSQ Quantum Access triple quadrupole mass spectrometer was used in this study for sensitivity and selectivity, which allows minimum sample preparation. A matrix diverter valve was used to divert high concentrations of inorganic anions to waste to prevent entrance cone fouling and to maintain long-term system stability. As seen in Figure 8.114, two different water samples, Lake Tahoe water and highly salty lake water ( $\approx 1000$  mg/L sulfate, estimated by suppressed conductivity detection), were spiked with 5  $\mu\text{g/L}$  endothall and analyzed by this method. The quantitation of endothall was carried out in SRM mode, the precursor ion was observed as the deprotonated molecular ion  $[M-H]^-$  at  $m/z$  185, and the predominant product ion was observed as  $[M-H-\text{CO}_2]^-$  at  $m/z$  141, and used as the quantitative SRM transition. Isotope labeled glutaric acid- $\text{d}_6$  was used as the internal standard due to its similarity in chemical structure and chromatographic retention to endothall. Method performance

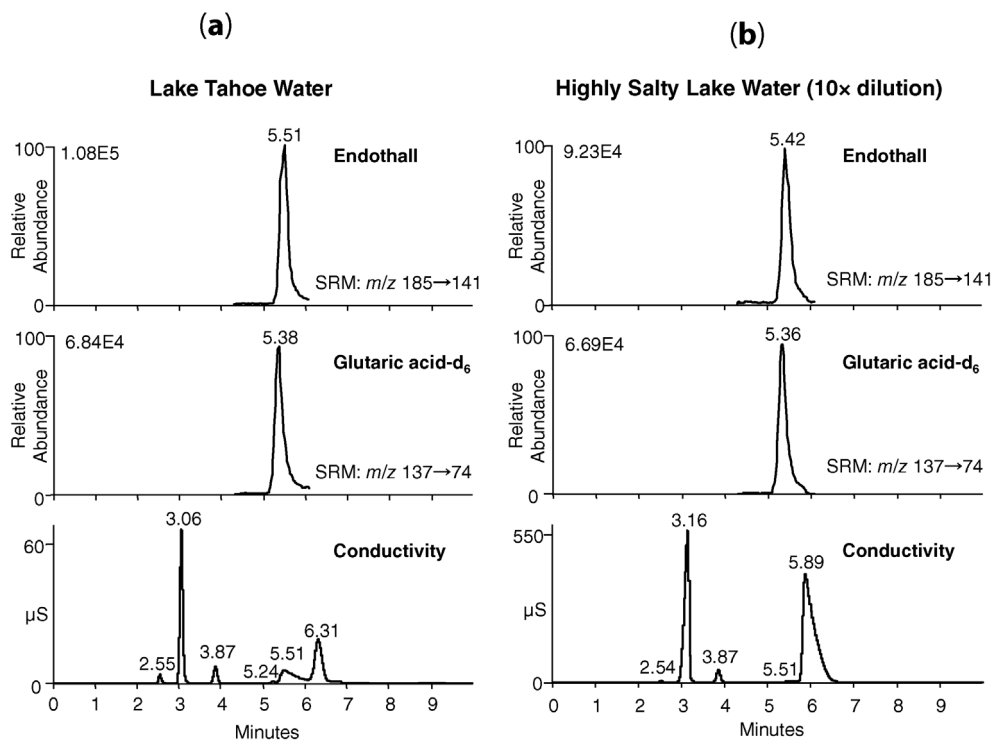


**Figure 8.114** Suppressed conductivity and SRM chromatograms of endothall spiked into different water samples. Separator column: IonPac AS16 with guard; column dimensions: 250 mm  $\times$  2 mm i.d.; column temperature: 30 °C; eluent: KOH (EG); gradient: 15 mmol/L for 0–15 min, 15–80 mmol/L for 5–6 min, and then 80 mmol/L for 6–9 min; flow rate: 400  $\mu$ L/min; detection: suppressed conductivity and MS (TSQ Quantum Access triple quadrupole);

ESI source: negative ionization mode; source voltage: 3 kV; needle temperature: 350 °C; collision gas: argon; collision gas pressure: 1.5 mTorr; operating mode: SRM (185 → 41) and (185 → 123) for endothall and SRM (137 → 74) for glutamic acid-d<sub>6</sub>; samples: 5  $\mu$ g/L of endothall spiked into Lake Tahoe water (a) and 50  $\mu$ g/L endothall spiked into salty lake water with 10-fold dilution (b).

was evaluated against quality parameters such as linearity, reproducibility, precision, accuracy, detection limits, and recovery, as outlined in the respective application note [266]. The method detection limit was calculated following the equation  $MDL = s \times t$ , where  $s$  is the standard deviation and  $t$  is the Student's  $t$  at 99% confidence interval. The calculated MDL is 0.56  $\mu$ g/L in deionized water ( $n = 7$ ).

The most commonly used agricultural pesticide is glyphosate [*N*-(phosphonomethyl)glycine], which controls woody and herbaceous weeds in forestry, cropped, and noncropped sites. Although the bacteria in soil break down glyphosate into aminomethylphosphonic acid (AMPA), wastewater discharge and drinking water samples in the United States and in Europe have tested positive for glyphosate. In 2006, the US EPA set the maximum contaminant level (MCL)

for glyphosate at 0.7 µg/L. Long-term exposure at levels above the MCL may cause kidney damage and reproductive defects in human biological systems. The standard liquid chromatographic method for quantitation of glyphosate is cation-exchange chromatography under isocratic conditions at elevated temperature, followed by analyte oxidation with calcium hypochlorite. The reaction product – glycine – is then derivatized with *o*-phthaldialdehyde/2-mercaptoethanol to incorporate a fluorophore, which can be detected with a fluorescence detector (excitation wavelength: 340 nm; emission wavelength >455 nm). US EPA Method 547 describes this procedure in more detail [267] and specifies glyphosate in reagent water of 6 and 9 µg/L in groundwater. Using ion chromatography to quantitate glyphosate and AMPA accurately at this level without sample preparation requires the use of a mass spectrometer. However, the ion sources of such instruments can be subject to fouling from routine analysis of high-ionic strength samples. The use of a heart-cutting technique significantly reduces the introduction of matrix ions to the mass spectrometer, while increasing method robustness in challenging sample matrices. In the IC–MS/MS method, the first chromatographic channel separates matrix ions from glyphosate and AMPA using a high-capacity IonPac AS19 column. Both analytes are heart-cut and trapped onto a concentrator column, which is backflushed onto an IonPac AS21 column, the second analytical column in the second chromatographic channel. This second low-capacity column significantly improves the peak shapes of glyphosate and AMPA, and reduces the introduction of matrix ions into the mass spectrometer. Figure 8.115 shows the data collected from the conductivity detectors in both channels, which reveal that low-level quantitation of both compounds by suppressed conductivity is not possible due to the high-ionic strength matrix. In both channels, separation of all compounds occurred in 30 min. For final quantitation, samples were run in SRM mode on the TSQ Quantum Access triple quadrupole mass spectrometer. SRM 110 → 63 and 110 → 79 transitions were used to quantitate AMPA, whereas SRM 168 → 150 and 168 → 79 transitions were used for the quantitation of glyphosate. Minimum detection limits for glyphosate and AMPA in matrix (250 mg/L chloride and sulfate, 150 mg/L bicarbonate, and 20 mg/L nitrate) were calculated to be 0.31 µg/L for AMPA and 0.25 µg/L for glyphosate. The TIC trace of 5 µg/L glyphosate and AMPA spiked into the high-ionic strength matrix as well as the SRM for AMPA (110 → 79) and glyphosate (168 → 150) are illustrated in Figure 8.116. These data show the recoveries of 97.2% for AMPA and 82.1% for glyphosate.

IC–MS has also been applied for the characterization of ionic liquids (IL) and for the investigation of their long-term stability under process-like conditions. The term “ionic liquid” commonly refers to a class of molten salts that are by definition liquid below 100 °C. They usually consist of bulky organic cations such as alkylated imidazole, pyrrole, or pyridine derivatives, or quaternized alkyl amines and alkyl phosphines. Common counterions are halides, alkyl sulfates, fluorinated hydrocarbons, carboxylic acids, or amino acids [268]. The physical and chemical properties of ILs are customizable by different cation–anion combinations and by the length of the alkyl chain of the cation. Depending on the



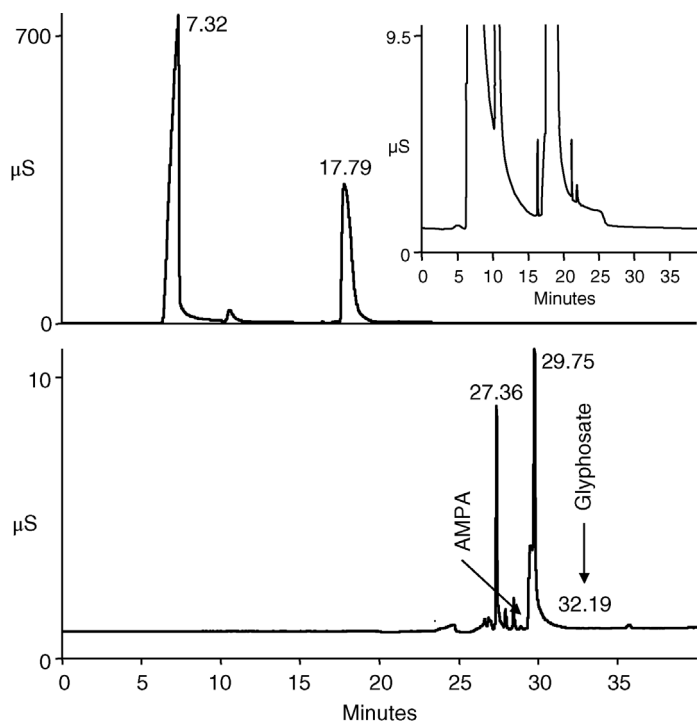


**Figure 8.115** IC  $\times$  IC separation of glyphosate and AMPA with suppressed conductivity detection. Channel 1: separator column: IonPac AS19; column dimensions: 250 mm  $\times$  2 mm i.d.; column temperature: 30  $^{\circ}$ C; eluent: KOH (EG); gradient: 8 mmol/L for 0–12 min, 8–40 mmol/L for 12–16 min, and then 40 mmol/L for 16–21 min; flow rate: 300  $\mu$ L/min; detection: suppressed conductivity; injection volume: 200  $\mu$ L; channel 2: separator

column: IonPac AS21; column dimensions: 250 mm  $\times$  2 mm i.d.; column temperature: 35  $^{\circ}$ C; eluent: KOH (EG); gradient: 1 mmol/L for 0–20 min, 1–40 mmol/L for 20–30 min, and then 40 mmol/L for 30–35 min; flow rate: 300  $\mu$ L/min; detection: suppressed conductivity; sample: 5  $\mu$ g/L glyphosate and AMPA spiked into high-ionic strength matrix consisting of 250 mg/L chloride and sulfate, 150 mg/L bicarbonate, and 20 mg/L nitrate.

chosen combination, hydrophobicity, solubility, acidity, and other properties can be adapted according to the specific task, which is the reason why ILs are known as tailor-made fluids [269]. Ionic liquids have unique properties, including extremely low vapor pressure, excellent thermal stability, electrical conductivity, and high polarity. Due to these outstanding and versatile properties, a wide range of applications using ILs have been reported in many areas such as catalysis, organic chemistry, and electrochemistry. However, production monitoring of ionic liquids and process control during their use necessitate efficient analysis of the qualitative and quantitative composition of ionic liquids in complex reaction systems. Considering the charge of the anions and cations in ionic liquids, ion chromatography with suppressed conductivity detection is a suitable analytical method for separating these complex electrolyte systems. König *et al.* were able

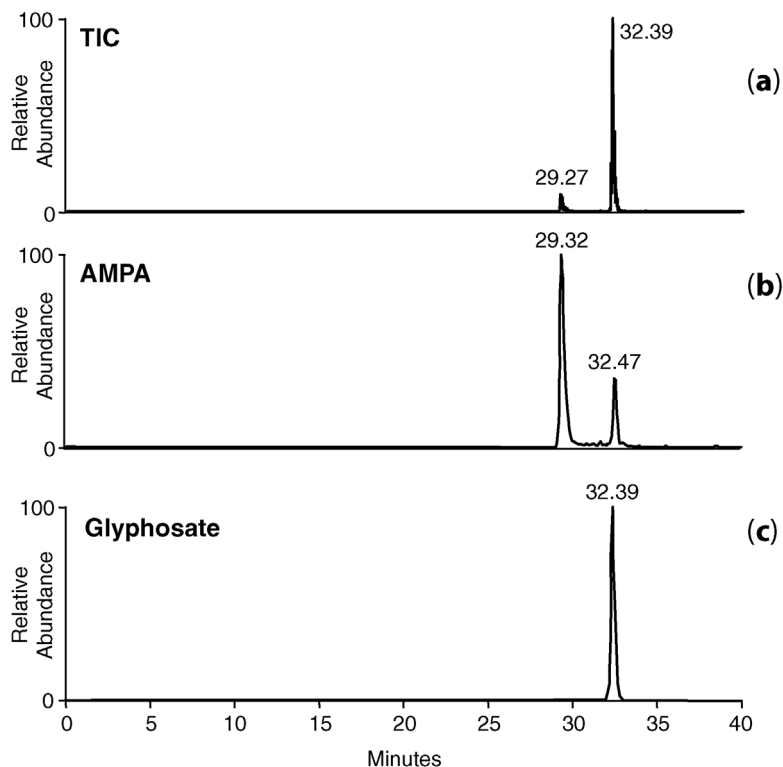


**Figure 8.116** TIC of glyphosate and AMPA with IC  $\times$  IC-MS/MS detection (a), SRM for AMPA (110  $\rightarrow$  79) (b), and SRM for glyphosate (168  $\rightarrow$  150) (c). MS: TSQ Quantum Access triple quadrupole; ESI source: negative ionization mode; source voltage: 3 kV; needle temperature: 400 °C; collision gas pressure: 1.5 bar.

to show this in their investigations of homologous imidazolium derivatives [270] and anion analysis in ionic liquids [271].

Little information is available for ensuring the quality of ILs, especially for catalysis and pharmaceutical or electrochemical applications. Impurities in an ionic liquid can change its physicochemical properties, reduce catalytic efficiency, or cause other adverse effects due to the toxicity of some ionic liquids. Exposure to elevated temperatures, pressure, friction, or electrochemical stress over a long period of time renders ILs prone to decompose. Consequently, decomposition of ILs has been studied and reported, mainly focusing on thermal or electrochemical stability. Both LC-MS and IC-MS methods have been developed for the characterization of ionic liquids. The LC-MS method benefits from Acclaim Trinity P1 (see Section 6.7.2), a mixed-mode column able to separate cationic, anionic, and neutral species in a single run [272]. This approach suits qualitative, confirmative, and semiquantitative applications. The IC-MS method applies an ion-exchange separation and provides detailed anionic profiles including anionic ILs, counterions, and impurities [273]. This second approach can be

used for quality assurance, impurity analysis, and trace-level residue analysis. Using the LC–MS approach on Acclaim Trinity P1, the chromatographic behavior of the analytes is affected by eluent strength (percentage of organic solvent and buffer concentration), eluent pH, and column temperature. Chromatographic conditions can be optimized to simultaneously separate organic cations such as imidazolium and lidocaine species, inorganic cations, inorganic anions, and organic anions. As shown in Figure 8.117, 13 different analytes were eluted in groups from an Acclaim Trinity P1 column following this elution order. When used in a confirmative analysis mode, this LC–MS method can detect submicrogram/Liter levels of major ionic liquid analytes (lidocaine, 1-butyl-3-methylimidazolium, 1-ethyl-3-methylimidazolium, hexafluorophosphate, and docusate), submilligram/Liter levels of halide impurities (chloride, bromide, and iodide), and microgram/Liter levels of cationic counterions (sodium and potassium). However, analytes are eluted in a mobile phase of higher ionic strength

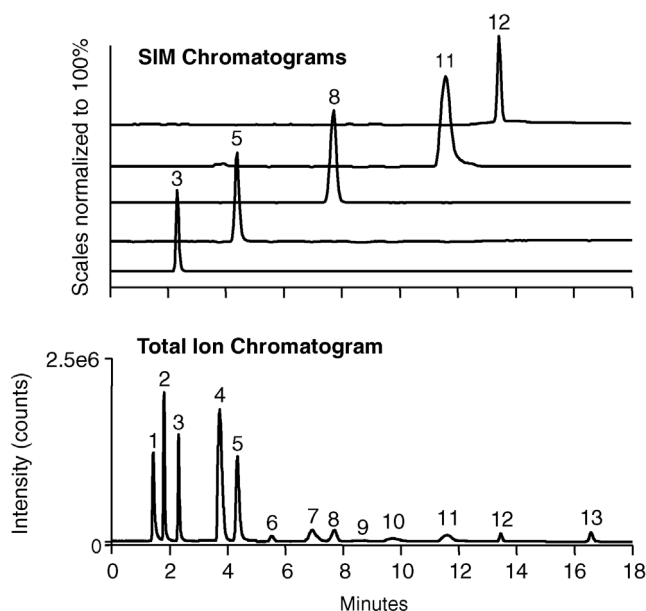


**Figure 8.117** LC–MS for simultaneous analysis of ionic liquids, counterions, and impurities. Separator column: Acclaim Trinity P1, 3  $\mu\text{m}$ ; column dimensions: 100 mm  $\times$  2.1 mm i.d.; eluent: MeCN/5 mmol/L  $\text{NH}_4\text{OAc}$ , pH 5.2; gradient: 55% MeCN (v/v) for 0–2 min, to 60% (v/v) in 8 min, and then to 90% (v/v) in 1 min and isocratic for 7 min; flow rate: 0.4 mL/min; detection: MS (Thermo Scientific MSQ Plus); source voltage: 1 kV; needle temperature: 500  $^\circ\text{C}$ ; nebulizer gas pressure: 85 psi; scan

mode: SIM; injection volume: 5  $\mu\text{L}$ ; peaks: (1) lidocaine  $m/z$  235, (2) 1-butyl-3-methylimidazolium  $m/z$  139, (3) 1-ethyl-3-methylimidazolium  $m/z$  111, (4) sodium  $m/z$  269 ( $\text{Na} + 6 \text{ MeCN}$ ), (5) potassium  $m/z$  39, (6) methanesulfonate  $m/z$  95, (7) tetrafluoroborate  $m/z$  87, (8) hexafluorophosphate  $m/z$  145, (9) chloride  $m/z$  35, (10) bromide  $m/z$  81, (11) iodide  $m/z$  127, (12) tosylate  $m/z$  171, and (13) docusate  $m/z$  421.

( $c = 5$  mmol/L ammonium acetate), that is, analytes are detected with less efficacy in comparison to IC–MS.

The IC–MS approach provides better sensitivity, because the hydroxide eluent used for the separation of anions is converted into water in the suppressor system prior to entering the MS detector. This keeps the electrospray current at a very low level and thus analytes can be detected very efficiently. Chromatographic separation of anionic ILs, anionic counterions, and anionic impurities is achieved on the hydroxide-selective IonPac AS20 anion exchanger, applying a 30 min multistep gradient to separate 17 anionic analytes as shown in Figure 8.118. MDLs are at low microgram/Liter levels for all analytes, ranging from 1.04  $\mu\text{g/L}$  for tosylate to 6.13  $\mu\text{g/L}$  for sulfate. The detection limits using the IC–MS method are significantly lower than the MDLs using the LC–MS method with Acclaim Trinity P1, making IC–MS the preferred method for low-level quantitation.

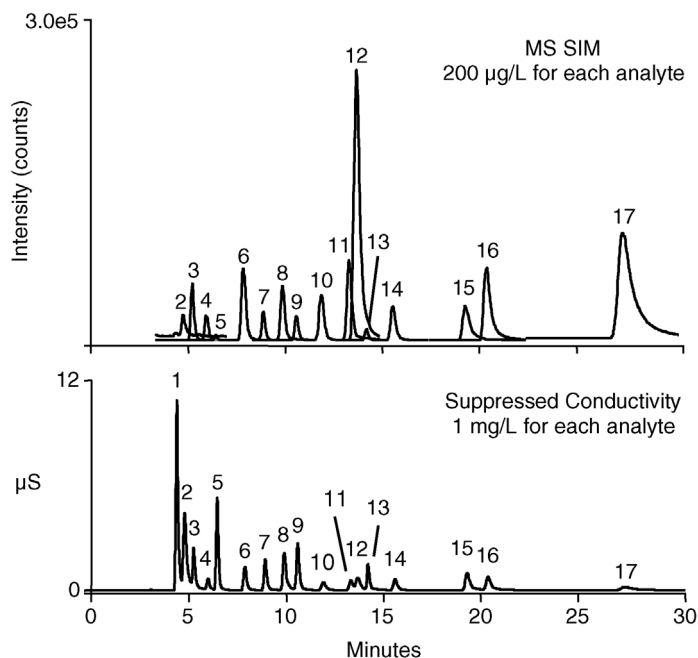
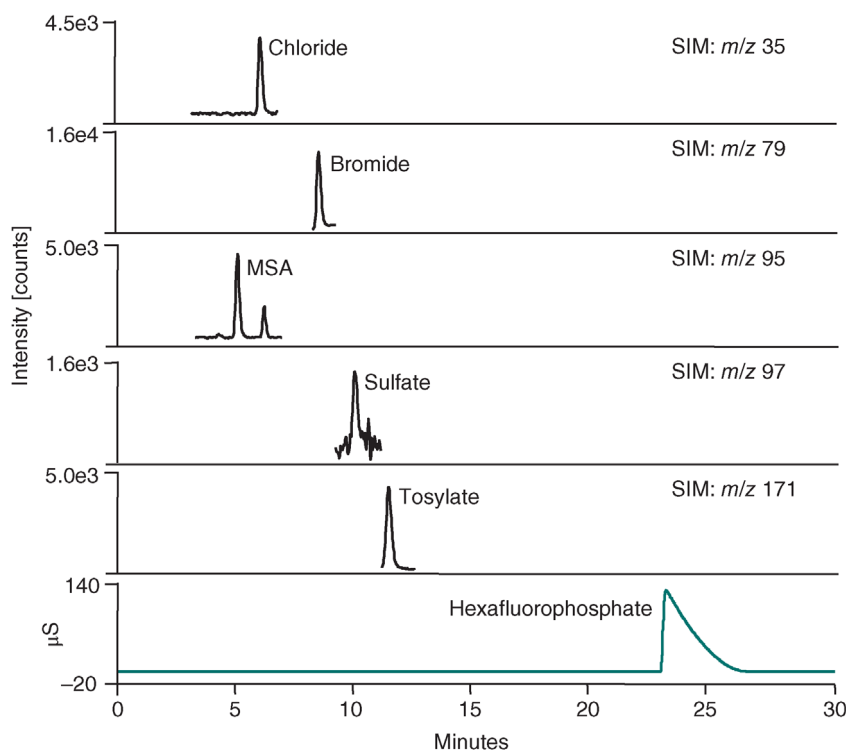


**Figure 8.118** Suppressed conductivity and MS SIM chromatograms for ionic liquids and anions. Separator column: IonPac AS20; column dimensions: 250 mm  $\times$  2 mm i.d.; column temperature: 35  $^{\circ}\text{C}$ ; eluent: KOH (EG); gradient: 10 mmol/L from 0 to 6 min, 30 mmol/L from 6 to 14 min, 60 mmol/L from 14 to 16 min, and 100 mmol/L from 16 to 30 min; flow rate: 0.25 mL/min; detection: MS (Thermo Scientific MSQ Plus); source voltage: 1 kV; needle temperature: 500  $^{\circ}\text{C}$ ; nebulizer gas pressure: 85 psi;

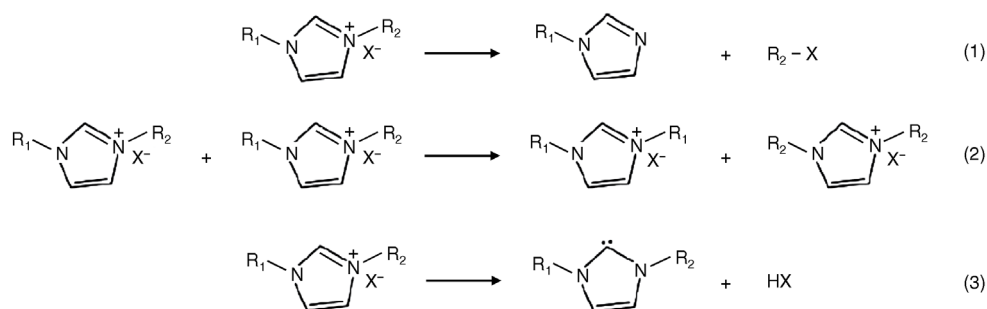
scan mode: SIM; injection volume: 20  $\mu\text{L}$ ; peaks: (1) fluoride  $m/z$  39.2, (2) acetate  $m/z$  59.1, (3) methanesulfonate  $m/z$  95.0, (4) butanesulfonate  $m/z$  137.2, (5) chloride  $m/z$  35.0, (6) trifluoroacetate  $m/z$  113.1, (7) bromide  $m/z$  78.9, (8) nitrate  $m/z$  62.0, (9) sulfate  $m/z$  97.1, (10) tosylate  $m/z$  171.0, (11) tetraborate  $m/z$  87.0, (12) triflate  $m/z$  149.1, (13) orthophosphate  $m/z$  97.1, (14) iodide  $m/z$  127.0, (15) thiocyanate  $m/z$  58.0, (16) perchlorate  $m/z$  99.0, and (17) hexafluorophosphate  $m/z$  145.1.

The two methods described here can be used for the analysis of commercially available ionic liquids. After a simple dilution with deionized water at 2 mg/mL, samples can be injected directly for IC–MS analysis. For LC–MS analysis, the standard solution has first to be diluted to 1  $\mu\text{mol/L}$ . As an example, Figure 8.119 shows the suppressed conductivity and the MS SIM traces of 1-butyl-3-methylimidazolium/ $\text{PF}_6$  and detected anionic impurities. Chloride and bromide were observed as the major impurities

König *et al.* [274] investigated the long-term stability of two selected ILs over several months under process-like conditions with a subsequent IC–MS analysis to identify the resulting decomposition products. As an example, samples of the imidazolium-based ILs 1-ethyl-3-methylimidazolium chloride (EMIM Cl) and 1-ethyl-3-methylimidazolium acetate (EMIM Ac) were thermally and catalytically stressed. The most obvious decomposition of a dialkylimidazolium cation is the reverse reaction of the quaternization reaction. The typical products are imidazole derivatives and alkylated anions (reaction (1) in Figure 8.120). Further considerable decomposition products are cations with scrambled alkyl chains. These cations can be formed either due to a realkylation of a previously dealkylated



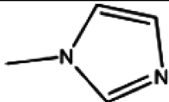
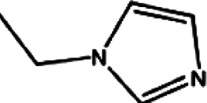
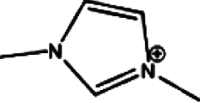
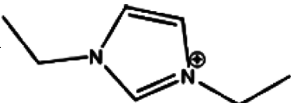
**Figure 8.119** MS SIM chromatograms of hexafluorophosphate and anionic impurities in a commercially available ionic liquid (1-butyl-3-methylimidazolium/ $\text{PF}_6$ ). Chromatographic conditions: see Figure 8.118; sample: 2 mg/mL ionic liquid.



**Figure 8.120** Decomposition mechanisms of dialkylimidazolium cations (see also [273]).

cation with an anion, which carries an alkyl chain of the same type, or by a direct exchange of the alkyl chains of two cations (reaction (2) in Figure 8.120). The resulting components are charged, and together with the initial anion, again ILs. Naturally, these decomposition species are nonvolatile. Another decomposition variation of imidazolium-derived cations, which is quite intensely discussed, is the deprotonation of the C2-atom of the fused ring by strong nucleophiles. The resulting carbenes are reactive components that react either with other IL cations (reaction (3) in Figure 8.120) or any dissolved decomposition products present in the liquid phase [273]. In summary, decomposition products of ILs can be volatile or not, uncharged or charged, and fragments or higher structures compared to the original species. Table 8.9 summarizes selected decomposition

**Table 8.9** Selected decomposition products identified in long-term thermally stressed 1-ethyl-3-methylimidazolium ionic liquids [273].

Component	Structure	<i>m/z</i>	
<i>N</i> -Methylimidazole	MIM 	83	$[M + H]^+$
<i>N</i> -Ethylimidazole	EIM 	97	$[M + H]^+$
1,3-Dimethylimidazolium	MMIM <sup>+</sup> 	97	$[M]^+$
1,3-Diethylimidazolium	MMIM <sup>+</sup> 	125	$[M]^+$

products that König *et al.* identified in long-term thermally stressed 1-ethyl-3-methylimidazolium ionic liquids.

**Pharmaceutical Applications** The quantitative analysis of bisphosphonates and excipients is taken as an example for the application of IC–MS in the pharmaceutical industry. Bisphosphonates are a group of compounds that are used as active pharmaceutical ingredients to treat bone disorders including osteoporosis, Paget's disease, and hypercalcemia [275]. Separation methods for bisphosphonate analysis include liquid chromatography with derivatization and/or ion pair reagents, ion chromatography, capillary electrophoresis (CE), and gas chromatography with derivatization, summarized in a review article by Zacharis and Tzanavaras [276]. This review concluded that for quality control analyses of bisphosphonates, ion chromatography with suppressed conductivity detection is a suitable solution because of its simplicity, avoidance of derivatization steps, adequate sensitivity, and simultaneous analysis of ionic impurities. The authors also indicated that mass spectrometry would be a sensitive approach, but the application to bisphosphonate analysis is limited due to the incompatibility of ion-pair reagents used in the mobile phase for LC separations.

Direct analysis of bisphosphonates and excipients in pharmaceuticals can be carried out using capillary ion chromatography with suppressed conductivity and mass spectrometric detection. The target analytes can be separated with high resolution on an IonPac AS18-Fast capillary anion exchanger. Due to the elimination of derivatization steps, the workflow is simplified and the sample throughput is improved. The detection by suppressed conductivity provides sufficient sensitivity for QC analysis, while MS offers additional selectivity and sensitivity for bisphosphonates in complex matrices such as biological fluids. Capillary IC offers improved sensitivity when coupled with a capillary electrospray interface to a mass spectrometric detector [277]. The IonPac AS18-Fast anion exchanger in the capillary format was selected for its excellent resolution for the three targeted bisphosphonates (clodronate, etidronate, and tiludronate) and the three excipients (citrate, benzoate, and *p*-hydroxybenzoate). The shorter length of this column (150 mm) in comparison to regular 250 mm columns allows a higher sample throughput while still offering sufficient chromatographic resolution. The optimized separation is shown in Figure 8.121 with standard inorganic anions eluting first, followed by the excipients and bisphosphonates. All compounds are well separated within 15 min, thus allowing simultaneous accurate quantitation of each individual component.

Capillary IC features a flow rate in the range of 10–30  $\mu\text{L}/\text{min}$ , thus requiring modifications and reoptimization of existing electrospray interfaces that are usually optimized for either analytical flow (100  $\mu\text{L}/\text{min}$  to several milliliters/minute) or nanoflow (<1  $\mu\text{L}/\text{min}$ ) rates. The optimization of interface parameters such as probe temperature, nebulizer gas, needle voltage, type of desolvation solvent, and the flow rate plays a critical role in establishing instrument sensitivity. When capillary IC is operated at a flow rate of 10–20  $\mu\text{L}/\text{min}$ , a probe temperature of 300 °C, a needle voltage of 3 kV, a nebulizer gas pressure of 65 psi, and the use of

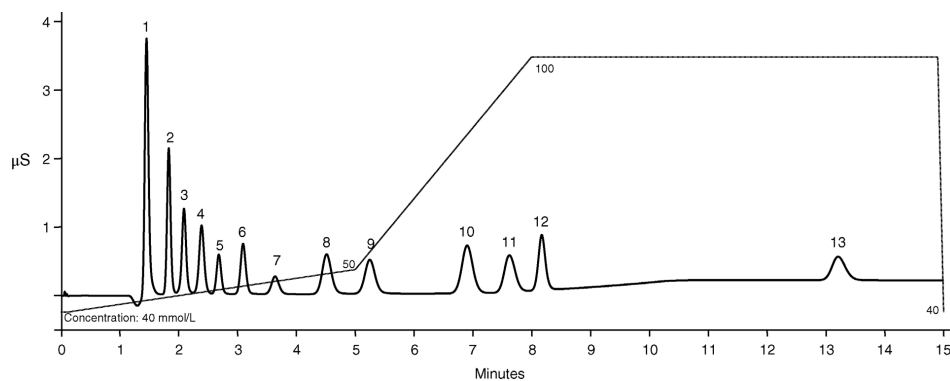


**Figure 8.121** Separation of selected bisphosphonates, excipients, and anionic impurities by capillary IC. Separator column: IonPac AS18-Fast; column dimensions: 150 mm  $\times$  0.4 mm i.d.; column temperature: 40 °C; eluent: KOH (EG); gradient: 40–50 mmol/L from 0 to 5 min and 50–100 mmol/L from 5 to 8 min; flow rate: 20  $\mu\text{L}/\text{min}$ ; detection: suppressed conductivity; injection volume: 10  $\mu\text{L}$ ; peaks: 20–100  $\mu\text{g}/\text{L}$  each of (1) fluoride, (2) chloride, (3) nitrite, (4) sulfate, (5) bromide, (6) nitrate, (7) orthophosphate, (8) benzoate, (9) *p*-hydroxybenzoate, (10) citrate, (11) etidronate, (12) clodronate, and (13) tiludronate.



acetonitrile as the desolvation solvent with the same flow rate as the capillary IC are recommended. All target analytes predominantly show deprotonated molecular ions  $[M-H]^-$  in negative polarity, which can be used in the SIM scans for quantitation. As shown in the full scan spectra in Figure 8.122, the observed pseudomolecular ions for etidronate, clodronate, and tiludronate are  $m/z$  205, 243, and 317, respectively. Figure 8.122 also shows the observed isotopic peaks for clodronate and tiludronate. Matching the observed and theoretical isotope patterns can assist in compound confirmation. Figure 8.123 shows the SIM chromatograms of the target analytes under optimized conditions, each analyte selectively detected as seen by the single peak in each monitored SIM channel. Using SIM acquisition and citric acid- $d_4$  as an isotope-labeled internal standard, sensitive and selective quantitation can be achieved at 5  $\mu\text{g/L}$  for excipients and 50  $\mu\text{g/L}$  for bisphosphonates. Method performance parameters such as calibration range, correlation coefficients, and detection limits are summarized in Table 8.10. Precision and accuracy were evaluated at 50 and 500  $\mu\text{g/L}$ , and the results are listed in Table 8.11.

**Forensic Applications** Analytical methods to measure biomarkers of exposure to chemicals that have potential use as chemical terrorism agents also include IC-MS. The nitrogen mustards bis(2-chloroethyl)ethylamine (HN1), bis(2-chloroethyl)methylamine (HN2), and tris(2-chloroethyl)amine (HN3) are three such chemicals that are listed on the Chemical Weapons Convention Schedule of Chemicals [279]. Like sulfur mustards, nitrogen mustards possess strong vesicant properties, but nitrogen mustards are less suitable for military purposes because of low volatility. Intact nitrogen mustards have been identified in blood and plasma, but the reactivity, extent of metabolism, and short half-life of the mustards [280] limit the usefulness of such measurements for biomonitoring. HN1, HN2, and HN3 are alkylating agents that rapidly react with biomolecules such as DNA and proteins to form nitrogen mustard adducts. Nitrogen mustards also hydrolyze to *N*-ethyldiethanolamine (EDEA), *N*-methyldiethanolamine (MDEA), and triethanolamine (TEA), which have been identified as urinary metabolites. Thus, a quantitative analytical method is required to determine the extent of human exposure to nitrogen mustards. Reported methods for the analysis of ethanolamines include GC [281] or LC [282] with MS detection. While GC-MS methods involve labor-intensive derivatization, the reported LC methods demonstrate relatively poor chromatographic resolution using conventional C18 columns. Lemire *et al.* [282] used a 3  $\mu\text{m}$  BDS Hypersil Cyano column and achieved an almost baseline-resolved separation of the above-mentioned hydrolysis products in 6.5 min with a mobile phase consisting of 80:20 (v/v) methanol/10 mmol/L ammonium bicarbonate delivered at a flow rate of 300  $\mu\text{L/min}$  under isocratic conditions. The respective separation of a urine sample spiked with native and labeled analytes in Figure 8.124 reveals that MDEA and EDEA are not perfectly resolved under these chromatographic conditions. However, high chromatographic resolution is not necessary, because both MDEA and EDEA differ significantly in their mass-to-charge ratio and SRM transitions.

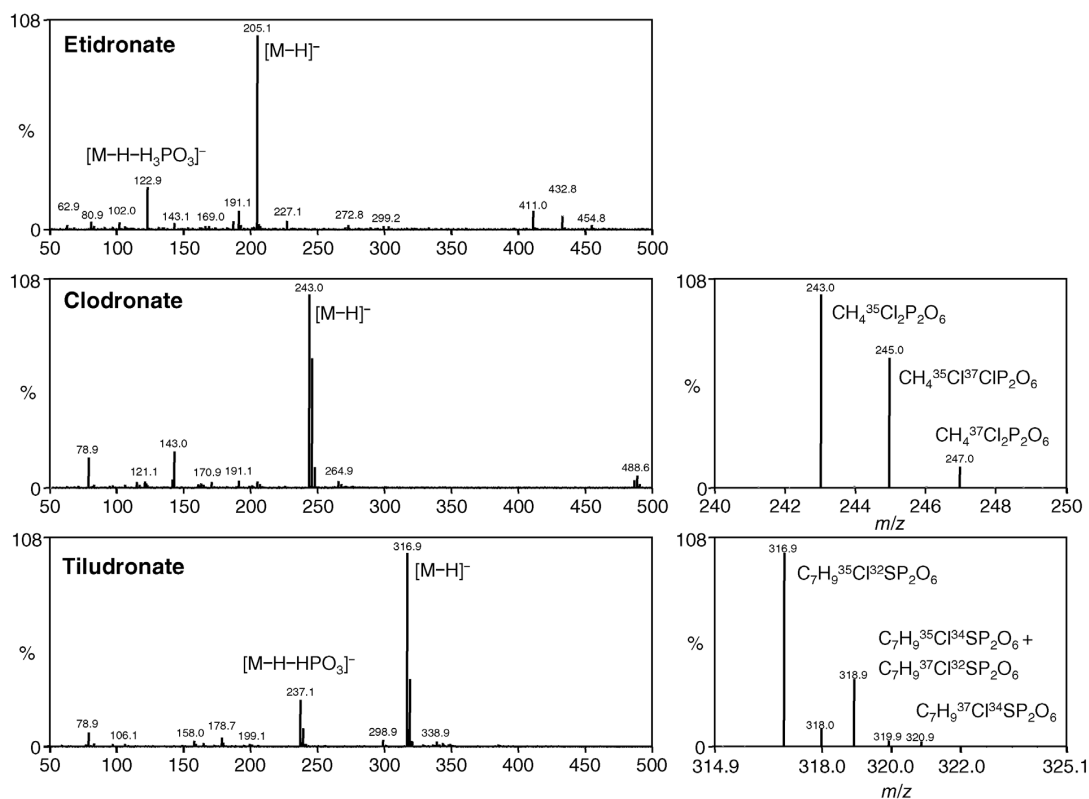
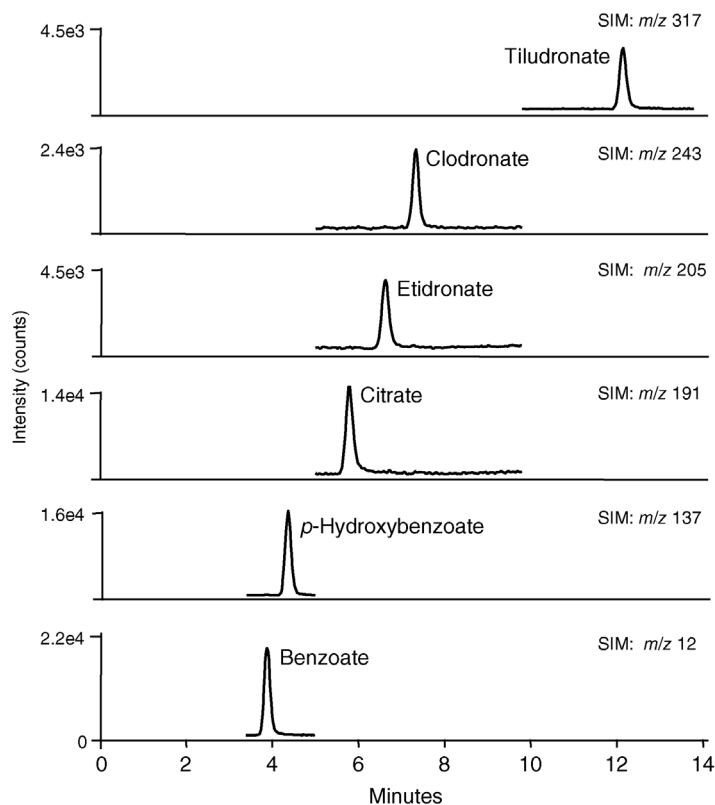


Figure 8.122 MS spectra of three selected bisphosphonate pharmaceuticals.



**Figure 8.123** SIM chromatograms of bisphosphonates and excipients.

**Table 8.10** Calibration range, correlation coefficients, standard deviation, and MDLs for bisphosphonates and excipients [277].

Analyte	Calibration range ( $\mu\text{g/L}$ )	Correlation coefficient $r^2$	Fit	% RSD <sup>a)</sup> ( $n = 5$ )	MDL <sup>b)</sup>
Benzoate	5–500	0.9994	Quadratic	8.00	2.48
<i>p</i> -Hydroxybenzoate	5–500	0.9998	Quadratic	5.31	1.20
Citrate	5–500	0.9997	Linear	3.82	1.31
Etidronate	50–500	0.9978	Quadratic	5.33	9.36
Clodronate	50–500	0.9970	Quadratic	10.28	15.5
Tiludronate	50–500	0.9957	Quadratic	4.51	7.19

a) % RSD calculated based on 20 pg injection for benzoate, *p*-hydroxybenzoate, and citrate; 100 pg injection for bisphosphonates.

b) Calculated as  $\text{MDL} = s \times t_{99\%, n=5}$ , where  $s$  is the standard deviation and  $t$  the Student's  $t$  at 99% confidence interval.

**Table 8.11** Accuracy, precision, and recovery for bisphosphonates and excipients [278].

Analyte	50 µg/L (n = 3)			200 µg/L (n = 3)			Original	Observed	% Recovery <sup>a)</sup>
	Mean	% RSD	% Accuracy	Mean	% RSD	% Accuracy			
Benzoate	54.2	2.75	108	499	4.71	99.9	ND	89.5	89.5
<i>p</i> -Hydroxybenzoate	52.4	1.53	105	499	7.07	99.9	ND	93.5	93.5
Citrate	49.4	2.58	98.7	497	0.76	99.5	ND	102	102
Etidronate	43.4	4.27	86.8	498	2.18	99.5	424	542	117
Clodronate	44.8	4.30	89.7	498	1.05	99.6	ND	134	134
Tiludronate	41.5	3.26	83.0	497	1.28	99.4	ND	121	121

a) Recovery calculated based on [observed amount (original sample + 100 µg/L spiked each analyte) – original amount]/100 × 100%.

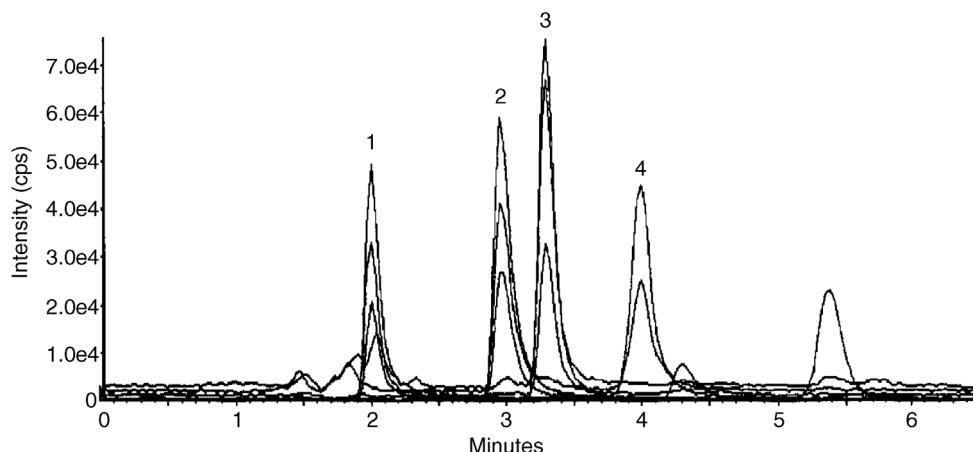


**Figure 8.124** SRM chromatogram of a urine sample spiked with native and labeled EDEA, MDEA, and TEA. Separator column: BDS Hypersil Cyano, 3  $\mu\text{m}$ ; column dimensions: 150 mm  $\times$  2.1 mm i.d.; column temperature: 30  $^{\circ}\text{C}$ ; eluent: 80:20 (v/v) MeOH/10 mmol/L ammonium bicarbonate; flow rate: 0.3 mL/min;

detection: ESI-MS with an API 4000 in the positive ion SRM mode; injection volume: 10  $\mu\text{L}$ ; sample: urine spiked with approximately 25 ng/mL of (1) triethanolamine, (2) *N*-methyldiethanolamine, and (3) *N*-ethyldiethanolamine, and (4) MDEA interference (see [282]).

Alternatively, cation-exchange chromatography can be selected to overcome the relatively poor separation of ethanolamines on conventional C18 columns. Significant retention for all target analytes is observed with low-capacity cation exchangers such as IonPac CS19 or with crown ether modified cation exchangers such as IonPac CS15. The latter one also provides sufficient separation of the target analytes from major common cations that may interfere with and contribute to ion suppression, mainly from sodium and potassium. Figure 8.125 shows the SRM chromatograms of four target ethanolamines and the isotope labeled internal standard diethanolamine- $\text{d}_8$  (IS). Matrix effects can be evaluated by comparing quantification results of standards both prepared in deionized water and prepared in a simulated matrix of 20 mg/L each of sodium chloride and potassium chloride. While no matrix effects are observed for retention times, diethanolamine (DEA) and TEA show slightly higher MDLs. Matrix also affects the % RSD, with a much higher variation for TEA. Method performance parameters for the analysis of ethanolamines are summarized in Table 8.12.

**Carbohydrate Applications** Carbohydrates and their derivatives play an important role in a wide variety of biological processes. Analysis of carbohydrates in complex matrices requires very sensitive and selective techniques to discriminate between the analytes and the background noise. The separation of carbohydrates is usually based on chromatographic methods such as gas chromatography, reversed-phase liquid chromatography, normal-phase liquid chromatography, anion-exchange chromatography (IC), HILIC, and CE. Detection is carried out

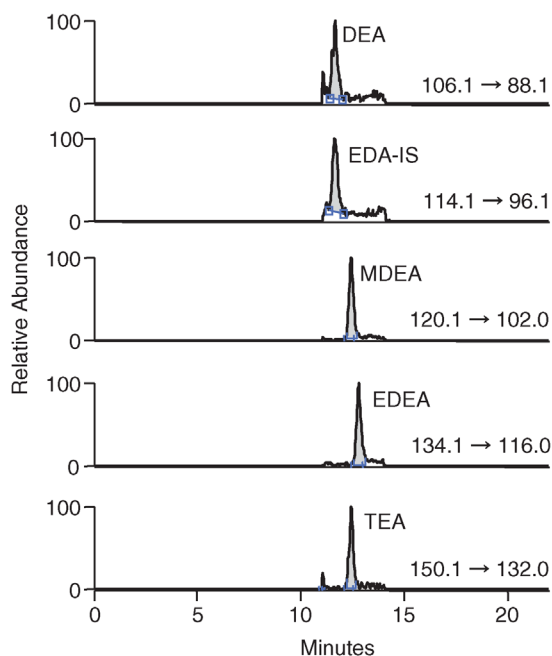


**Figure 8.125** SRM chromatogram of ethanolamines. Separator column: IonPac CS15 with guard; column temperature: 40 °C; eluent: MSA (EG); gradient: 2 mmol/L from 0 to 8 min and then to 30 mmol/L in 10 min; flow rate: 0.4 mL/min; detection: ESI-MS with an TSQ Quantum

Access in the positive ion SRM mode; spray voltage: 4 kV; needle temperature: 300 °C; desolvation solvent: 0.2 mL/min 2-propanol; injection volume: 20 µL; peaks: 10 µg/L each of DEA, IS, MDEA, EDEA, and TEA.

**Table 8.12** Method performance parameters for the analysis of ethanolamines.

Matrix	Analyte	Calibration range (µg/L)	Correlation coefficient $r^2$	Mean <sup>a)</sup>	% Deviation	% RSD ( $n = 7$ )	MDL <sup>b)</sup>
DI water	DEA	5–200	0.9997	5.38	7.6	5.65	0.89
	MEDA	1–200	0.9990	5.87	17.4	5.87	0.92
	EDEA	1–200	0.9997	5.25	5.0	6.10	0.96
	TEA	5–200	0.9997	5.84	16.8	3.64	0.57
20 mg/L NaCl + 20 mg/L KCl	DEA	5–200	0.9999	6.17	23.4	8.80	1.71
	MEDA	1–200	0.9996	4.60	–8.0	4.35	0.63
	EDEA	1–200	0.9979	4.41	–11.8	4.32	0.60
	TEA	5–200	0.9981	4.90	–2.0	10.59	1.63

a) Mean is calculated as the average of the observed amount of seven replicate injections.

b) MDL is evaluated by seven replicate injections of a 5 µg/L mixed standard and calculated as  $MDL = s \times t_{99\%, n=7}$ , where  $s$  is the standard deviation and  $t$  the Student's  $t$  at 99% confidence interval.

using electrochemical, mass spectrometric, or near-universal evaporative light scattering and charged aerosol detectors. A well-established technique for determining underivatized carbohydrates is anion-exchange chromatography in combination with integrated pulsed amperometric detection (HPAE-PAD), which allows the separation of mono-, di-, and oligosaccharides up to a degree of polymerization (DP) of 70. Although HPAE-PAD is highly selective and its ability to separate isomeric carbohydrates is unmatched, the only verification of the identity of individual sugars is the retention time. However, size and composition of an unknown carbohydrate are not easily derived from its retention time. In the past, fractions of unknown sugars were collected and identified offline by MS, NMR, or other techniques [283]. Therefore, IC-MS is the method of choice for structural elucidation of unknown peaks and for analyzing more complex samples. Moreover, tandem MS represents an even more advanced method, because structural information can be obtained by fragmentation. Cleavage of glycosidic linkages provides information on sugar composition and sequence, while cross-ring fragments yield data on linkage isomerism [284].

Many strategies in LC-MS interfacing have been followed for carbohydrate ionization. In the early 1990s, Niessen *et al.* used a thermospray interface for hyphenating anion-exchange chromatography with tandem mass spectrometry, and analyzed oligosaccharides after enzymatic degradation of plant cell wall polysaccharides [285]. Based on the work by Simpson *et al.* [233], Niessen *et al.* also employed membrane-based suppressor systems to convert the NaOH/NaOAc eluent to water/acetic acid prior to entering the thermospray interface. Today, electrospray ionization mass spectrometry (ESI-MS) is the dominant LC-MS technique for carbohydrate analysis. However, the use of a desalting device (suppressor) between the column and the MS is still required. To enhance sensitivity of neutral carbohydrates, LiCl ( $c = 0.5$  mmol/L) is added between the desalter and the MS using a T-piece and an auxiliary pump [285]. Because LiCl forms charged complexes with carbohydrates, sugars can be detected as lithium adducts  $[M + Li]^+$  at  $[M + 7]^+$  in the positive mode or as chloride adducts  $[M + Cl]^-$  in the negative mode; positively charged complexes, however, are detected with higher sensitivity. In-source collision-induced fragmentation of carbohydrates after electrospray ionization can be achieved in single quadrupole MS by accelerating the ions into the focusing RF lens region with a high enough voltage applied to the exit cone. Because the formed fragment ions are from glycosidic cleavage, they can confirm whether an unknown eluting peak is a carbohydrate or not. If the analytical system comprises an amperometric detector in addition to an MS detector for confirmation purpose, both detectors should be placed in parallel after the separator column using a flow splitter. Although only 3–5% of the analytes are oxidized in an amperometric detector, the respective oxidation products could interfere with MS detection if the MS detector would be installed in series. Hence, the schematics of the complete chromatographic system for IC-MS of carbohydrates is illustrated in Figure 8.126.

Figure 8.127 shows an isocratic separation of glucose, fructose, and sucrose on CarboPac PA200. As expected, all three carbohydrates are well separated under

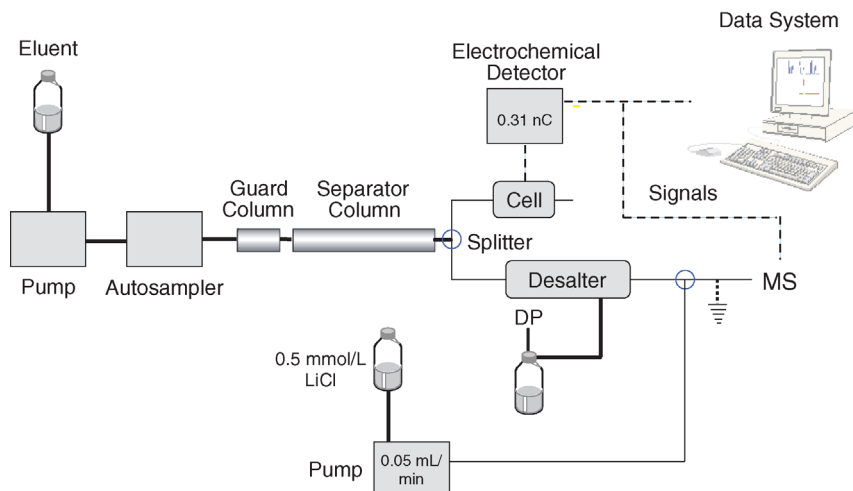


**Figure 8.126** Schematics of a chromatographic system for carbohydrate analysis with integrated pulsed amperometric and MS detection.

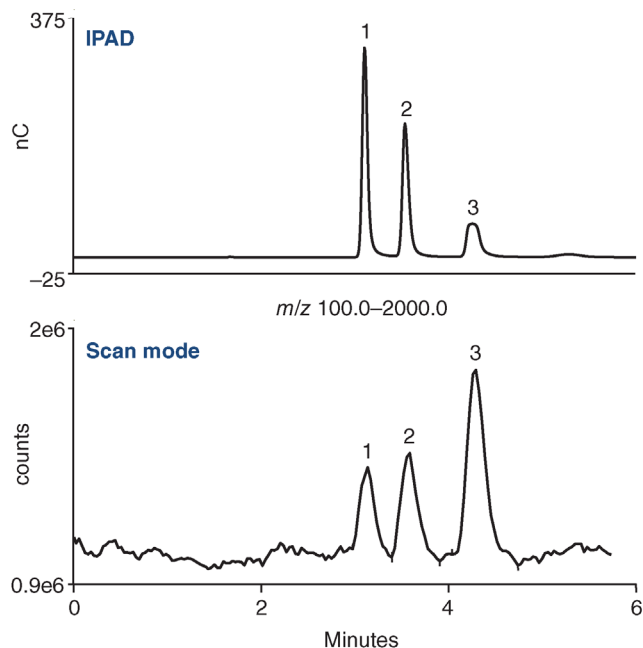


**Figure 8.127** Isocratic separation of glucose, fructose, and sucrose with integrated pulsed amperometric and MS detection. Separator column: CarboPac PA200; column dimensions: 250 mm × 3 mm i.d.; eluent: 60 mmol/L NaOH; flow rate: 0.5 mL/min; detection: IPAD and ESI–

MS (positive ion mode, probe temperature: 525 °C, cone voltage: 75 V); injection volume: 25 µL; peaks: 500 pmol each of glucose (1), fructose (2), and sucrose (3) (with permission © 2005 Elsevier B.V., [287]).



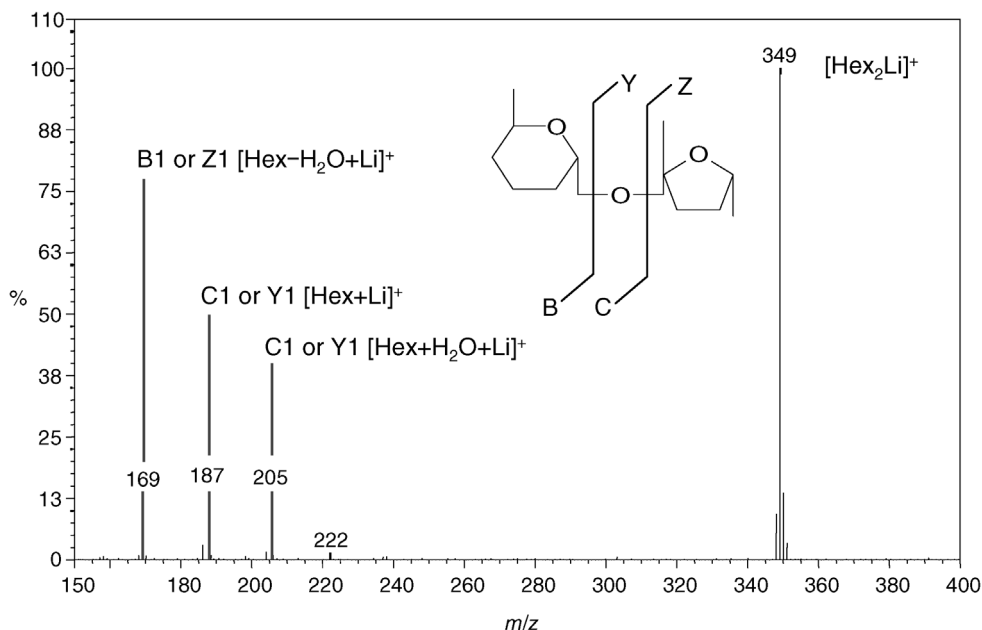
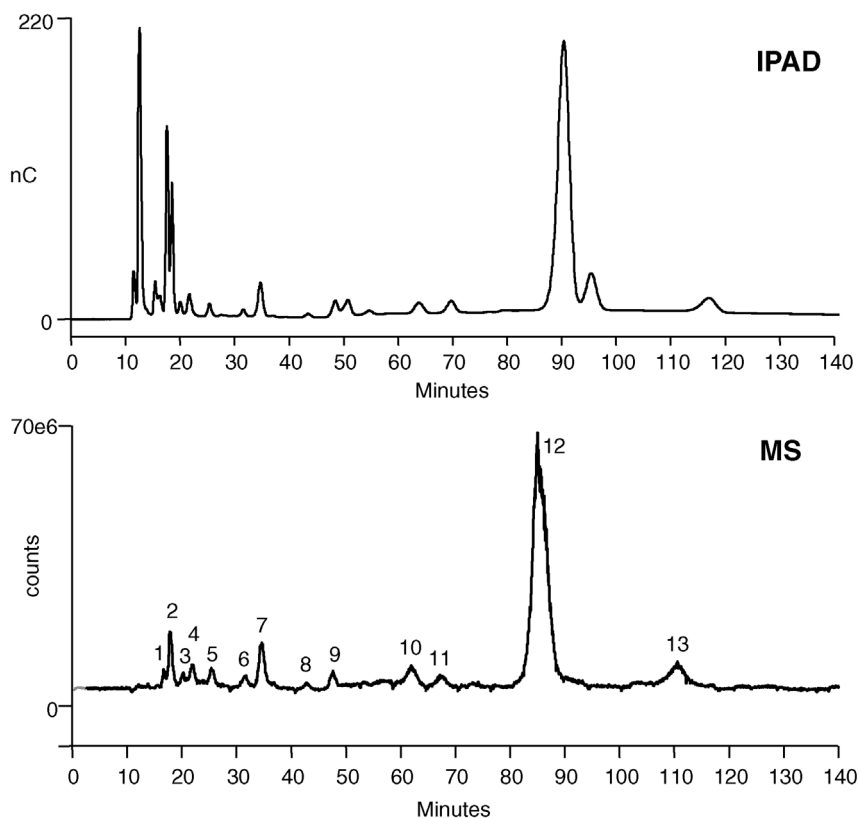


Figure 8.128 Mass spectrum of sucrose.

the given chromatographic conditions. Based on a 500 pmol injection, the mass spectrum obtained for sucrose (Figure 8.128) features a good signal-to-noise ratio. At a cone voltage of 75 V, the quasimolecular ion at  $m/z$  349 is clearly the base peak of sucrose. Fragment ions from glycosidic cleavages are also observed. In reference to the most commonly adopted Domon and Costello nomenclature [286] for glycosidic cleavages, the most universal pair of fragment ions afforded by all different MS instruments is the B and Y ions resulting from a glycosidic cleavage that contains the reducing end of the sugar, as shown in Figure 8.128. Glycosidic cleavages containing the nonreducing end of the sugar are called B and C ions. The mass loss of 162 Da (Y fragment at  $m/z$  187) can be attributed to a hexose, while the fragment ion at  $m/z$  205 is a water adduct of the Y fragment. Such water adducts are easily formed in electrospray ionization using single quadrupole mass spectrometers. The B fragment ion at  $m/z$  169 is a glycosidic cleavage on the other side of the oxygen atom. Bruggink *et al.* [287] studied sensitivity and minimum detection limits by repeated injections of 5 pmol of the three carbohydrates mentioned above. They employed selected ion monitoring, because the signal-to-noise ratio in this mode is better than in scan mode with a single quadrupole MS. The MDLs in SIM mode range from 1.49 pmol for glucose to 0.36 pmol for sucrose and are inferior to IPAD that is approximately 3–10 times more sensitive in comparison to MS.

A very topical application of the HPAE-PAD-MS system is the complete characterization of carbohydrates as hydrolysis products of biomass, which is a

biological material derived from living or recently living organisms. It usually refers to plants or plant-derived materials such as lignocellulosic biomass. As an energy source, biomass can be converted to biofuels (e.g., ethanol, biodiesel, etc.) or chemicals, using thermal, chemical, or biochemical methods. There is also a great deal of research involving algae-derived biomass, because it is a nonfood resource and can be produced much faster than land-based agricultural products such as corn, sugar cane, and soy. Converting biomass into fuels and chemicals represents a challenge as researchers have to understand which feedstock gives the best conversion to the final products. Biomass contains sugars, but they are locked in cellulose, so that microorganisms such as cellulase enzymes are used to break down cellulose into monosaccharides, a process that is called saccharification. Once the sugars are released in the saccharification step, they can undergo microbial fermentation to produce alcohols or other precursor chemicals such as diols, glycols, or organic acids. Once the sugars are released in the saccharification step they can undergo microbial fermentation to produce alcohols or other precursor chemicals such as diols, glycols, or organic acids. Cellulose and hemicellulose hydrolysis produce a wide variety of sugars in a complex matrix that have to be accurately quantified. This is a difficult task because monosaccharides have many different stereoisomers with similar physicochemical properties. To overcome the difficulty of separating these structurally similar sets of isomers, high-resolution chromatography is necessary. Capillary GC gives excellent resolution of monosaccharides but requires expensive and time-consuming derivatization prior to injection. HPLC is more convenient because the sugars can be directly injected into the chromatography column without prior derivatization; however, chromatographic resolution is not as high as in GC. On the other hand, the use of anion-exchange chromatography with mass spectrometric detection permits baseline-resolved separations of the most important saccharides in complex lysate mixtures without labor- and time-consuming derivatization steps. Figure 8.129 shows the IPAD and the total ion chromatogram of sugars detected in a microalgae whole-cell lysate. The lysate was centrifuged at 12 000 rpm for 60 min. The supernatant was collected and centrifuged for an additional 30 min, filtrated through a 0.2  $\mu\text{m}$  filter, and passed through an OnGuard-RP cartridge to remove molecular hydrophobic components. The sample was finally injected onto a CarboPac MA1 column. CarboPac MA1 is a high-capacity column that is well suited for the high sample loading often associated with biomass samples. As can be seen from Figure 8.129, more than 12 peaks could be separated under isocratic conditions. Mass spectrometric analysis of the same sample was used to confirm the carbohydrate identity of the peaks. MS detection permits the quantitation of multiple coeluting components of interest in a single analytical run. The full scan spectrum of each peak is shown in Figure 8.130. Because many mono- and disaccharides have identical mass-to-charge ratios, HPAE-PAD-MS allows the separation and verification of the components on the basis of their retention time and their molecular weights (Figure 8.131). In this way, monosaccharide alditols (fucitol, arabitols, and inositol), monosaccharides (glucose, mannose, and others), and disaccharides



**Figure 8.129** Separation of carbohydrates derived from a microalgae whole-cell lysate with integrated pulsed amperometric and MS detection. Separator column: CarboPac MA1; column dimensions: 250 mm  $\times$  4 mm i.d.; column temperature: 30  $^{\circ}$ C; eluent: 0.5 mol/L

NaOH; flow rate: 0.2 mL/min; detection: integrated pulsed amperometry on a Au working electrode and MS (positive ion scan mode  $m/z$  120–600, cone voltage: 50 V); sample: microalgae whole-cell lysate.

(sucrose, maltose, and others) could be identified in this particular sample, with sucrose being the most abundant sugar.

Bruggink also employed analytical-scale gradient anion-exchange chromatography to separate a mix of *N*-glycans that were released from a therapeutic glycoprotein [288]. The separation was carried out on CarboPac PA200 at a flow rate of 360  $\mu$ L/min (Figure 8.132). The column end was connected with a PEEK flow splitter, directing 90  $\mu$ L/min to the electrochemical cell and 270  $\mu$ L to a desalter (suppressor). The effluent of the desalter was combined with a makeup solution at 90  $\mu$ L/min, comprising a mixture of acetonitrile and 0.6 mmol/L NaCl (50:50 v/v) for MS detection. In this particular setup, the MS was a Bruker HCT Ultra ion trap equipped with an electrospray interface, detecting the glycans in the positive mode as protonated ions. The different peaks shown in Figure 8.132 were identified on the basis of MS and tandem MS spectra. In those cases where

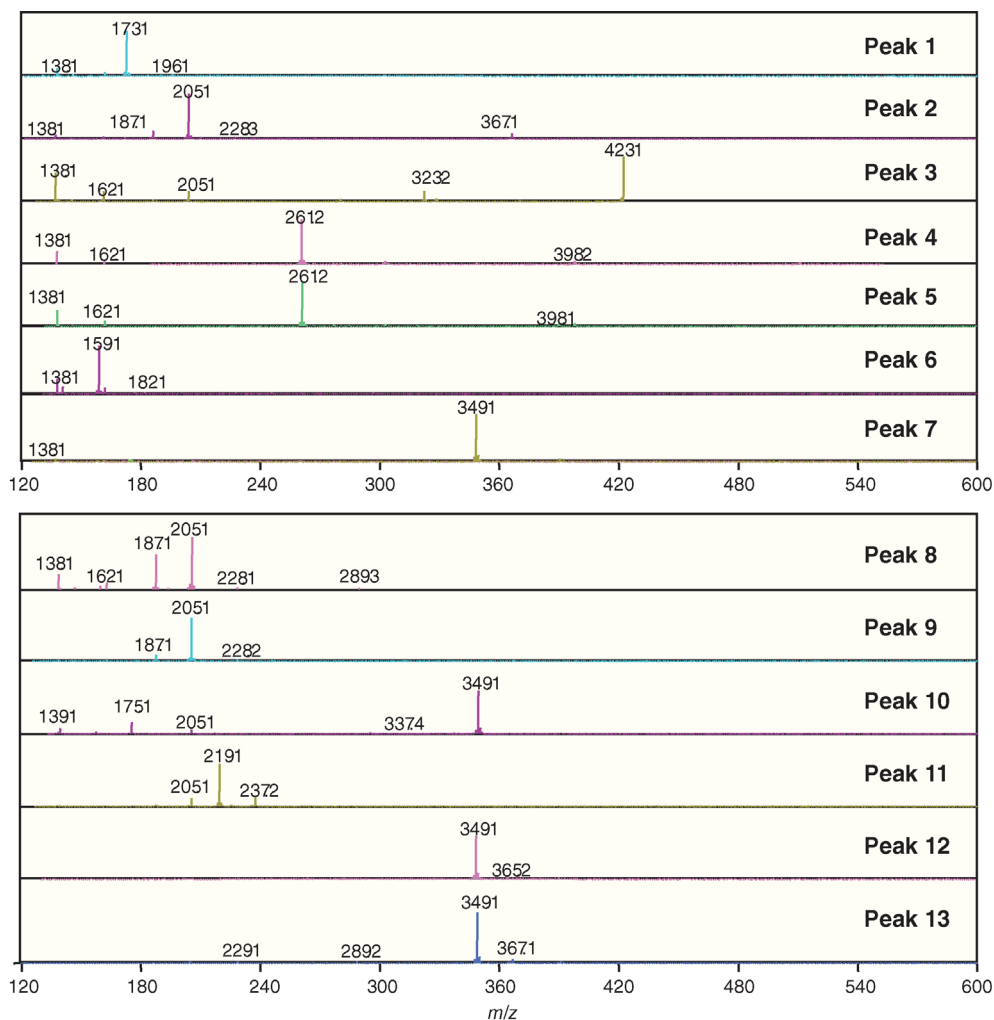


**Figure 8.130** Background-subtracted ESI mass spectra of peaks shown in Figure 8.129.

MS can only partly elucidate structures, confirmation can be effected by comparing retention times of the respective glycans. As can be seen from the chromatogram in Figure 8.132, fucosylated glycans are eluting earlier than their respective nonfucosylated counterparts, which is consistent with literature [289].

In order to meet current standards in biomedical research, scaling of column dimensions down to the capillary or even nanoscale, and hyphenation with mass spectrometry are required for the development of glycan analysis technology. These requirements have already been fulfilled utilizing normal-phase [290] and reversed-phase chromatography [291]; in the case of HPAE-PAD, however,

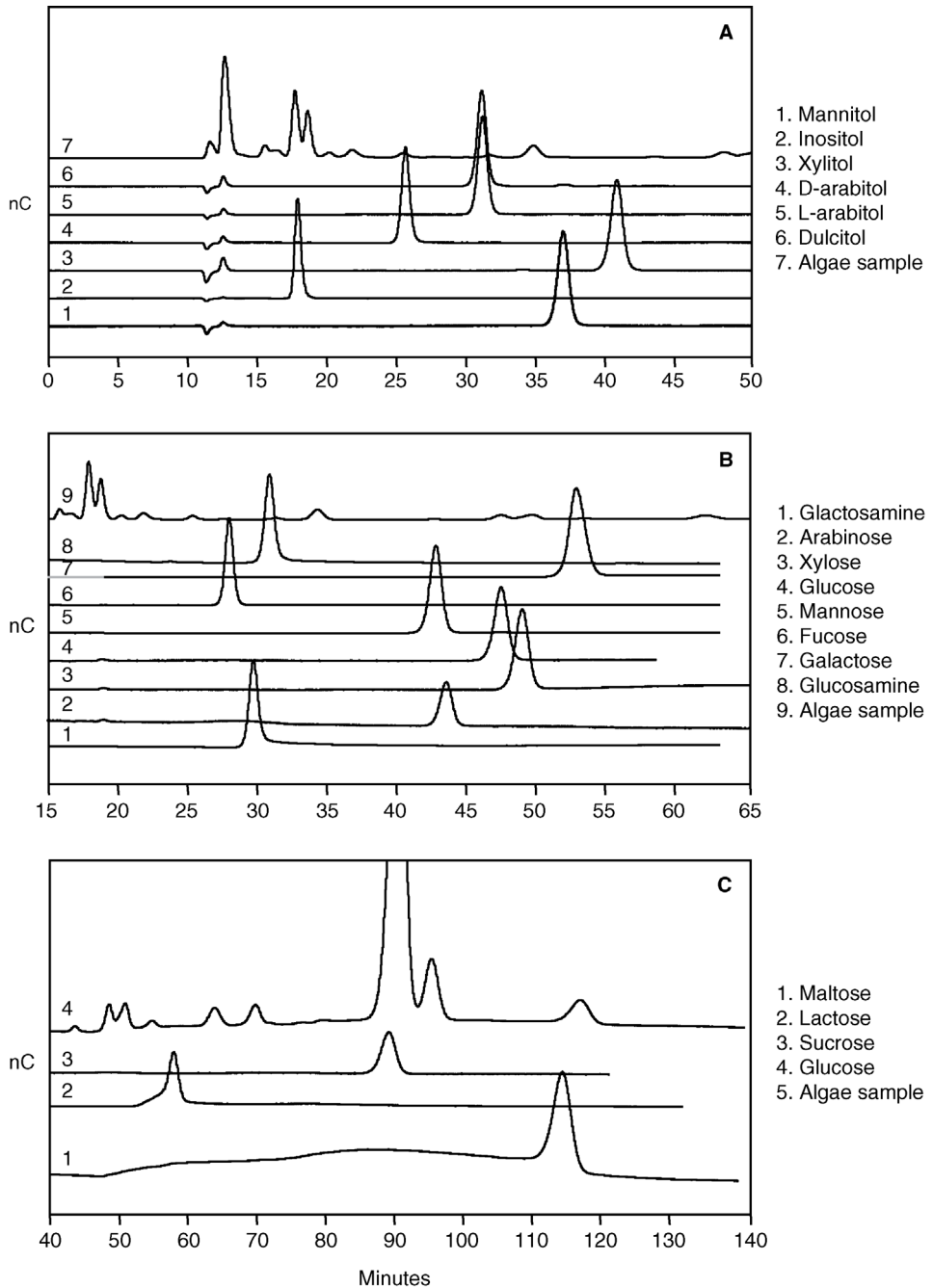


**Figure 8.131** Overlay comparisons of microalgae whole cell lysate samples with (a) alditol standards, (b) monosaccharide standards, and (c) disaccharide standards. Chromatographic conditions: see Figure 8.129.

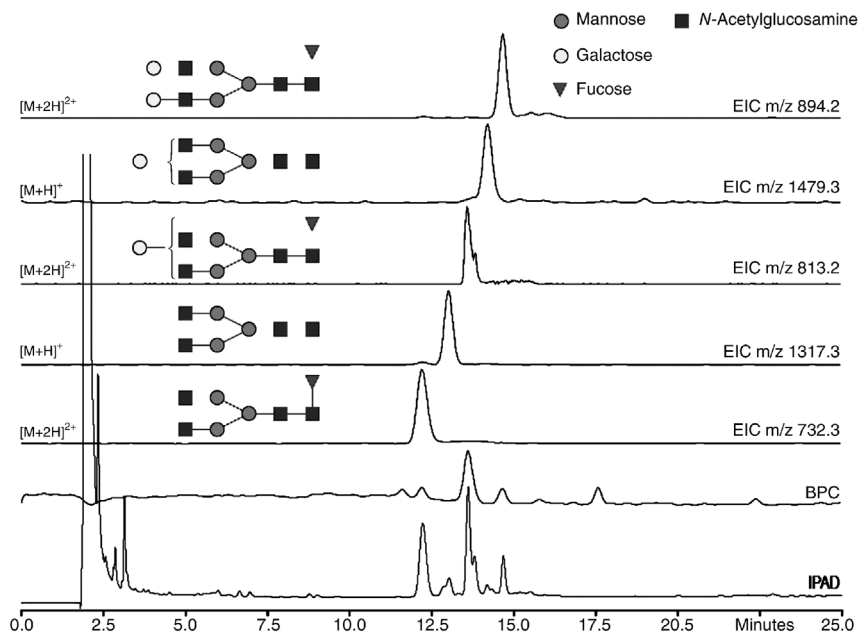


**Figure 8.132** Separation of *N*-linked glycans with HPAE-PAD-MS. Separator column: Carbo-Pac PA200; column dimensions: 250 mm × 3 mm i.d.; column temperature: 30 °C; eluent: NaOH/NaOAc; gradient: 100 mmol/L NaOH from 0 to 5 min and then linearly to

100 mmol/L NaOH + 200 mmol/L NaOAc in 60 min; flow rate: 360  $\mu$ L/min; detection: integrated pulsed amperometry and MS; sample: PNGase F released *N*-glycans from a therapeutic glycoprotein (with permission © 2005 Elsevier B.V., [287]).

oligosaccharide separations with online mass spectrometric detection has so far only been demonstrated at analytical scale (2–4 mm column i.d.) [292]. The first implementation of a capillary anion exchanger (0.4 mm column i.d.) for carbohydrate analysis in combination with two parallel online detection methods – integrated pulsed amperometry and electrospray ion trap mass spectrometry – was reported by Bruggink *et al.* [293]. Such system exhibits subpicomole sensitivity, both in amperometric and in mass spectrometric detection, and was found to be particularly useful for carbohydrate analysis in complex biological samples due to its high chromatographic resolution combined with the MS/MS capabilities of the ion trap mass spectrometer. Several components of the system had to be adapted to fulfill the requirements of capillary HPAE-PAD. The amperometric detector cell volume, for instance, has to be minimized to reduce band dispersion. Equally important is the use of a capillary suppressor (see Section 3.6.6) to convert the NaOH/NaOAc eluent into water/acetic acid prior to entering the electrospray interface. The suppression capacity of a capillary suppressor is high enough to convert eluents used for the elution of glycans with a maximum of three negative charges, for example, three sialic acids groups in oligosaccharide

structures, with only a minor loss of chromatographic resolution. By downscaling the separator column dimensions to the capillary format (0.4 mm i.d.), a significant sensitivity gain is observed in ESI-MS of carbohydrates. Minimum detection limits for underivatized glycans with capillary scale HPAE-PAD-MS were found to be 160 fmol, using a conventional electrospray ionization source [293].

Bruggink *et al.* demonstrated the applicability of capillary-scale HPAE-PAD-MS in biomedical research with the analysis of urinary oligosaccharides of a  $G_{M1}$ -gangliosidosis patient [293,294].  $G_{M1}$ -gangliosidosis is a neurosomatic disease that progressively destroys nerve cells. It is caused by mutations of the *GLB1* gene, which provides instructions for producing the enzyme  $\beta$ -galactosidase. This enzyme is located in lysosomes, which are compartments within cells that break down and recycle different types of molecules. Within lysosomes,  $\beta$ -galactosidase helps break down several molecules, including a substance called  $G_{M1}$ -ganglioside that is important for normal functioning of nerve cells in the brain. Mutations in the *GLB1* gene reduce or eliminate the activity of  $\beta$ -galactosidase. Without enough functional  $\beta$ -galactosidase,  $G_{M1}$ -ganglioside cannot be broken down when it is no longer needed. As a result, this substance accumulates to toxic levels in many tissues and organs, particularly in the brain. Progressive damage caused by the buildup of  $G_{M1}$ -ganglioside leads to the destruction of nerve cells in the brain, causing many of the signs and symptoms of  $G_{M1}$ -gangliosidosis. In general, the severity of  $G_{M1}$ -gangliosidosis is related to the level of  $\beta$ -galactosidase activity. Individuals with higher enzyme activity levels usually have milder signs and symptoms than those with lower activity levels, because they have less accumulation of  $G_{M1}$ -ganglioside within the body. Conditions such as  $G_{M1}$ -gangliosidosis that cause molecules to build up inside the lysosomes are called lysosomal storage disorders. The oligosaccharides in urine samples were isolated utilizing solid-phase extraction with graphitized carbon (Carbograp, Alltech Associates, Deerfield, IL, USA), according to the method described by Packer *et al.* [295]. Extracted ion chromatograms of disease-related glycans found in the urine of a  $G_{M1}$ -gangliosidosis patient are illustrated in Figure 8.133. Twenty glycan compositions were detected, of which six glycans with the composition  $\text{Hex}_{3-7}\text{HexNAc}_{2-5}$  are presumably disease related. The compositions together with the MS/MS data suggest these glycans to be endo- $\beta$ -*N*-acetylglucosaminidase cleavage products of complex-type *N*-glycans.  $\text{Hex}_3\text{-HexNAc}_2$  was interpreted as a monoantennary structure and  $\text{Hex}_5\text{HexNAc}_3$  as a diantennary structure. Species carrying additional  $\text{Hex}_1\text{HexNAc}_1$  units were found to be attached in species such as  $\text{Hex}_6\text{HexNAc}_4$  and  $\text{Hex}_7\text{HexNAc}_5$  with a higher number of antennae and LacNAc repeats. The tandem MS spectrum of the disodiated diantennary *N*-glycan with the composition  $\text{Hex}_5\text{HexNAc}_3$  ( $m/z$  742.1) is shown in Figure 8.134. The cross-ring fragments  $^{0,2}A_5$  and  $^{2,4}A_5$  are typical for the 4-substituted reducing end HexNAc, while the fragment ion  $B_4Y_{2\alpha}$  (D-ion,  $m/z$  712.3) reveals the composition of the 6-antenna [284]. The two oligosaccharides A and B of the composition  $H_3N_2$  in Figure 8.133 were detected in a sodiated form with a monoisotopic mass of 933.5 Da. The MS/MS data of the two isomeric species in Figure 8.135, which can be completely

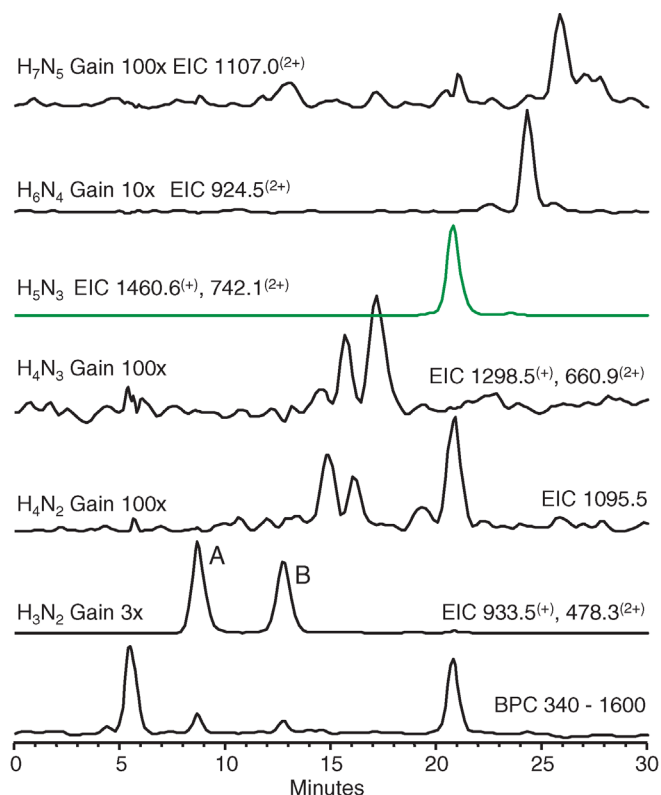


**Figure 8.133** Separation of oligosaccharides in urine of a GM1-gangliosidosis patient utilizing HPAE-PAD-MS. Separator column: CarboPac PA200; column dimensions: 250 mm × 0.4 mm i.d.; column temperature: 25 °C; eluent: NaOH/NaOAc; gradient: 60–200 mmol/L NaOH from 0 to 9.1 min, 200 mmol/L NaOH isocratically to 12.5 min, then linearly from 60 mmol/L NaOH to 60 mmol/L NaOH + 14 mmol/L NaOAc from 12.5 to 21.6 min, and then linearly to 60 mmol/L NaOH + 137.5 mmol/L NaOAc from 21.6 to

104 min; flow rate: 10 µL/min; detection: integrated pulsed amperometry and MS (Bruker Esquire 3000 ion trap, positive ion mode, dry temperature: 325 °C, capillary voltage: –3.5 kV, scan range:  $m/z$  150–2000); injection volume: 0.4 µL; sample: urine from a  $G_{M1}$ -gangliosidosis patient after SPE with Carbograph; H = hexose, N = *N*-acetylhexosamine, BPC = base peak chromatogram (reproduced with permission from Ref. [294]. Copyright 2012, Springer).

resolved by capillary anion-exchange chromatography, could be assigned based on linkage-specific fragmentation. Both oligosaccharides seemed to contain a *N*-acetylhexosamine at the reducing end, which displayed specific ring fragmentations ( $^{0,2}A$  at  $m/z$  832 and  $^{2,4}A$  at  $m/z$  772). These fragments, together with the lack of a  $^{0,3}A$  ring cleavage (no signal at  $m/z$  802), are characteristic for a 4-substituted *N*-acetylhexosamine, according to the ring fragmentation rules established for sodiated oligosaccharides. The observed series of B-ions results in a monosaccharide sequence of H–N–H–H–N for both isomers (Figure 8.135a and b). For compound A, the observed ring fragmentations ( $^{0,2}A$  at  $m/z$  670,



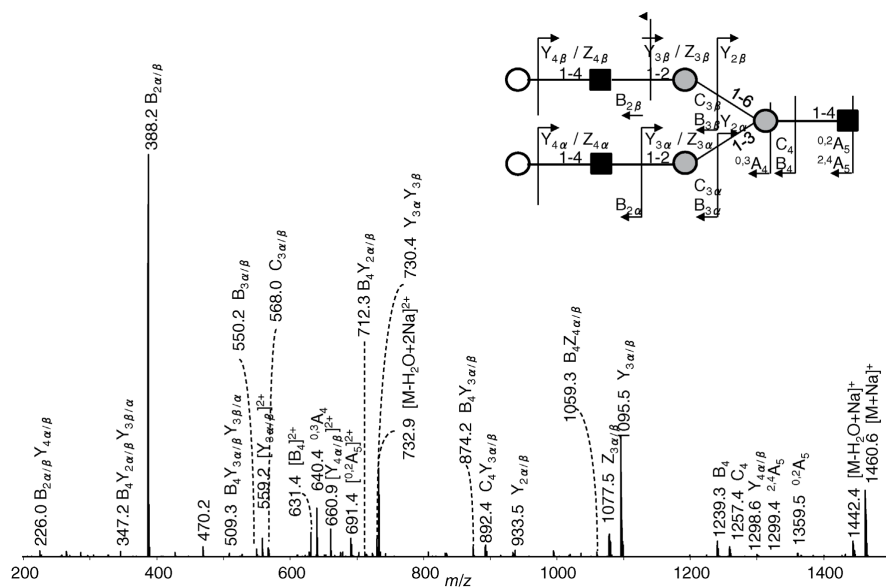


**Figure 8.134** Positive ion fragmentation mass spectrum of the disociated diantennary oligosaccharide Hex<sub>3</sub>HexNAc<sub>3</sub> (precursor ion at  $m/z$  742.1) from urine of a GM1-gangliosidosis patient. Empty circle = galactose, gray circle = mannose, black square = *N*-acetylglucosamine (reproduced with permission from Ref. [294]. Copyright 2012, Springer).

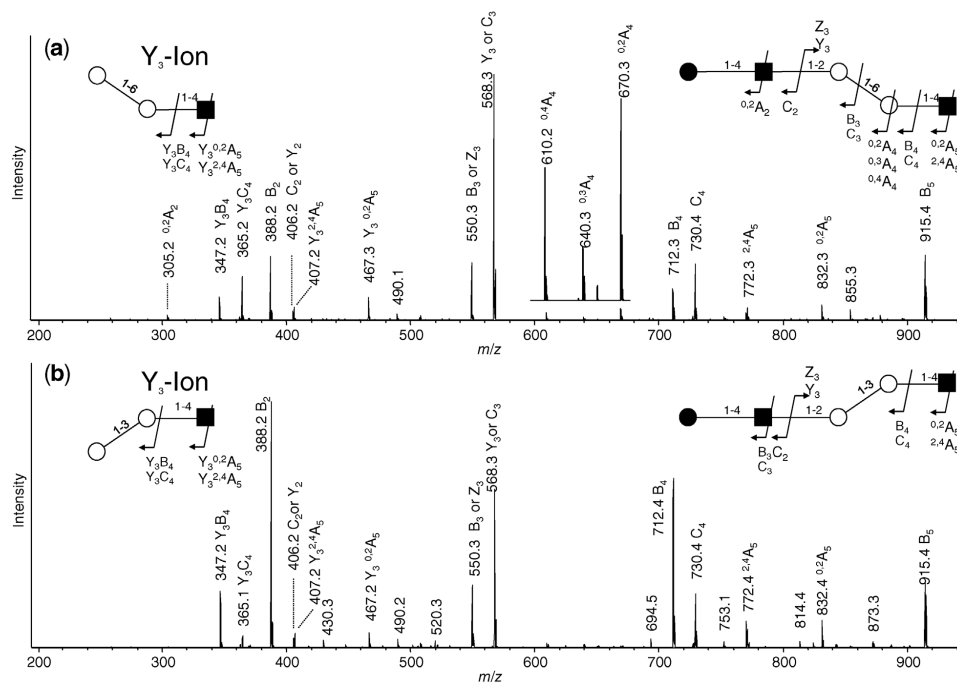


**Figure 8.135** Fragment ion analysis of H<sub>3</sub>N<sub>2</sub> species A and B in Figure 8.133. Both species were subjected to MS<sup>2</sup> analysis in their sodiated form (*m/z* 933.5); empty circle = mannose, black circle = galactose, black square = *N*-acetylglucosamine (reproduced with permission from Ref. [293]. Copyright 2005, Elsevier B.V.).

$^{0,3}A$  at  $m/z640$ , and  $^{0,4}A$  at  $m/z610$ ) of the hexose next to the reducing end *N*-acetylhexosamine are typical for a substituent in the 6 position (Figure 8.135a). Based on this information, Bruggink *et al.* concluded compound A to be the  $G_{M1}$ -gangliosidosis urinary oligosaccharide Gal(1–4)GlcNAc(1–2)Man(1–6)Man(1–4)GlcNAc (Figure 8.135a), which has been characterized before [296]. A lack of these ring fragments is typical for a substituent in the 3-position. Therefore, compound B is concluded to be the isomer Gal(1–4)GlcNAc(1–2)Man(1–3)Man(1–4)GlcNAc (Figure 8.135b), which has also been found previously in  $G_{M1}$ -gangliosidosis urine [295]. In addition to the analysis of urinary oligosaccharides from  $G_{M1}$ -gangliosidosis patients, Bruggink *et al.* also registered glycan fingerprints from patients suffering from other lysosomal storage disorders such as fucosidosis,  $\alpha$ -mannosidosis, and sialidosis [294]. The capillary HPAE-PAD-MS approach allowed structural analysis of the excreted oligosaccharides and revealed several previously unpublished structures.

**Other Applications** Anion-exchange chromatography in the capillary format coupled with a high-resolution mass spectrometer is increasingly used for metabolomic analysis. Metabolomics is a rapidly growing technique for the simultaneous analysis of small molecules in biological systems, the metabolome. In contrast to proteomics and genomics, the enormous heterogeneity of biological small molecules precludes comprehensive analysis of metabolites by a single generic technique. For this reason, multiple techniques are required to obtain maximal coverage of the metabolome. In recent years, liquid chromatography/mass spectrometry (LC–MS) has become the standard technique for metabolomic analysis. The two major reasons for this development are (i) the use of electrospray ionization as an ionization technique that emphasizes the production of molecular ions and (ii) the huge variety of stationary phases in liquid chromatography that allows the separation of a wide variety of different compounds. Although recent developments in accurate mass spectrometry have enabled determination of a limited set of potential empirical formulas for each detected molecular ion, in-source fragments, contaminant ions, and isomeric compounds often prevent identification and quantitation of metabolites based on MS data. Hence, isomeric compounds with their varying roles in biochemical pathways have to be separated chromatographically in order to be able to distinguish between them. The most common stationary phases coupled to MS for metabolite analysis are reversed-phase [297] and HILIC [298] columns, effectively separating hydrophobic and polar metabolites, respectively. However, compounds such as nucleoside di- and triphosphates and organic acids that are important elements of metabolic pathways are poorly resolved on HILIC columns or not retained at all on reversed-phase columns using MS-compatible buffers. Especially reports on MS-compatible separations of organic acids are not that common in literature. Luo *et al.* [299], for instance, used tetrabutylammonium acetate as a volatile ion-pair reagent to separate carboxylic acids in addition to sugar phosphates and nucleotides on a conventional C18 reversed-phase column. They applied this method to determine these metabolites in cell extracts

of *Escherichia coli*. Anion-exchange chromatography, on the other hand, is a very powerful separation technique for anionic compounds, but so far was not widely used in the field of metabolomics due to the high electrolyte concentrations in the mobile phase, which can lead to deleterious ion suppression effects when directly coupled to MS. Kiefer *et al.* [300] used a suppressor system for converting the eluent into a less conductive form and applied this technique to the analysis of phosphorylated metabolites, although the relatively high flow rate limits sensitivity. Based on the experience of Bruggink *et al.* [293] with capillary flow rates, Burgess *et al.* [301] applied capillary anion-exchange chromatography to metabolomic analysis for semitargeted, high-resolution analysis of metabolite standards. They also demonstrated the effectiveness of this approach for semi-quantitative analysis of samples of the protozoan parasite *Trypanosoma brucei* grown using two different carbon sources.

Although HILIC using sulfobetaine stationary phases has been reported to provide the broadest application range for untargeted metabolomic analysis under standard buffer conditions (pH ~2–4), there are a number of critical compounds with a major role in metabolism that exhibit very poor peak shapes in HILIC mode. A typical example of an important metabolite with poor peak shape under HILIC conditions is adenosine diphosphate (ADP), which is essential to the flow of energy in living cells. The respective triphosphate, where the terminal phosphate is very labile, is even less tractable, as shown by the corresponding mass spectra in Figure 8.136. The peak at  $m/z$  505.9889 corresponds to the true mass of ATP. The loss of a phosphate group in source results in the dominant peak in the mass spectrum corresponding to ADP ( $m/z$  426.0226). Thus, coelution of ADP and ATP would result in overlapping signals at  $m/z$  426.0226, making identification and quantitation impossible. Separated by HILIC, ADP is retained but with very poor peak shape. While ATP does not produce a detectable peak under HILIC conditions at all, both ADP and ATP are very well separated by anion-exchange chromatography using IonPac AS19 or AS20. Both columns differ in anion-exchange capacity and in the hydrophobicity of the functional groups. The slightly higher capacity of the IonPac AS20 column makes it more suitable for the analysis of biological samples, which typically exhibit a greater variation of metabolite concentrations and a larger potential for contaminants. In general, all nucleoside di- and triphosphates are poorly separated on conventional HILIC columns such as ZIC-HILIC (see Section 6.7.2), but are well separated with Gaussian peak shapes by anion-exchange chromatography (Figure 8.137). Burgess *et al.* reported LODs of approximately 100 pmol for this class of compounds.

The only limitation of capillary anion-exchange chromatography hyphenated with high-resolution mass spectrometry is the suppressor device that exchanges all cations from the eluent and from the samples for hydronium ions. Therefore, detection is limited to negative ions. The analysis of positively charged species can be performed, but it would require a separate run using a cation-exchange column and the corresponding suppressor device.

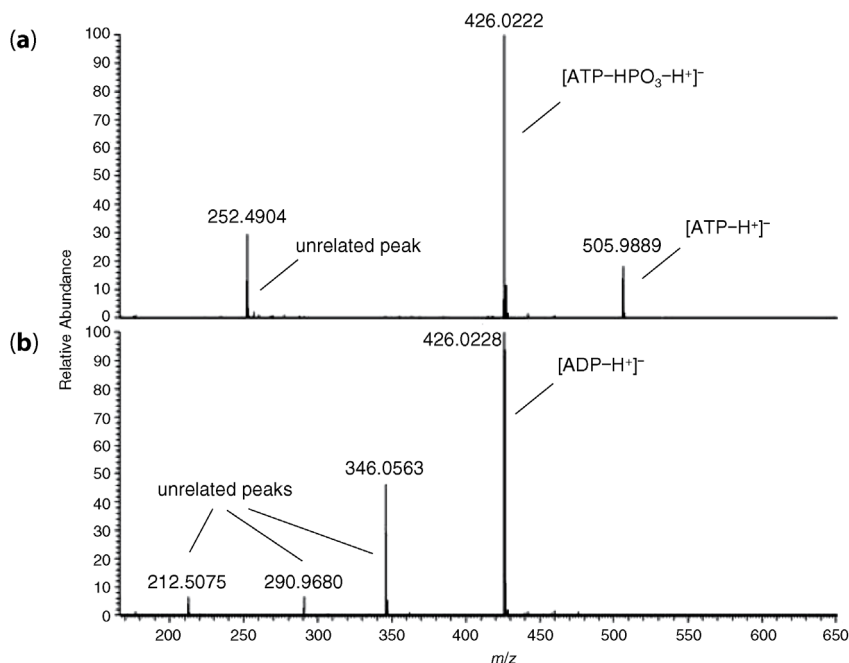


**Figure 8.136** Negative ion high-resolution mass spectrum of ATP (a) and ADP (b). MS: LTQ Orbitrap Velos; negative ion mode; voltage:  $-3$  kV; resolution: 60 000 (reproduced with permission from Ref. [301]. Copyright 2011, John Wiley & Sons, Ltd.).

As discussed in Section 10.5.1, ICP–MS is the most popular detection system for arsenic species, but it detects them all as As, at  $m/z$  75. Speciation is commonly provided by chromatographic separation using a high-capacity anion exchanger such as IonPac AS7, for instance, to achieve retention of the most common arsenic species. While arsenite, arsenate, monomethylarsonic acid (MMA), and dimethylarsinic acid (DMA) are retained on this column, arsenobetaine (AsB) as a zwitterionic compound elutes close to the void volume, making it susceptible to matrix interference. The only way to retain arsenobetaine is using cation-exchange chromatography at low pH. Thus, there is no single chromatographic separation to date that provides sufficient retention for both anionic and zwitterionic arsenic species using ESI–MS-compatible mobile phases. Slingsby *et al.* [302] solved this problem by coupling a dual-channel ion chromatography system with electrospray ionization mass spectrometry (IC–MS or IC–MS/MS) to provide retention of all five arsenic species and structural information using ESI–MS detection. The use of MS/MS detection is required for the analysis of samples with complex matrices, especially in the determination of arsenite.

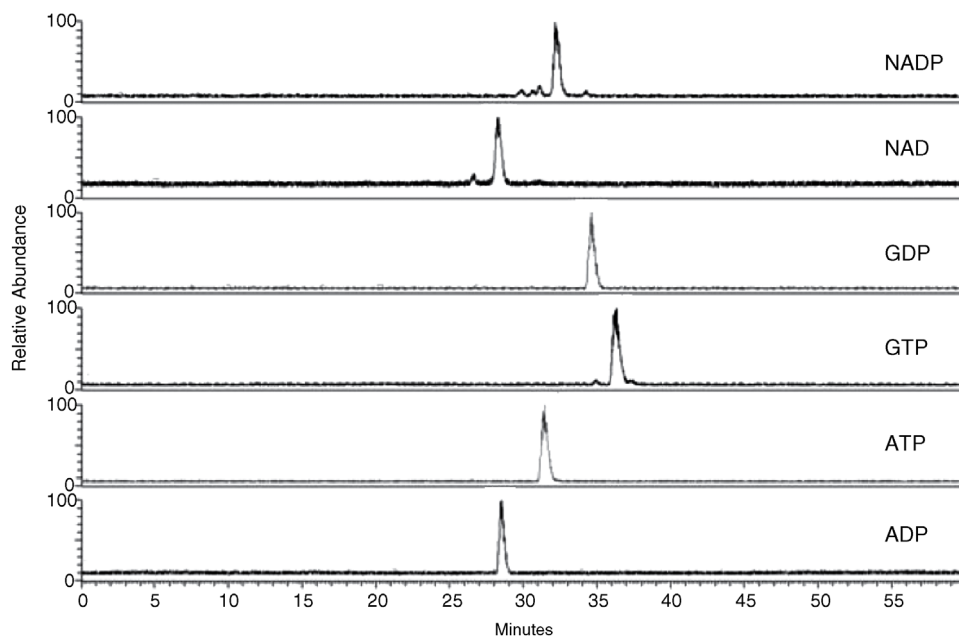


**Figure 8.137** Separation of nucleoside di- and triphosphates together with NAD and NADP by capillary anion-exchange chromatography coupled with high-resolution mass spectrometry. Separator column: IonPac AS19; column dimensions: 250 mm  $\times$  0.4 mm i.d.; eluent: KOH (EG); gradient: 8–40 mmol/L linearly from 0 to 15 min, then to 80 mmol/L in 10 min, to 100 mmol/L in 5 min, and then isocratic at 100 mmol/L for 22 min; flow rate: 10  $\mu$ L/min; detection: LTQ Orbitrap Velos (see Figure 8.136), makeup flow of MeOH at a flow rate of 10  $\mu$ L/min (reproduced with permission from Ref. [301]. Copyright 2011, John Wiley & Sons, Ltd.).

The analytical method developed by Slingsby *et al.* combines an anion-exchange separation with electrolytic suppression in Channel 1 and a mixed-mode anion/cation separation without suppression in Channel 2. Within the set of five arsenic species mentioned above, MMA, DMA, and AsB are best detected in the positive ion mode, while arsenite and arsenate are best detected in the negative ion mode. DMA needs to be separated by anion-exchange without suppression, because it crosses the membrane inside the suppressor device. Injections into the two columns are made sequentially, 13 min apart, so that the data from the conductivity and the ESI-MS detector can be collected in one data file. The anion-exchange separation is carried out on the hydroxide-selective, high-capacity IonPac AS18 column in the microbore format. Hydroxide selectivity is important, because it allows the use of a hydroxide eluent that can be converted to water in the suppressor device. The selectivity of IonPac AS18 also permits the elution of the trivalent arsenate while at the same time retaining the monovalent arsenite. Using a hydroxide gradient, MMA is well separated from common matrix anions such as chloride and sulfate. Chloride, on the other hand, is

well separated from arsenite, which is very important because chloride can cause significant signal suppression of coeluting analytes. Mixed-mode separation can be accomplished on a microbore IonPac CS5A column, which has an anion-exchange capacity of 10  $\mu\text{equiv/column}$  and a cation-exchange capacity of 5  $\mu\text{equiv/column}$ , enabling both anions and cations to be retained at this stationary phase. The formic acid eluent supplies formate ions for the elution of anions and hydronium ions for the elution of cations. Thus, DMA and AsB can be separated on the same stationary phase, although DMA requires an anion-exchange mechanism for separation. Using an IonPac CS5A column with a formic acid eluent, chloride elutes very close to AsB and signal suppression is observed on the +SIM channel at  $m/z$  179 for AsB during the elution of chloride. However, additional anion-exchange capacity for an adequate separation of chloride and AsB can be provided by using an IonPac AC15 column instead of the regular guard column.

Figure 8.138 shows an overlay of SIM chromatograms of the five arsenic standards, including the conductivity trace for chloride. Arsenite is retained by anion

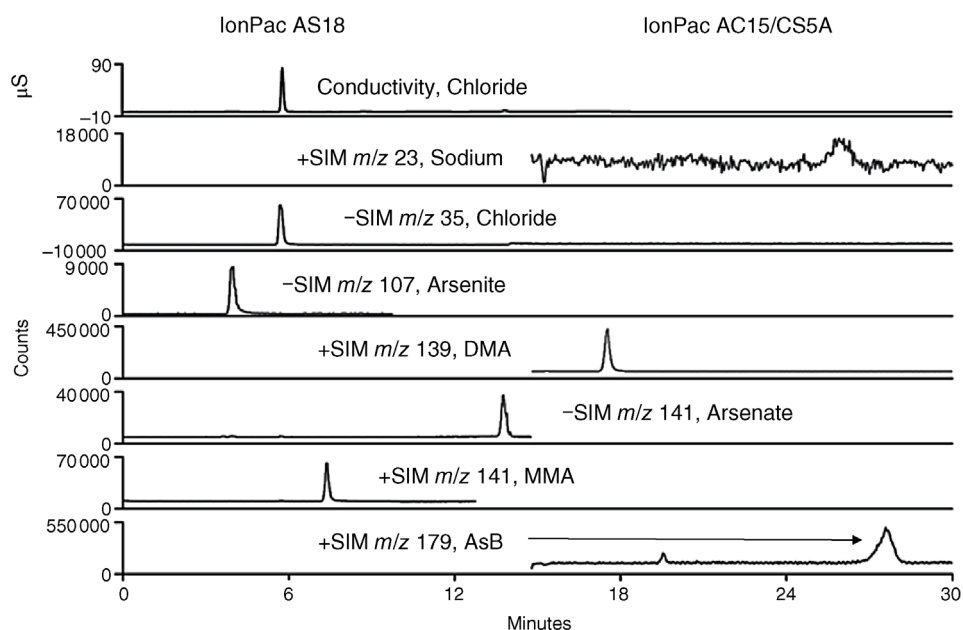


**Figure 8.138** SIM chromatograms of the five most common arsenic species together with the conductivity trace for chloride based on a dual-channel ion chromatography system coupled with ESI-MS. Channel 1. Separator column: IonPac AS18; column dimensions: 250 mm  $\times$  2 mm i.d.; eluent: KOH (EG); gradient: 6–52 mmol/L linearly in 15 min; flow rate:

0.3 mL/min; Channel 2. Separator column: IonPac AC15 + CS5A; column dimensions: 250 mm  $\times$  2 mm i.d.; eluent: 80 mmol/L formic acid; flow rate: 0.37 mL/min; detection: MSQ Plus (needle voltage: 3 kV; cone voltages: 50 V for arsenite, 30 V for arsenate, 60 V for MMA, 80 V for DMA, and 70 V for AsB) (see also [302]).

exchange on IonPac AS18 and can be detected as  $\text{AsO}_2^-$  ion. Arsenate is retained by anion exchange on both columns and is detected with best sensitivity as the  $\text{H}_2\text{AsO}_3^-$  ion. Monomethylarsonic acid is also retained as an anion but detected with good sensitivity as the protonated species in the positive ion mode. Arsenobetaine is also protonated in the formic acid eluent and is, therefore, retained by cation exchange on the IonPac AC15/CS5A column set. It is detected as a cation because As bears a permanent positive charge under these conditions. Dimethylarsinic acid is not only retained as an anion but also detected as a cation. The method is linear for all analytes over the range of 5–100  $\mu\text{g/L}$ . Method detection limits in a drinking water matrix of 100 mg/L each of chloride, bicarbonate, and sulfate were determined based on seven replicates and the standard student's test calculation, ranging from 1  $\mu\text{g/L}$  for DMA to 20  $\mu\text{g/L}$  for arsenite.

At present, electrospray interfacing is the most widely used technique for introducing liquid into a mass spectrometer. In addition, electrospray ionization is a very efficient ionization technique that significantly extended the analytical potential of mass spectrometry. Today, both electrospray ionization and chemical ionization at atmospheric pressure (APCI) are standard methods in LC–MS. Although the majority of current publications deal with the characterization of biologically relevant macromolecules, the few examples introduced above underline the significance of electrospray interfaces for the sensitive detection and structural elucidation of ionic compounds. The dominating role of electrospray is attributed, above all, to its ease of use, high sensitivity, reliability, and robustness.

## References

- Ackermann, G., Jugelt, W., Möbius, H.-H., Suschke, H.D., and Werner, G. (1974) *Elektrolytgleichgewichte und Elektrochemie*, VEB Verlag für Grundstoffindustrie, Leipzig.
- Göbl, M. (1983) *GIT Fachz. Lab.*, **27**, 261–265 and 373–375.
- Fritz, J.S. and Gjerde, D.T. (1987) *Ion Chromatography*, Dr. Alfred Hüthig-Verlag, Heidelberg.
- Gjerde, D.T. and Fritz, J.S. (1981) *Anal. Chem.*, **53**, 2324.
- Gjerde, D.T., Fritz, J.S., and Schmuckler, G. (1979) *J. Chromatogr.*, **186**, 509.
- Girard, J.E. and Glatz, J.E. (1981) *Am. Lab.*, **13**, 26.
- Okada, T. and Kuwamoto, T. (1983) *Anal. Chem.*, **55**, 1001.
- Ivey, J.P. (1984) *J. Chromatogr.*, **287**, 128.
- Irgum, K. (1987) *Anal. Chem.*, **59**, 358.
- Small, H. (1989) *Ion Chromatography*, Plenum Press, New York, p. 180 ff.
- Rocklin, R.D. and Johnson, E.L. (1983) *Anal. Chem.*, **55**, 4.
- Han, K. and Koch, W.F. (1987) *Anal. Chem.*, **59**, 1016.
- Tan, L.K. and Dutrizac, J.E. (1986) *Anal. Chem.*, **58**, 1383.
- Kolb, T., Bogenschütz, G., and Schäfer, J. (1998) *LaborPraxis*, **5**, 66.
- Hughes, S. and Johnson, D.C. (1981) *Anal. Chim. Acta*, **149**, 1.
- Rocklin, R.D. and Johnson, E.L. (1982) *Anal. Chem.*, **55**, 392.
- Weiss, J. (1986) *GIT Supplement Chromatogr.*, **3**, 65.
- Johnson, D.C. and LaCourse, W.R. (1990) *Anal. Chem.*, **62**, 589A.
- Jensen, M.B. and Johnson, D.C. (1997) *Anal. Chem.*, **69**, 1776.



- 20 Rocklin, R.D., Clarke, A.P., and Weitzhandler, M. (1998) *Anal. Chem.*, **70**, 1496.
- 21 Weitzhandler, M., Pohl, C., Narayanan, L., Slingsby, R., and Avdalovic, N. (1996) *Anal. Biochem.*, **241**, 128.
- 22 Johnson, D.C. and LaCourse, W.R. (1994) *Carbohydrate Analysis: High Performance Liquid Chromatography and Capillary Electrophoresis* (ed. Z.El Rassi), Elsevier Science, Amsterdam, Chapter 10.
- 23 Chassaniol, K., Cheng, J., Jandik, P., and Pohl, C.A. (2011) Utilization of palladium hydrogen reference electrode for amperometric detection in ion chromatography. Presentation No. 1210-2P at Pittcon 2011, Atlanta, GA, USA.
- 24 Tomilov, A.P., Mairanovskij, S.G., Fioshin, M.Y., and Smironov, V.A. (1972) *Electrochemistry of Organic Compounds*, Halsted, New York, p. 314.
- 25 Hughes, S., Meschi, L., and Johnson, D.C. (1981) *Anal. Chim. Acta*, **132**, 1.
- 26 LaCourse, W.R. and Owens, G.S. (1995) *Anal. Chim. Acta*, **307**, 301.
- 27 Dasenbrock, C.O. and LaCourse, W.R. (1998) *Anal. Chem.*, **70**, 2415.
- 28 Hanko, V. and Rohrer, J. (1999) Determination of sulfur-containing antibiotics by improved HPLC-pulsed electrochemical detection. Presentation No. 636, Pittsburg Conference, Orlando, FL, USA.
- 29 Polta, J.A. and Johnson, D.C. (1983) *J. Liq. Chromatogr.*, **6**, 1727.
- 30 Martens, D.A. and Frankenberger, W.T. (1992) *J. Liq. Chromatogr.*, **15**, 423.
- 31 Welch, L.E., LaCourse, W.R., Mead, D.A., and Johnson, D.C. (1989) *Anal. Chem.*, **61**, 555.
- 32 Clarke, A.P., Jandik, P., Rocklin, R.D., Liu, Y., and Avdalovic, N. (1999) *Anal. Chem.*, **71**, 2774.
- 33 Edwards, P. and Haak, K. (1983) *Am. Lab.*, **April**.
- 34 Small, H., Stevens, T.S., and Bauman, W.C. (1975) *Anal. Chem.*, **47**, 73.
- 35 Yang, B., Chen, Y., Mori, M., Ohira, S., Azad, A.K., Dasgupta, P.K., and Srinivasan, K. (2010) *Anal. Chem.*, **82**, 951.
- 36 Yang, B., Takeuchi, M., and Dasgupta, P.K. (2008) *Anal. Chem.*, **80**, 40.
- 37 Doury-Berthod, M., Giampoli, P., Pitsch, H., and Poitrenaud, C. (1985) *Anal. Chem.*, **57**, 2257.
- 38 Buck, R.P., Singhadeja, S., and Rogers, L.B. (1954) *Anal. Chem.*, **26**, 1240.
- 39 Reeve, R.N. (1979) *J. Chromatogr.*, **177**, 393.
- 40 Leuenberger, U., Gauch, R., Rieder, K., and Baumgärtner, E. (1980) *J. Chromatogr.*, **202**, 461.
- 41 Williams, R.J. (1983) *Anal. Chem.*, **55**, 851.
- 42 Kola, S.H., Buckle, K.A., and Wooton, M. (1983) *J. Chromatogr.*, **260**, 189.
- 43 Jackson, P.E., Haddad, P.R., and Dilli, S. (1984) *J. Chromatogr.*, **295**, 471.
- 44 Rocklin, R.D. (1984) *Anal. Chem.*, **56**, 1959.
- 45 Shibata, S. (1972) Chelates, in *Analytical Chemistry*, vol. 4 (eds H.A. Flaschka and A.J. Barnard), Marcel Dekker, New York, Chapter 1.
- 46 Yan, D.-R. and Schwedt, G. (1987) *LaborPraxis*, **January/February**, 48.
- 47 Yan, D.-R. and Schwedt, G. (1987) *Fresenius' Z. Anal. Chem.*, **327**, 503.
- 48 Lucy, C.A. and Dinh, H.N. (1994) *Anal. Chem.*, **66**, 793.
- 49 Smith, R.M. and Martell, A.E. (1975) *Critical Stability Constants, Amines*, 2nd edn, Plenum Press, New York.
- 50 Martell, A.E. and Smith, R.M. (1975) *Critical Stability Constants*, 2nd edn, First Supplement, Plenum Press, New York.
- 51 Stillian, J. (1984) Trace analysis via post-column chemistry in ion chromatography: silica and ppb calcium and magnesium in brines. Presentation at the Pittsburgh Conference 1984, Atlantic City, NJ, USA.
- 52 Wang, W., Chen, Y., and Wu, M. (1984) *Analyst (London)*, **109**, 281.
- 53 Application Note C-106, Metrohm AG, Herisau, Switzerland.
- 54 Knight, C.H., Cassidy, R.M., Recoskie, B.M., and Green, L.W. (1984) *Anal. Chem.*, **56**, 474.
- 55 Hautman, D.P. and Bolyard, M.J. (1991) *J. Chromatogr.*, **602**, 7.
- 56 Charles, L. and Pépin, D. (1998) *Anal. Chem.*, **70**, 353.
- 57 Joyce, R.J. and Dhillon, H.S. (1994) *J. Chromatogr. A*, **671**, 165.
- 58 Charles, L., Pépin, D., and Casetta, B. (1996) *Anal. Chem.*, **68**, 2554.

- 59 Heitkemper, D.T., Kaine, L.A., Jackson, D.S., and Wolnik, K.A. (1994) *J. Chromatogr. A*, **67**, 101.
- 60 Weinberg, H.S. and Yamada, H. (1998) *Anal. Chem.*, **70**, 1.
- 61 Wagner, H.P., Pepich, B.V., Hautmann, D.P., and Munch, D.J. (1999) Performance evaluation of EPA Method 302.0 and validation of EPA Method 303.0. Presentation at the International Ion Chromatography Symposium 1999, San Jose, CA, USA.
- 62 Hautmann, D.P., Munch, D.J., and Pfaff, J.D. (1997) NERL, US EPA, Method 300.1.
- 63 Warner, C.R., Daniels, D.H., Joe, F.L., and Diachenko, G.W. (1996) *Food Addit. Contam.*, **13**, 633.
- 64 Wagner, H.P., Pepich, B.V., Hautman, D.P., and Munch, D.J. (2001) US EPA Method 317.0.
- 65 US EPA Appendix B to Part 136-Definition and Procedure for the Determination of the Method Detection Limit-Revision 1.11. Fed. Reg. 40:136B:141.
- 66 Wagner, H.P., Pepich, B.V., Hautman, D.P., and Munch, D.J. (2000) *J. Chromatogr. A*, **882**, 309.
- 67 Iatrou, A. and Knocke, W.R. (1992) *AWWA*, **11**, 63.
- 68 Wagner, H.P., Pepich, B.V., Hautman, D.P., and Munch, D.J. (2002) *J. Chromatogr. A*, **956**, 93.
- 69 Wagner, H.P., Pepich, B.V., Hautman, D.P., Munch, D.J., Sahli, E., and von Gunten, U. (2002) USEPA, Method 326.0.
- 70 Delcomyn, C.A., Weinberg, H.S., and Singer, P.C. (2001) *J. Chromatogr. A*, **920**, 213.
- 71 De Borba, B.M., Rohrer, J.S., Pohl, C.A., and Saini, C. (2005) *J. Chromatogr. A*, **1085**, 23.
- 72 De Borba, B.M. and Rohrer, J.S. (2012) Application Note No. 171. Thermo Fisher Scientific, Sunnyvale, CA, USA.
- 73 Bichsel, Y. and von Gunten, U. (1999) *Anal. Chem.*, **71**, 34.
- 74 Weiß, J. (1987) *Fresenius' Z. Anal. Chem.*, **328**, 46.
- 75 Baba, Y., Yoza, N., and Ohashi, S. (1984) *J. Chromatogr.*, **295**, 153.
- 76 Baba, Y., Yoza, N., and Ohashi, S. (1985) *J. Chromatogr.*, **348**, 27.
- 77 Baba, Y., Yoza, N., and Ohashi, S. (1985) *J. Chromatogr.*, **350**, 119.
- 78 Vaeth, E., Sladek, P., and Kenar, K. (1987) *Fresenius' Z. Anal. Chem.*, **239**, 584.
- 79 Small, H. and Miller Jr., T.E. (1982) *Anal. Chem.*, **54**, 462.
- 80 Cochrane, R.A. and Hillman, D.E. (1982) *J. Chromatogr.*, **241**, 392.
- 81 Kolthoff, I.M. and Sandell, E.B. (1949) *Textbook of Quantitative Inorganic Analysis*, Macmillan, New York, p. 662–668.
- 82 Dreux, M., Lafosse, M., and Pequinet, M. (1982) *Chromatographia*, **15**, 653.
- 83 Haddad, P.R. and Heckenberg, A.L. (1982) *J. Chromatogr.*, **252**, 177.
- 84 Haddad, P.R. and Heckenberg, A.L. (1983) *Chem. Aust.*, **50**, 275.
- 85 Roth, M. and Hampai, H. (1973) *J. Chromatogr.*, **83**, 353.
- 86 de Montigny, P., Stobaugh, J.F., Givens, R.S., Carlson, R.G., Srinivasachar, K., Sternson, L.A., and Higuchi, T. (1987) *Anal. Chem.*, **59**, 1096.
- 87 Dionex Corporation (1997) Dionex Application Note No. 109: Determination of Glyphosate by Cation Exchange Chromatography with Postcolumn Derivatization. Dionex Corporation (now part of Thermo Fisher Scientific), Sunnyvale, CA, USA.
- 88 Lee, S.H. and Field, L.R. (1984) *Anal. Chem.*, **56**, 2647.
- 89 Wolkoff, A.W. and Larose, R.H. (1974) *J. Chromatogr.*, **99**, 731.
- 90 Katz, S., Pitt Jr., W.W., Mrochek, J.E., and Dinsmore, S.J. (1974) *J. Chromatogr.*, **101**, 193.
- 91 Sherman, J.H. and Danielson, N.D. (1987) *Anal. Chem.*, **59**, 490.
- 92 Sherman, J.H. and Danielson, N.D. (1987) *Anal. Chem.*, **59**, 1483.
- 93 Bächmann, K. and Blaskowitz, K.-H. (1989) *Fresenius' Z. Anal. Chem.*, **333**, 15.
- 94 Mho, S. and Yeung, E.S. (1985) *Anal. Chem.*, **57**, 2253.
- 95 Takeuchi, T. and Yeung, E.S. (1986) *J. Chromatogr.*, **370**, 83.
- 96 Nimura, N. and Kinoshita, T. (1980) *Anal. Lett.*, **13**, 191.

- 97 Nakaya, T., Tomomoto, T., and Imoto, M. (1967) *Bull. Chem. Soc. Jpn.*, **40**, 691.
- 98 IUPAC (1997) *IUPAC Compendium of Chemical Technology*, 2nd edn, International Union of Pure and Applied Chemistry, Research Triangle, NC, USA.
- 99 Joshi, P.B., Bhoir, S.L., and Bhagwat, M. (2010) *J. Sep. Sci.*, **2**, 12.
- 100 Charlesworth, J.M. (1978) *Anal. Chem.*, **50**, 1414.
- 101 Megoulas, N.C. and Koupparis, M.A. (2005) *Crit. Rev. Anal. Chem.*, **35**, 301.
- 102 Young, C.S. and Dolan, J.W. (2003) *LC-GC N. Am.*, **21**, 120.
- 103 Deschamps, F.S., Baillet, A., and Chaminade, P. (2002) *Analyst*, **127**, 35.
- 104 Megoulas, N.C. and Koupparis, M.A. (2004) *J. Chromatogr. A*, **1057**, 125.
- 105 Petritis, K., Elfakir, C., and Dreux, M. (2002) *J. Chromatogr. A*, **961**, 9.
- 106 Peterson, J.A., Lorenz, L.J., Risley, D.S., and Sandmann, B.J. (1999) *J. Liq. Chromatogr. Relat. Technol.*, **22**, 1009.
- 107 Allgeier, M.C., Nussbaum, M.A., and Risley, D.S. (2003) *LC-GC N. Am.*, **21**, 376.
- 108 Taylor, E.W., Qian, M.G., and Dollinger, G.D. (1998) *Anal. Chem.*, **70**, 3339.
- 109 Koropchak, J.A., Heenan, C.L., and Allen, L.B. (1996) *J. Chromatogr. A*, **736**, 11.
- 110 Vervoort, N., Daemen, D., and Török, G. (2008) *J. Chromatogr. A*, **1189**, 92.
- 111 Vogel, R., DeFillipo, K., and Reif, V. (2001) *J. Pharm. Biomed. Anal.*, **24**, 405.
- 112 Clarot, I., Chaimbault, P., Hasdenteufel, F., Netter, P., and Nicolas, A. (2004) *J. Chromatogr. A*, **1031**, 281.
- 113 Megoulas, N.C. and Koupparis, M.A. (2005) *Anal. Bioanal. Chem.*, **382**, 290.
- 114 Park, M.K., Park, J.H., Han, S.B., Shin, Y.G., and Park, I.H. (1996) *J. Chromatogr. A*, **736**, 77.
- 115 Li, W. and Fitzloff, J.F. (2001) *J. Pharm. Biomed. Anal.*, **25**, 257.
- 116 Wei, Y. and Ding, M.Y. (2002) *J. Liq. Chromatogr.*, **25**, 1769.
- 117 Allen, L.B. and Koropchak, J.A. (1993) *Anal. Chem.*, **65**, 841.
- 118 Allen, L.B., Koropchak, J.A., and Szostek, B. (1995) *Anal. Chem.*, **67**, 659.
- 119 Bartz, H., Fissan, H., Helsper, C., Kousaka, Y., Okuyama, K., Fukushima, N., Keady, S., Kerrigan, P.B., Fruin, S.A., McMurry, P.H., Pui, D.Y., and Stolzenburg, M.R. (1985) *J. Aerosol Sci.*, **16**, 443.
- 120 Ahn, K. and Liu, B.Y.H. (1990) *J. Aerosol Sci.*, **21**, 263.
- 121 Koropchak, J.A., Heenan, C.L., and Allen, L.B. (1996) *J. Chromatogr. A*, **736**, 11.
- 122 Dixon, R.W. and Peterson, D.S. (2002) *Anal. Chem.*, **74**, 2930.
- 123 Gamache, P.H., McCarthy, R.S., Freeto, S.M., Asa, D.J., Woodcock, M.J., Laws, K., and Cole, R.O. (2005) *LC-GC Europe*, **18**, 345.
- 124 Dasgupta, P.K., Chen, Y., Serrano, C.A., Guiochon, G., Liu, H., Fairchild, J.N., and Shalliker, R.A. (2010) *Anal. Chem.*, **82**, 10143.
- 125 Shalliker, R.A., Stevenson, P.G., Shock, D., Mnatsakanyan, M., Dasgupta, P.K., and Guiochon, G. (2010) *J. Chromatogr. A*, **1217**, 5693.
- 126 Crafts, C., Plante, M., Bailey, B., and Acworth, I. (2012) Enhancement of linearity and response in charged aerosol detection. Poster presented at Pittcon 2012, Orlando, FL, USA.
- 127 Cobb, Z., Barret, D., Shaw, P., Meehan, E., Watkins, J., O'Donohue, S., and Wrench, N. (2001) *J. Microcolumn Sep.*, **13**, 169.
- 128 Mathews, B.T., Higginson, P.D., Lyons, R., Mitchell, J.C., Sach, N.W., Snowdon, M.J., Taylor, M.R., and Wright, A.G. (2004) *Chromatographia*, **60**, 625.
- 129 Górecki, T., Lynen, F., Scucs, R., and Sandra, P. (2006) *Anal. Chem.*, **78**, 3186.
- 130 Steiner, F., Waraska, J., Crafts, C., Fehrenbach, T., and McLeod, F. (2010) An investigation on the approach of inverse compensation gradients in liquid chromatography with mobile phase dependent detectors. Presentation at HPLC 2010, Boston, MA, USA.
- 131 Almeling, S., Ilko, D., and Holzgrabe, U. (2012) *J. Pharm. Biomed. Anal.*, **69**, 50.
- 132 Reilly, J., Everatt, B., and Aldcroft, C. (2008) *J. Liq. Chrom. Relat. Tech.*, **31**, 3132.
- 133 Schönherr, C., Touchene, S., Wilser, G., Peschka-Süss, R., and Francese, G. (2009) *J. Chromatogr. A*, **1216**, 781.
- 134 Lisa, M., Lynen, F., Holcapek, M., and Sandra, P. (2007) *J. Chromatogr. A*, **1176**, 135.

- 135 Sun, P., Wang, X., Alquier, L., and Maryanoff, C.A. (2008) *J. Chromatogr. A*, **1177**, 87.
- 136 Forsatz, B. and Snow, N.H. (2007) *LC–GC N. Am.*, **25**, 960.
- 137 Nováková, L., Lopéz, S.A., Solichová, D., Šatínský, D., Kulichová, B., Horna, A., and Solich, P. (2009) *Talanta*, **78**, 834.
- 138 Liu, X.K., Fang, J.B., Cauchon, N., and Zhou, P. (2008) *J. Pharm. Biomed. Anal.*, **46**, 639.
- 139 Huang, Z., Richards, M.A., Zha, Y., Francis, R., Lozano, R., and Ruan, J. (2009) *J. Pharm. Biomed. Anal.*, **50**, 809.
- 140 International Conference on Harmonisation (2006) ICH Harmonised Tripartite Guideline: Impurities in New Drug Substances: Q3A(R2).
- 141 Zhang, K., Dai, L., and Chetwyn, N.P. (2010) *J. Chromatogr. A*, **1217**, 5776.
- 142 Stypulkowska, K., Blazewicz, A., Fijalek, Z., and Sarna, K. (2010) *Chromatographia*, **72**, 1225.
- 143 Joseph, A., Patel, S., and Rustum, A. (2010) *J. Chromatogr. Sci.*, **48**, 607.
- 144 Holzgrabe, U., Nap, C.-J., Kunz, N., and Almeling, S. (2011) *J. Pharm. Biomed. Anal.*, **56**, 271.
- 145 Adams, E., Schepers, R., Roets, E., and Hoogmartens, J. (1996) *J. Chromatogr. A*, **741**, 233.
- 146 Adams, E., Dalle, J., Bie, E.De., De Smedt, I., Roets, E., and Hoogmartens, J. (1997) *J. Chromatogr. A*, **766**, 133.
- 147 Adams, E., van Vaerenbergh, G., Roets, E., and Hoogmartens, J. (1998) *J. Chromatogr. A*, **819**, 93.
- 148 Adams, E., Roetlands, W., de Paepe, R., Roets, E., and Hoogmartens, J. (1998) *J. Pharm. Biomed. Anal.*, **18**, 689.
- 149 Adams, E., Puelings, D., Raffiee, M., Roets, E., and Hoogmartens, J. (1998) *J. Chromatogr. A*, **812**, 151.
- 150 Adams, E., Raffiee, M., Roets, E., and Hoogmartens, J. (2000) *J. Pharm. Biomed. Anal.*, **24**, 219.
- 151 Szunyog, J., Adams, E., Roets, E., and Hoogmartens, J. (2000) *J. Pharm. Biomed. Anal.*, **23**, 891.
- 152 Debremaeker, D., Adams, E., Nadal, E., van Hove, B., and Hoogmartens, J. (2002) *J. Chromatogr. A*, **953**, 123.
- 153 Kawano, S.J. (2009) *Rapid Commun. Mass Spectrom.*, **23**, 907.
- 154 Arul, J. and Abu, R. (2010) *J. Pharm. Biomed. Anal.*, **51**, 521.
- 155 Jia, S., Lee, W.J., Ee, J.W., Park, J.H., Kwon, S.W., and Lee, J. (2010) *J. Pharm. Biomed. Anal.*, **51**, 973.
- 156 Jia, S., Park, J.H., Lee, J., and Kwon, S.W. (2011) *Talanta*, **85**, 2301.
- 157 Jia, S., Lee, H.-S., Choi, M.-J., Sung, S.H., Han, S.B., Park, J.H., Hong, S.-S., Kwon, S.W., and Lee, J. (2012) *Curr. Anal. Chem.*, **8**, 159.
- 158 Taylor, G.E. (1997) *J. Chromatogr. A*, **770**, 261.
- 159 Crafts, C., Plante, M., Bailey, B., and Acworth, I. (2012) Sensitive analysis of underivatized amino acids with charged aerosol detection. Poster at Pittcon 2012, Orlando, FL, USA.
- 160 Holzgrabe, U., Nap, C.-J., and Almeling, S. (2010) *J. Chromatogr. A*, **1217**, 294.
- 161 Holzgrabe, U., Nap, C.-J., Beyer, T., and Almeling, S. (2010) *J. Sep. Sci.*, **33**, 2402.
- 162 Council of Europe (2007) *European Pharmacopoeia*, 6th edn, Strasbourg.
- 163 United States Pharmacopeial Convention Inc. (2007) *United States Pharmacopoeia*, vol. **32**, Rockville.
- 164 Wang, Z., Hilder, T.L., van der Drift, K., Sloan, J., and Wee, K. (2013) *Anal. Biochem.*, **437**, 20.
- 165 Carrel, R., Jeppsson, J., Vaughan, L., Brennan, S., Owen, M., and Boswell, D. (1981) *FEBS Lett.*, **135**, 301.
- 166 Buytenhuys, F.A. (1981) *J. Chromatogr.*, **218**, 57.
- 167 Haddad, P.R. and Heckenberg, A.L. (1984) *J. Chromatogr.*, **300**, 357.
- 168 Pfeiffer, P. and Radler, F. (1985) *Z. Lebensm. Unters. Forsch.*, **181**, 24.
- 169 Pecina, R., Bonn, G., Burtcher, E., and Bobleter, O. (1984) *J. Chromatogr.*, **287**, 245.
- 170 Stadlbauer, E.A., Trieu, C., Hingmann, H., Rohatzsch, H., Weiß, J., and Maushart, R. (1988) *Fresenius' Z. Anal. Chem.*, **330**, 1.
- 171 Marina-Sánchez, M.A., Díaz-García, M.E., and Sanz-Medel, A. (1992) *Microchim. Acta*, **106**, 227.

- 172 Lu, C., Lin, J.-M., Huie, C.W., and Yamada, M. (2003) *Anal. Sci.*, **19**, 557.
- 173 Mottola, H.A. and Perez-Bendito, D. (1996) *Anal. Chem.*, **68**, 257R.
- 174 Augusti, R., Dias, A.O., Rocha, L.L., and Lago, R.M. (1998) *J. Phys. Chem.*, **102**, 10723.
- 175 Xiao, C.-B., King, D.W., Palmer, D.A., and Wesolowski, D.J. (2000) *Anal. Chim. Acta*, **415**, 209.
- 176 Fujinari, E.M. and Courthaudon, L.O. (1992) *J. Chromatogr.*, **592**, 209.
- 177 Taylor, E.W., Qian, M.G., and Dollinger, G.D. (1998) *Anal. Chem.*, **70**, 3339.
- 178 Bizanek, R., Manes, J.D., and Fujinari, E.M. (1996) *Pep. Res.*, **9**, 40.
- 179 Allgeier, M.C., Nussbaum, M.A., and Risley, D.S. (2003) *LC-GC N. Am.*, **21**, 377.
- 180 Courthaudon, L.O. and Fujinari, E.M. (1991) *LC-GC*, **9**, 732.
- 181 Brannegan, D., Ashraf-Khorassani, M., and Taylor, L.T. (2001) *J. Chromatogr. Sci.*, **39**, 217.
- 182 Pettersen, J.M. (1984) *Anal. Chim. Acta*, **160**, 263.
- 183 Woolson, E.A. and Aharonson, N. (1980) *J. Assoc. Off. Anal. Chem.*, **63**, 523.
- 184 Montaser, A. and Golightly, D.W. (1987) *Inductively Coupled Plasmas in Analytical Atomic Spectroscopy*, VCH Publishers, New York.
- 185 Nölte, J. (2002) *ICP Emissionsspektrometrie für Praktiker*, Wiley-VCH Verlag GmbH, Weinheim.
- 186 Horlick, G., Tan, S.H., Vaughan, M.A., and Shao, Y. (1987) *Inductively Coupled Plasma – Mass Spectrometry, Radiation Chemistry: Principles and Applications*, VCH Publishers, New York.
- 187 Montaser, A. (ed.) (1998) *Inductively Coupled Plasma Mass Spectrometry*, Wiley-VCH Verlag GmbH, Weinheim.
- 188 Nelms, S. (ed.) (2005) *Inductively Coupled Plasma Mass Spectrometry Handbook*, John Wiley & Sons, Inc., Hoboken.
- 189 Hill, S. (ed.) (2006) *Inductively Coupled Plasma Mass Spectrometry and its Applications*, John Wiley & Sons, Inc., Hoboken.
- 190 Jensen, D. and Blödnorn, W. (1995) *GIT Fachz. Lab.*, **7**, 654.
- 191 Powell, M.J. and Boomer, D.W. (1995) *Anal. Chem.*, **67**, 2474.
- 192 Roehl, R., Alforque, M., and Riviello, J. (1992) Comparison of the determination of hexavalent chromium by ion chromatography coupled with ICP-MS or with colorimetry. Presentation at the Plasma Winter Conference on Plasma Spectrochemistry 1992, San Diego, CA, USA.
- 193 Hagendorfer, H. and Goessler, W. (2008) *Talanta*, **76**, 656.
- 194 Knoell, J. and Seubert, A. (2009) *GIT Fachz. Lab.*, **53**, 151.
- 195 Boomer, D.W., Powell, M.J., and Hipfner, J. (1990) *Talanta*, **37**, 127.
- 196 Powell, M.J., Quan, E.S.K., Boomer, D.W., and Wiederin, D.R. (1992) *Anal. Chem.*, **64**, 2253.
- 197 Roehl, R. and Alforque, M.M. (1990) *Atomic Spectrosc.*, **11**, 211.
- 198 Ammann, A. (2011) *Am. J. Anal. Chem.*, **2**, 27.
- 199 Jain, C.K. and Ali, I. (2000) *Water Res.*, **34**, 4304.
- 200 Urasa, I.T. and Ferede, F. (1987) *Anal. Chem.*, **59**, 1563.
- 201 De Menna, G.J. The speciation and structure elucidation of transition metal complexes by HPLC-DCP. Presentation at the Pittsburgh Conference 1986, Atlantic City, NJ, USA.
- 202 Heitkemper, D.T., Kaine, L.A., Jackson, D.S., and Wolnik, K.A. (1994) *J. Chromatogr. A*, **671**, 101.
- 203 Gong, Z.L., Lu, X., Ma, M., Watt, C., and Le, X.C. (2002) *Talanta*, **58**, 77.
- 204 B'Hymer, C. and Caruso, J.A. (2004) *J. Chromatogr. A*, **1045**, 1.
- 205 Bissen, M. and Frimmel, F.H. (2000) *Fresenius' J. Anal. Chem.*, **367**, 51.
- 206 Vela, N.P., Heitkemper, D.T., and Stewart, K.R. (2001) *Analyst*, **126**, 1011.
- 207 Suzuki, K.T., Tomita, T., Ogra, Y., and Ohmichi, M. (2001) *Chem. Res. Toxicol.*, **14**, 1604.
- 208 B'Hymer, C. and Caruso, J.A. (2002) *J. Liq. Chromatogr. Relat. Technol.*, **25**, 639.
- 209 Riviello, J.M., Siriraks, A., Manabe, R.M., Roehl, R., and Alforque, M. (1991) *LC-GC*, **9**, 704.
- 210 Schlegel, D., Mattusch, J., and Dittrich, K. (1994) *J. Chromatogr. A*, **683**, 261.

- 211 Mattusch, J. and Wennrich, R. (1998) *Anal. Chem.*, **70**, 3649.
- 212 Chen, Z., Akter, K.F., Rahman, M.M., and Naidu, R. (2006) *J. Sep. Sci.*, **29**, 2671.
- 213 Brätter, P., Blasco, I.N., and Negretti-Brätter, V.E., and Raab, A. (2000) *Metal Ions in Biology and Medicine*, vol. **6**, John Libbey Eurotext, Montrouge, pp. 751–754.
- 214 Michalke, B. (2006) *Pure Appl. Chem.*, **78**, 79.
- 215 Preedy, V.R., Burrow, G.N., and Watson, R.R. (eds) (2009) *Comprehensive Handbook of Iodine. Nutritional, Biochemical, Pathological, and Therapeutic Aspects*, Academic Press, Burlington, MA, USA.
- 216 Shah, M., Wuilloud, R.G., Kannamkumarath, S.S., and Caruso, J.A. (2005) *J. Anal. At. Spectrom.*, **20**, 176.
- 217 Gilfedder, B.S., Petri, M., and Biester, H. (2007) *Atmos. Chem. Phys.*, **7**, 2661.
- 218 Jackie, M., Vikki, A.C., and Philip, H.E.G. (2002) *J. Anal. At. Spectrom.*, **17**, 377.
- 219 Chen, D., Jing, M., and Wang, X. (2005) Determination of methyl mercury in water and soil by HPLC-ICP-MS. Application Note 5989-3572EN, Agilent Technologies.
- 220 Wallschläger, D. and Roehl, R. (2001) *J. Anal. At. Spectrom.*, **16**, 922.
- 221 Conde, J.E. and Sanz Alaejos, M. (1997) *Chem. Rev.*, **97**, 1979.
- 222 Krachler, M. and Emons, H. (2001) *Anal. Chim. Acta*, **429**, 125.
- 223 Andrae, M.O., Asmode, J.-F., Foster, P., and Van't Dack, L. (1981) *Anal. Chem.*, **53**, 1766.
- 224 Krachler, M. and Emons, H. (2000) *J. Anal. At. Spectrom.*, **15**, 281.
- 225 Lintschinger, J., Schramel, O., and Kettrup, A. (1998) *Fresenius' J. Anal. Chem.*, **361**, 96.
- 226 Lindemann, T., Prange, A., Dannecker, W., and Neidhart, B. (1999) *Fresenius' J. Anal. Chem.*, **364**, 462.
- 227 Lintschinger, J., Michalke, B., Schulte-Hostede, S., and Schramel, P. (1998) *Int. J. Environ. Anal. Chem.*, **67**, 1.
- 228 Krachler, M. and Emons, H. (2001) *Trends Anal. Chem.*, **20**, 79.
- 229 Lintschinger, J., Koch, I., Serves, S., Feldmann, J., and Gullen, W.R. (1997) *Fresenius' J. Anal. Chem.*, **359**, 484.
- 230 Yergey, A.L., Edmonds, C.G., Lewis, I.A.S., and Vestal, M.L. (1990) *Liquid Chromatography/Mass Spectrometry, Techniques and Applications*, Plenum Press, New York.
- 231 Niessen, W.M.A. (1999) *Liquid Chromatography–Mass Spectrometry*, 2nd edn, Marcel Dekker, New York.
- 232 Buchberger, W. and Ahrer, W. (1999) *J. Chromatogr. A*, **850**, 99.
- 233 Simpson, R.C., Fenselau, C.C., Hardy, M.R., Townsend, R.R., Lee, Y.C., and Cotter, R.J. (1990) *Anal. Chem.*, **62**, 248.
- 234 Conboy, J.J., Henion, J.D., Martin, M.W., and Zweigenbaum, J.A. (1990) *Anal. Chem.*, **62**, 800.
- 235 Cole, R.B. (ed.) (1997) *Electrospray Ionization Mass Spectrometry: Fundamentals, Instrumentation, and Applications*, John Wiley & Sons, Inc., New York.
- 236 Yamashita, M. and Fenn, J.B. (1984) *J. Phys. Chem.*, **88**, 4451 and 4671.
- 237 Aleksandrov, M.L., Gall, L.N., Krasnov, V.N., Nikolaev, V.I., Pavlenko, V.A., and Shkurov, V.A. (1984) *Dokl. Akad. Nauk SSSR*, **277**, 379.
- 238 Taylor, G. (1964) *Proc. R. Soc. London A*, **280**, 383.
- 239 Last, I., Levy, Y., and Jortner, J. (2002) *Proc. Natl. Acad. Sci. USA*, **99**, 9107.
- 240 Fenn, J.B., Mann, M., Meng, C.K., Wong, S.F., and Whitehouse, C.M. (1990) *Mass Spectrom. Rev.*, **9**, 37.
- 241 Doyle, M., Mack, L.L., Hines, R.L., Mobley, R.C., Ferguson, L.D., and Alice, M.B. (1968) *J. Chem. Phys.*, **49**, 2240.
- 242 Iribarne, J.V. and Thomson, B.A. (1976) *J. Chem. Phys.*, **64**, 2287.
- 243 Kebarle, P. and Ho, Y. (1997) On the mechanism of electrospray mass spectrometry, in *Electrospray Ionization Mass Spectrometry: Fundamentals, Instrumentation, and Applications* (ed. R.B. Cole) John Wiley & Sons, Inc., New York.
- 244 Lee, E.D. and Henion, J.D. (1992) *Rapid Commun. Mass Spectrom.*, **6**, 727.
- 245 Banks Jr., J.F., Shen, S., Whitehouse, C.M., and Fenn, J.B. (1994) *Anal. Chem.*, **66**, 406.
- 246 Smith, R.D., Loo, J.A., Brarinaga, C.J., Edmonds, C.G., and Hudspeth, H.R. (1990) *J. Am. Soc. Mass Spectrom.*, **1**, 53.

- 247 Armentrout, P.B., Ervin, K.M., and Rodgers, M.T. (2008) *J. Phys. Chem.*, **112**, 10071.
- 248 Wang, J. and Schnute, W.C. (2009) *Rapid Commun. Mass Spectrom.*, **23**, 3439.
- 249 Charles, L., Pépin, D., and Casetta, B. (1996) *Anal. Chem.*, **68**, 2554.
- 250 Charles, L. and Pépin, D. (1998) *Anal. Chem.*, **70**, 353.
- 251 Rabin, S. and Stillian, J. (1994) *J. Chromatogr. A*, **671**, 63.
- 252 Slingsby, R., Saini, C., and Pohl, C., and Jack, R. (2008) The Measurement of haloacetic acids in drinking water using IC-MS/MS – method performance. Poster at IICS 2008, Portland, OR, USA.
- 253 US EPA (2009) Method 557: Determination of Haloacetic Acids, Bromate, and Dalapon in Drinking Water by Ion Chromatography Electrospray Ionization Tandem Mass Spectrometry (IC-ESI-MS-MS). US Environmental Protection Agency, Cincinnati, OH, USA.
- 254 US EPA (1999) Method 314.0: Determination of Perchlorate in Drinking Water by Ion Chromatography. US Environmental Protection Agency, Cincinnati, OH, USA.
- 255 US EPA (2005) Method 332.0: Determination of Perchlorate in Drinking Water by Ion Chromatography with Suppressed Conductivity and Electrospray Ionization Mass Spectrometry. US Environmental Protection Agency, Cincinnati, OH, USA.
- 256 US EPA (2005) Method 331.0: Determination of Perchlorate in Drinking Water by Liquid Chromatography Electrospray Ionization Mass Spectrometry (LC-ESI/MS). US Environmental Protection Agency, Cincinnati, OH, USA.
- 257 Roehl, R., Slingsby, R., Avdalic, N., and Jackson, P.E. (2002) *J. Chromatogr. A*, **956**, 245.
- 258 Di Rienzo, R.P., Lin, K., McKay, T.T., and Wade, R.W. (2004) *Fed. Fac. Environ. J.*, **15**, 27.
- 259 Proudfoot, A.T., Bradberry, S.M., and Vale, J.A. (2006) *Toxicol. Rev.*, **25**, 213.
- 260 Koryagina, N.L., Savelieva, E.I., Khlebnikova, N.S., Goncharov, N.V., Jenkins, R.O., and Radilov, A.S. (2006) *Anal. Bioanal. Chem.*, **386**, 1395.
- 261 Collins, D.M., Fawcett, J.P., and Rammell, C.G. (1981) *Bull. Environ. Contam. Toxicol.*, **26**, 669.
- 262 Mori, M., Nakajima, H., and Seto, Y. (1996) *J. Chromatogr. A*, **736**, 229.
- 263 Mohsin, S.B. (1999) *Anal. Chem.*, **71**, 3603.
- 264 Mohsin, S.B. (2000) *J. Chromatogr. A*, **884**, 23.
- 265 US EPA (1992) Method 548.0: Determination of Endothall in Drinking Water by Ion-Exchange Extraction, Acidic Methanol Methylation and Gas Chromatography/Mass Spectrometry. US Environmental Protection Agency, Cincinnati, OH, USA.
- 266 Thermo Fisher Scientific (2011) Application Note No. 263: Sensitive and Fast Determination of Endothall in Water Samples by IC-MS/MS. Thermo Fisher Scientific, Waltham, MA, USA.
- 267 US EPA (1990) Method 547: Determination of Glyphosate in Drinking Water by Direct-Aqueous-Injection HPLC, Post-Column Derivatization, and Fluorescence Detection. US Environmental Protection Agency, Cincinnati, OH, USA.
- 268 Hallet, J.P. and Welton, T. (2011) *Chem. Rev.*, **111**, 3508.
- 269 Wasserscheid, P. and Welton, T. (2003) *Ionic Liquids in Synthesis*, Wiley-VCH Verlag GmbH, Weinheim.
- 270 König, A., Weckesser, D., and Jensen, D. (2006) *GIT Fachz. Lab.*, **50**, 546.
- 271 König, A., Weckesser, D., and Jensen, D. (2008) *LC-GC The Peak*, **10**, 9.
- 272 Wang, L., Jensen, D., and Schnute, W. (2010) IC-MS and LC-MS determination of ionic liquids, counter-ions, and impurities. Poster at Pittcon 2010, Orlando, FL, USA.
- 273 Wang, L., and Jensen, D., and Schnute, W. (2010) IC-MS determination of anionic ionic liquids, counter-ions, and impurities. Poster at Pittcon 2010, Orlando, FL, USA.
- 274 Keil, P., Kick, M., and König, A. (2012) *Chemie Ingenieur Technik*, **84**, 859.
- 275 Svensson, M., Jones, M.L., Nigri, E.D., Brewer, N., Davis, S., and Oakley, J.A. (2005) *Health Tech. Assess.*, **9**, 1.

- 276 Zacharis, C. and Tzanavaras, P. (2008) *J. Pharm. Biomed.*, **48**, 483.
- 277 Abian, J., Oosterkamp, A.J., and Gelpi, E. (1999) *J. Mass Spectrom.*, **34**, 244.
- 278 Thermo Fisher Scientific (2012) Application Note No. 1001: Quantitative Determination of Bisphosphonate Pharmaceuticals and Excipients by Capillary IC-MS. Thermo Fisher Scientific, Waltham, MA, USA.
- 279 United Nations (1992) Conference on Disarmament. The Convention on the Prohibition of the Development, Production, Stockpiling and the Use of Chemical Weapons and on their Destruction. United Nations Document CD/1170, Geneva, Switzerland.
- 280 Black, R.M. and Read, R.W. (1998) *J. Chromatogr. A*, **449**, 261.
- 281 Ohsawa, I. and Seto, Y. (2006) *J. Chromatogr. A*, **1122**, 242.
- 282 Lemire, S.W., Barr, J.R., Ashley, D.L., Olson, C.T., and Hayes, T.L. (2004) *J. Anal. Toxicol.*, **28**, 320.
- 283 Lee, K.B., Loganathan, D., Merchant, Z.M., and Linhardt, R.J. (1990) *Appl. Biochem. Biotechnol.*, **23**, 53.
- 284 Harvey, D.J. (2000) *J. Am. Mass Spectrom.*, **11**, 900.
- 285 Niessen, W.M.A., van der Hoeven, R.A.M., van der Greef, J., Schols, H.A., Voragen, A.G.J., and Bruggink, C. (1992) *J. Chromatogr.*, **627**, 63.
- 286 Domon, B. and Costello, C.E. (1988) *Glycoconj. J.*, **5**, 397.
- 287 Bruggink, C., Maurer, R., Herrmann, H., Cavalli, S., and Höfler, F. (2005) *J. Chromatogr. A*, **1085**, 104.
- 288 Bruggink, C. (2012) Oligosaccharide analysis by high-performance anion exchange chromatography hyphenated to integrated pulsed amperometric detection and on-line ion-trap mass spectrometry, in *Applications of Ion Chromatography for Pharmaceutical and Biological Products* (eds L. Bhattacharyya and J.S. Rohrer), John Wiley & Sons, Inc., Hoboken, pp. 379–391.
- 289 Hardy, M.R. and Townsend, R.R. (1989) *Carbohydr. Res.*, **188**, 1.
- 290 Wuhler, M., Koeleman, C.A., Deeler, A.M., and Hokke, C.H. (2004) *Anal. Chem.*, **76**, 833.
- 291 Gennaro, L.A., Harvey, D.J., and Vouras, P. (2003) *Rapid Commun. Mass Spectrom.*, **17**, 1528.
- 292 van der Hoeven, R.A.M., Tjaden, U.R., van der Greef, J., van Casteren, W.M.H., Schols, H.A., Voragen, A.G.J., and Bruggink, C. (1998) *J. Mass Spectrom.*, **33**, 377.
- 293 Bruggink, C., Wuhler, M., Koeleman, C.A.M., Barreto, V., Liu, Y., Pohl, C., Ingendoh, A., Hokke, C.H., and Deelder, A.M. (2005) *J. Chromatogr. B*, **829**, 136.
- 294 Bruggink, C., Poorthuis, B.J.H.M., Deelder, A.M., and Wuhler, M. (2012) *Anal. Bioanal. Chem.*, **403**, 1671.
- 295 Packer, N.H., Lawson, M.A., Jardine, D.R., and Redmond, J.W. (1998) *Glycoconj. J.*, **15**, 737.
- 296 Yamashita, K., Okhura, T., Okada, S., Yabuuchi, H., and Kobata, A. (1981) *J. Biol. Chem.*, **256**, 4789.
- 297 De Vos, R.C.H., Moco, S., Lommen, A., Keurentjes, J.J.B., Bino, R.J., and Hall, R.D. (2007) *Nat. Protocols*, **2**, 778.
- 298 t'Kindt, R., Jankevics, A., Scheltema, R.A., Zheng, L., Watson, D.G., Dujardin, J., Breitling, R., Coombs, G.H., and Decuyper, S. (2010) *Anal. Bioanal. Chem.*, **398**, 2059.
- 299 Luo, B., Groenke, K., Takors, R., Wandrey, C., and Oldiges, M. (2007) *J. Chromatogr. A*, **1147**, 153.
- 300 Kiefer, P., Nicolas, C., Letisse, F., and Portais, J.C. (2007) *Anal. Biochem.*, **360**, 182.
- 301 Burgess, K., Creek, D., Dewsbury, P., Cook, K., and Barrett, M.P. (2011) *Rapid Commun. Mass Spectrom.*, **25**, 3447.
- 302 Slingsby, R.W., Al-Horri, R., Pohl, C.A., and Lee, J.H. (2007) *Amer. Lab.*, **10**, 42.